INVESTIGATIVE STUDIES ON VIBRATION ENERGY HARVESTING USING PIEZOELECTRIC DISC TYPE ACTUATORS

A Dissertation

Submitted in Partial Fulfillment of the Requirements

for the award of the degree of

DOCTOR OF PHILOSOPHY

in

MECHANICAL ENGINEERING

by

K.VISWANATH ALLAMRAJU

(Roll No.701419)

Under the Guidance of

Dr. Srikanth Korla

Assistant Professor

DEPARTMENT OF MECHANICAL ENGINEERING

NATIONAL INSTITUTE OF TECHNOLOGY

WARANGAL-506004

2017

INVESTIGATIVE STUDIES ON VIBRATION ENERGY HARVESTING USING PIEZOELECTRIC DISC TYPE ACTUATORS

A Dissertation

Submitted in Partial Fulfillment of the Requirements

for the award of the degree of

DOCTOR OF PHILOSOPHY

in

MECHANICAL ENGINEERING

by

K.VISWANATH ALLAMRAJU

(Roll No.701419)

Under the Guidance of

Dr. Srikanth Korla

Assistant Professor

DEPARTMENT OF MECHANICAL ENGINEERING

NATIONAL INSTITUTE OF TECHNOLOGY

WARANGAL-506004

2017

DEPARTMENT OF MECHANICAL ENGINEERING
NATIONAL INSTITUTE OF TECHNOLOGY
WARANGAL-506004

This is to certify that the dissertation work entitled "**Investigative Studies on Vibration Energy Harvesting using Piezoelectric Disc Type Actuators**" which is being submitted by Mr.**K.Viswanath Allamraju (Roll No.701419)**. His bonafide work is submitted to National Institute of Technology, Warangal, in partial fulfilment of requirement for the award of degree of **Doctor of Philosophy in Mechanical Engineering**.

To the best of our knowledge, the work incorporated in this thesis has not been submitted elsewhere for the award of any degree.

Dr Srikanth Korla
Supervisor
Department of Mechanical Engineering
National Institute of Technology
Warangal-506004

Prof P. Bangaru Babu
Head & Chairman
Department of Mechanical Engineering
National Institute of Technology
Warangal-506004

DECLARATION

This is to certify that the work presented in the thesis entitled "**Investigative Studies on Vibration Energy Harvesting using Piezoelectric Disc Type Actuators"** is a bonafide work done by me under the supervision of Dr Srikanth Korla and was not submitted elsewhere for the award of any degree. I declare that this written submission represents my ideas in my own words and where others ideas or words have been included; I have adequately cited and referenced the original sources. I also declare that I have adhered to all principles of academic honesty and integrity and have not misrepresented or fabricated or falsified any idea/data/fact/source in my submission. I understand that any violation of the above will be a cause for disciplinary action by the institute and can also evoke penal action from the sources which have not been properly cited or from whom proper permission has not been taken when needed.

(K.Viswanath Allamraju)

(701419)

Date:

ACKNOWLEDGEMENT

I am grateful to my supervisor Dr. Srikanth Korla for giving me guidance in every moment and in every action of the accomplishment of my research work. I am very thankful to Prof. P.Bangarubabu, Head & Chairman of the Department and one of the DSC members for giving me support in nurturing the basics of my research work, because of him I got opportunity to visit DRDL Hyderabad and take help from Dr. Y. Krishna Scientist G and Dr. K. Kishore Kumar Scientist F.

I am very thankful to my DSC members Prof R.V.Chalam and Dr. D. Ravi Prasad for their valuable suggestions during and after progress report presentations. I am also thankful to Dr.Y. Krishna and Dr. K. Kishore Kumar for giving me valuable suggestions.

I am dedicating this thesis to the mentor of my life. It is a great privilege for me to work at NIT Warangal.

K.Viswanath Allamraju
Research Scholar
Department of Mechanical Engineering
National Institute of Technology
Warangal-506004, India

List of figures

List of Tables

List of symbols

$[\pm]$	Stress component
$[S]$	Strain component
$[E]$	Electric field component
$[D]$	Electric displacement component
$[s]$	Elastic Compliance coefficient
$[k]$	Stiffness coefficient
$[£]$	Electric permittivity
$[d]$	Piezoelectric coupling coefficients for Strain-Charge form
$[e]$	Piezoelectric coupling coefficients for Stress-Charge form
$[g]$	Piezoelectric coupling coefficients for Strain-Voltage form
$[q]$	Piezoelectric coupling coefficients for Stress-Voltage form
P_{max}	Maximum stress at the point of contact
W_{max}	Maximum load on one spherical contact component
PZT	Lead Zirconate Titanate
EH	Energy Harvester

Table of Contents

Abstract

The power requirements for electronic gadgets which work on micro level power supply is exponentially increasing day by day due to the rapid innovations taking place in electronics & instrumentation. Therefore researchers are putting effort to reduce the dependence on conventional batteries and investigating methods of obtaining electrical energy from other unconventional sources. In this context, vibration energy harvesting has received growing attention during the past decade. The research motivation is due to the reduced power requirement of small electronic components, which are often used in active and passive monitoring applications. Mechanical vibrations are found almost everywhere in the running automobile appliances, civil structures, railways and so on, and in most of the cases these vibrations will be dampened for the comfort. Recently, research is also carried out to generate electricity in shoes, dancing floors, generating energy in thread mills using human energy. The major advantage of vibration energy harvesting is that it is an unconventional source of energy which can utilize the ambient vibrations to generate micro level power. Vibration energy harvesting using piezoelectric materials is found to be a greatest attention for the researchers in recent past because the piezoelectric materials have large power densities when compared to the other basic transduction mechanisms. The disadvantage being usage of some of the piezoelectric materials which are environmentally unfriendly. However, there is a still large scope to develop these kind of harvesters for defense, nuclear and other applications.

Most of the piezoelectric vibration energy harvesters developed earlier are in the form of cantilever beams with one piezo ceramic layer called unimorph or two piezo ceramic layers called bimorph. These harvester beams are fixed on the host structure and dynamic strain is induced in piezo ceramic layers which results in an alternative voltage output across the electrodes. Experimental research on piezoelectric energy harvesters also conducted to estimate the device performance for AC power generation. As an electrical engineering point of view the alternating output voltage is also converted to a stable rectified voltage through a rectifier bridge and a smoothing capacitor.

Piezoelectric materials are molded as actuators in the form of cantilevers, discs and cylinders. some of the typical piezoelectric materials include quartz, barium titanate, lead

titanate, cadmium sulphide, lead zirconate titanate (PZT), lead lanthanum zirconate titanate, lead magnesium niobate, piezoelectric polymer polyvinylidene fluoride (PVDF), polyvinyl fluoride (PVF). These actuators are used in different applications starting from developing simple accelerometers to the complex ultrasonic surgical applications.

However, in the recent, piezoceramics are widely used to develop energy harvesting devices. Earlier PZT materials are used to develop cantilever type piezoelectric energy harvesters using bimorph structures PZT cantilever beams. PZT material is very much reliable for energy harvesting when compared to the other ceramics as well as piezoceramic series because their coupling factors and short circuit sensitivities, permittivity and compliance are very much high when compared to the other materials.

In the present work extensive studies are conducted on the PZT-5H type piezoelectric disc actuators, and the applicability of the energy harvesting actuators for vibration energy harvesting. A novel energy harvesting device which can generate micro level power is developed and tested under experimental conditions. Initially, the distribution of the composition and bonding levels of the PZT -5H materials also observed. Studies are also conducted to understand the characteristics of these PZT-5H actuators; the performance under different temperature conditions, fatigue conditions are observed. By conducting the above experiments the reliability and the durability of these PZT- 5H energy harvesting actuators is studied for the development of efficient energy harvesting device. Analytical studies are conducted using MEMS module to estimate the maximum voltage generated in the piezo electric materials. The significance of the PZT 5H materials is analytically checked during these studies. These actuators may be stacked to develop a device that can generate maximum output. A mathematical model is developed for the devices and vibration studies are conducted to identify the significant frequencies of vibration for maximum power output. Experiments are conducted on these novel PZT 5H based energy harvesting device to observe the maximum power output that could be generated at the significant frequencies.

Chapter 1

Introduction

Nowadays, technology is playing a crucial role for accomplishing the goals very quickly. The knowledge of Information technology, Electrical and Electronics Engineering, Computer Science Engineering, Mechanical Engineering, Civil Engineering etc. are required for the smooth running of any industry and research organization. For all these departments electrical energy is essential. Scientists and researchers worked to gain electrical energy through wind, solar, tidal waves and fossil fuels. Earlier trials were also made to generate electrical energy using vibrations of structures and operating machinery.

During past decade, the research of energy conversion techniques employing ambient vibration has been of high interest for many scientists and engineers. The electricity is taken out from vibrating machines and structures can be employed for powering the wireless sensors, micro power electronic devices, distributing direct current into rechargeable cells and electrical power storage devices. Especially by powering the smart wireless sensor instruments which can be used for structural health monitoring of machines, civil structures and air crafts. By using vibration energy generating electricity can be possible only by means of perovskite materials. PZT (Lead Zirconate Titanate) is one of the perovskite which is having high piezoelectric coupled constant. When the mechanical pressure or load is acted on the PZT, dynamic strain can be created. This dynamic strain leads to separate the anions and cations charges on to the surface; thus resulting in generation of electrical energy. Vibrations are often observed in automobiles, human motions, civil structures, rotating machines, hydraulic pipes, pneumatic pipes, aircrafts, missiles, rockets, rocket launching pads etc. The knowledge of piezoelectric materials and their behaviour such as crystal structure of material, mechanical and electrical properties of the material, manufacturing methods of the PZT discs, geometry properties, design concepts, vibration concepts, modal analysis, finite element methods, computational methods , signal processing, electrical circuit analysis are essentially needed for maximum energy generation. Piezoelectric materials are highly sensitive therefore they may be used for sensing purposes and for damage detection of bearing cracks, gears, bridges, fatigue cracks of aircrafts, plates in vibration analysis approach. Surface embedded piezoelectric materials can also be used for structural health monitoring of

aircraft structures when aerodynamic loads are severe and for continuous monitoring of civil structures.

1.1 Evaluation of Harvesting Energies

Based on the literature survey, text books and internet sources the collected data mentioned in Table.1.1. Comparison in power density is done for temperature gradient, rechargeable batteries, non-rechargeable batteries, solar panels ad vibrations. Power density is very low for rechargeable batteries and high for Temperature gradient power sources. For vibrations power density is 200μ W/cm^3, which is in the second high position amongst the power sources.

Table 1.1: Evaluation of the harvesting energies and the energy storage methods.

Sources of Power	Power density	Information source
Temperature gradient	320 μ W/cm^3 from 5^{0}C	Thermolife
Rechargeable Batteries	9 μ W/cm^3	Commonly available
Non rechargeable Batteries	48μ W/cm^3	Commonly available
Solar panel	20 to 60 μ W/cm^3	Commonly available
Vibrations	200 μ W/cm^3	Roundy [56]

1.1.1. Vibrations

The power density from vibrations is 200 μW/cm^3 , which may be observed from certain building structures. Vibrations are observed in plenty from automobile vehicles, operated production machines, air crafts, missiles, human body organs and due to aerodynamic loads. Vibrations beyond the designed value considered as negative effect on the life of the structures, therefore, a lot of research has been performed earlier to control the vibrations rather to utilize the vibrations to convert the vibration energy into electrical energy. Table1.2 gives some details of vibration sources, frequencies and amplitudes.

Table1.2. Frequency and Amplitude of Vibration Sources

Vibration Source	Frequency(Hz)	Amplitude(mm)
Air Compressors	4-20	$25.4x10^{-2}$
Handling Equipment	5-40	$25.4x10^{-3}$
Pumps	5-25	$25.4x10^{-3}$
Building Service	7-40	$25.4x10^{-4}$
Foot Traffic	0.5-6	$25.4x10^{-5}$
Acoustics	100-10000	$25.4\ x10^{-2}$ to $25.4x10^{-4}$
Punch Presses	Up to 20	$25.4\ x10^{-2}$ to $25.4x10^{-5}$
Transformers	50 -400	$25.4x10^{-4}$ to $25.4x10^{-5}$

1.2 Objectives of the Thesis

Based on the literature survey in the area of vibration energy harvesting, it is noticed that most of the researchers have worked profoundly on electromagnetic and electrostatic mechanisms but the amount of research work conducted on piezoelectric vibration based energy harvesting mechanisms is very less. The literature survey has been performed with the aim to understand the mathematical modelling, characteristics of materials, electromechanical coupled phenomenon, experimental setups, applications and merit and demerits of piezoelectric materials of the different transduction mechanisms.

The objectives of this research are to profoundly study the effectiveness of piezoelectric element (PZT-5H) for effective energy harvesting. The detail objectives of the study are given below.

- To study the effect of piezoelectric coupling coefficient on the electrical displacement by analyzing the piezoelectric constitutive equations.
- To conduct the characterization studies on the piezoelectric element (PZT-5H) to understand it's durable life under compression, fatigue and heat.
- To conduct experimental studies on by fabricating piezoelectric device and to estimate the output voltage and power under different frequency excitation.
- To validate the analytical results with the experimental results
- To understand the effect of temperature on the performance of energy harvester.
- To optimize the output voltage generated by the energy harvester for charging the electronic devices.

1.3 Significance of dissertation

This research work improves the confidence levels of scientists and researchers in the field of vibration based piezoelectric energy harvesters. It makes to aspire in the design of energy harvesting devices, to fabricate the piezoelectric disc type actuators for maximizing the output power generation.

1.4 Research Method of the thesis

After doing the rigorous literature survey, the research methodology of thevibration energy harvesting using piezoelectric disc type actuators in this dissertation covers the concept of basic linear constitutive equations, the mathematical modelling of vibration based piezoelectric disc with input base excitations, the experimental validations and the effect of environmental factor on energy harvester. In this research method, the effect of piezoelectric coefficient on the output parameters plays an important role in vibration energy harvesting devices. It is understood that scientists did not convey in-depth communication of the electromechanical relations. The most important mathematical equations are derived in order to evaluate the effect of piezoelectric coupling coefficient on the output voltage generation. The mechanical and electrical characteristics of piezoelectric disc type actuator are studied experimentally. By the process of characterization, the operating loading and life conditions of piezoelectric disc type actuator could be known. MATLAB Simulink is used as a method of optimizing the power output for charging the low power MEMS and the wireless sensor nodes.

1.5 Organization of the Dissertation

The total thesis contains six chapters, starting from the first chapter to final chapter linked together to give information about the method of generating the electricity by using piezoelectric materials with the means of utilizing vibrations. The overview of the each chapter is mentioned below. **Chapter 1** gives an introduction to piezoelectricity, currently used unconventional sources of energy, conversion principles and describes about the different sources of vibrations for generating piezoelectricity. **Chapter 2** presents the detailed summary of the literature published earlier by Academicians and Researchers in the field of Piezoelectricity and Vibration Energy Harvesting.

Chapter 3 describes the characterization of piezoelectric disc type actuators for their sustainability under mechanical and electrical loads. **Chapter 4** deals with modeling, simulation studies conducted on piezoelectric disc type actuators for maximum energy generation under

sustainable conditions (Frequency, Acceleration and Temperature). **Chapter 5** deals with proto type modeling of energy harvester and experimental studies conducted on piezoelectric disc type actuators under various accelerations from 25 Hz to 100 Hz. **Chapter 6** summarizes the significant conclusions of this research. The relationship between displacement field and piezoelectric coupling coefficient to analyze further the effect of output voltage with piezoelectric coupling coefficient is mentioned in Appendix A .

1.6 Back ground of Piezoelectricity

There are many materials which are useful for manufacturing automobile parts, sophisticated circuit boards, electronic components, defence equipments, armed devices etc. but some materials are having the property of generating the electricity by applying the mechanical pressure which are called piezoelectric materials. In the last two chapters described the introduction and literature survey parts of dissertation. In this chapter mentioned the linear constitutive equations of piezoelectricity which are applicable for analytical and experimental studies of piezoelectric disc type actuators and also mentioned the applications for designing the vibration energy harvester.

1.6.1 Lead Zirconate Titanate (PZT)

This section intends to mention the influence of the crystal structure of the piezoelectric nature of materials, it is by no means a detailed study on the crystallography of piezoelectric materials. In dielectric materials, the regular repetitive arrangement of atom, ions or molecules in a lattice is called the crystal structure. The presence of the piezoelectric phenomenon in materials depends on the internal crystal structure of the dielectric; unlike electrostriction which is independent of the internal structure and thus can occur in liquids and gases. In particular, the piezoelectric effect can only occur in crystals which do not possess a center of symmetry. From the direct piezoelectric effect point of view, when the material is elastically deformed, the center of gravity of the positive and negative charges are displaced and the lack of symmetry prevents a net electrical cancellation. The summation of these electric dipoles lead to a macroscopic non-zero polarization field. From a mathematical point of view, when the crystal possess a center of symmetry then the piezoelectric coefficients which are third rank tensors, must cease to exist . Therefore a material with a center of symmetry cannot exhibit piezoelectric effects. In the study of crystallography, there exist a total 32 different crystal classes out of which 20 possess the

piezoelectric capability. The 32 classes are divided into seven groups such as triclinic, monoclinic, orthorhombic, tetragonal, trigonal, hexagonal and cubic. These groups are also concomitant with the elastic nature of the material where triclinic represents anisotropic material, orthorhombic represents orthotropic material and cubic are usually isotropic materials. The choice of crystal structure of the piezoelectric to be adopted in this work were based on the following factors: the generality of the piezoelectric material to accommodate a greater variety of directional actuation, avoiding over-generalization of having more independent material coefficients than is necessary, the availability of numerical data from manufacturer or literature. Having considered this, the chosen crystal structural model for this research work is that of the "orthorhombic - class mm2". The piezoelectric material and the non-piezoelectric material (substrate) considered in this work will be, at most, orthotropic. This means that it can be anything up to orthotropic; including isotropic and transversely isotropic. In particular, two types of piezoelectric materials widely used in smart structure applications are piezo-ceramics which is usually poly-crystalline materials such as (Pb(Zr,Ti)O3) and piezo-polymers such as polyvinyl fluoride (PVF).

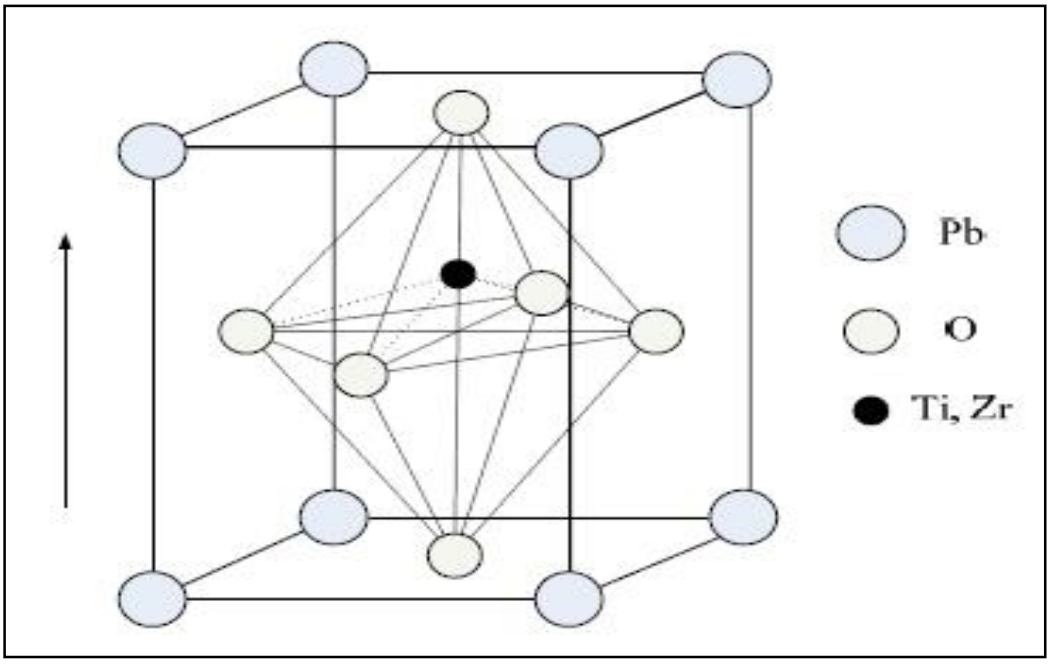

Fig.1.1 Atomic structure of PZT

Due to polarization methods (to initiate the piezoelectric properties), the piezoceramic often adopt the mm6 crystal structure whereas the piezopolymers are of the mm2 crystal structure. The

former can be considered as a degenerate subset of the latter crystal structure. Thus the choice of mm2 structure for the present work is general enough to cover the piezoelectric materials often associated with smart structures. Fig 1.1 shows the crystal structure of lead zirconate titanate perovskite at the room temperature. The chemical formula of lead zirconate titanate is $Pb[Zr_xTi_{(1-x)}]O_3$, x=0.52. It is also called PZT. At x=0.52, PZT shows a large dielectric constant, high piezoelectric response and poling efficiency. The lattice parameters **a, b, c** and ~ of PZT at different 'x' values is mentioned in table 1.3 [64].

Table1.3. Lattice parameters of PZT

x	Phase	Form	$a\left(\overset{o}{A}\right)$	$b\left(\overset{o}{A}\right)$ or ~	$c\left(\overset{o}{A}\right)$
0.00	O	P	5.85	11.77	8.23
0.10	R	SD	4.14	89.73^o	-
0.20	R	SD	4.12	89.71^o	-
0.30	R	SD	4.11	89.70^o	-
0.40	R	SD	4.09	89.70^o	-
0.48	R+T	SD	4.08	89.72^o	-
0.52	T	SD	4.01	-	4.14

Note - O: Orthorhombic , R: Rhombohedral , T: Tetragonal , P: Powder, SD: Sintered disk

1.6.2 Characteristics of PZT

i. Damping ratio is very low
ii. Good machinability
iii. High brittleness
iv. Sensitivity for voltage is very high
v. Castability is high

vi. PZTs are flexible. It can be usable for various voltage electrical drive circuits

vii. PZTs can also be usable under the various frequency environments.

1.6.3 History of Piezoelectricity

History of piezoelectricity since 1880 to 2017 is mentioned in Table 1.4. Curie brothers discovered the direct piezoelectric effect by using Tourmaline, Quartz, Topaz, Cane Sugar and Rachelle Salt in the year of 1880[54].

Table 1.4 History of piezoelectricity

Year	Name	Material	Remark
1880	Pierre Curie & Jacques Curie	tourmaline, quartz, topaz, cane sugar and Rochelle salt	Direct piezoelectric effect
1881	Lippman	Quartz	Converse piezoelectric effect
Early 1990	-	-	Topic of scientific interest
1916	Paul Langevin	Quartz crystals between two metal plates	Langevin transducer & Ultra sonic submarine detector
1917	Robert A	Quartz crystals between two metal plates	He supported the work of Langevin
1917-1940	W.G.Cady	Quartz crystals between two metal plates	Developed the devices based on the work of Langevin
1940-1965	US, Japan and Soviet Union	$BaTio_3$ family	Deemed in developing piezoelectric materials
1965-1980	Japaneese developments	$BaTio_3$ family	Piezoceramic ignitors, ultrasoninc transducers
1980-2017	India involved	Lead Zirconate Titanate	Piezoceramic products & Energy harvesters

1.6.4 Applications of Piezoelectricity

Fig 1.2 represents the pictorial presentation of the overall view of applications of piezoelectricity. There are two types of piezoelectric effects. One is the direct piezoelectric effect and the second one is indirect or converse piezoelectric effect. Converse piezoelectric effect is defined as it converts the voltage into mechanical strain or deformation. Converse piezoelectric effect is subdivided into two categories such as resonant applications and non-resonant

applications. Maximum applications are under resonant condition. Under resonant condition, the applications of converse piezoelectric effect are for ultrasonic cleaning, dental descaling, wave filters, scanning probe microscopy etc. Voltage and power generations takes place under the applications of direct piezoelectric effect. In this dissertation, research work is carried out on the application of direct piezoelectric effect that is voltage generation by applying impact load on the piezoelectric disc type actuators.

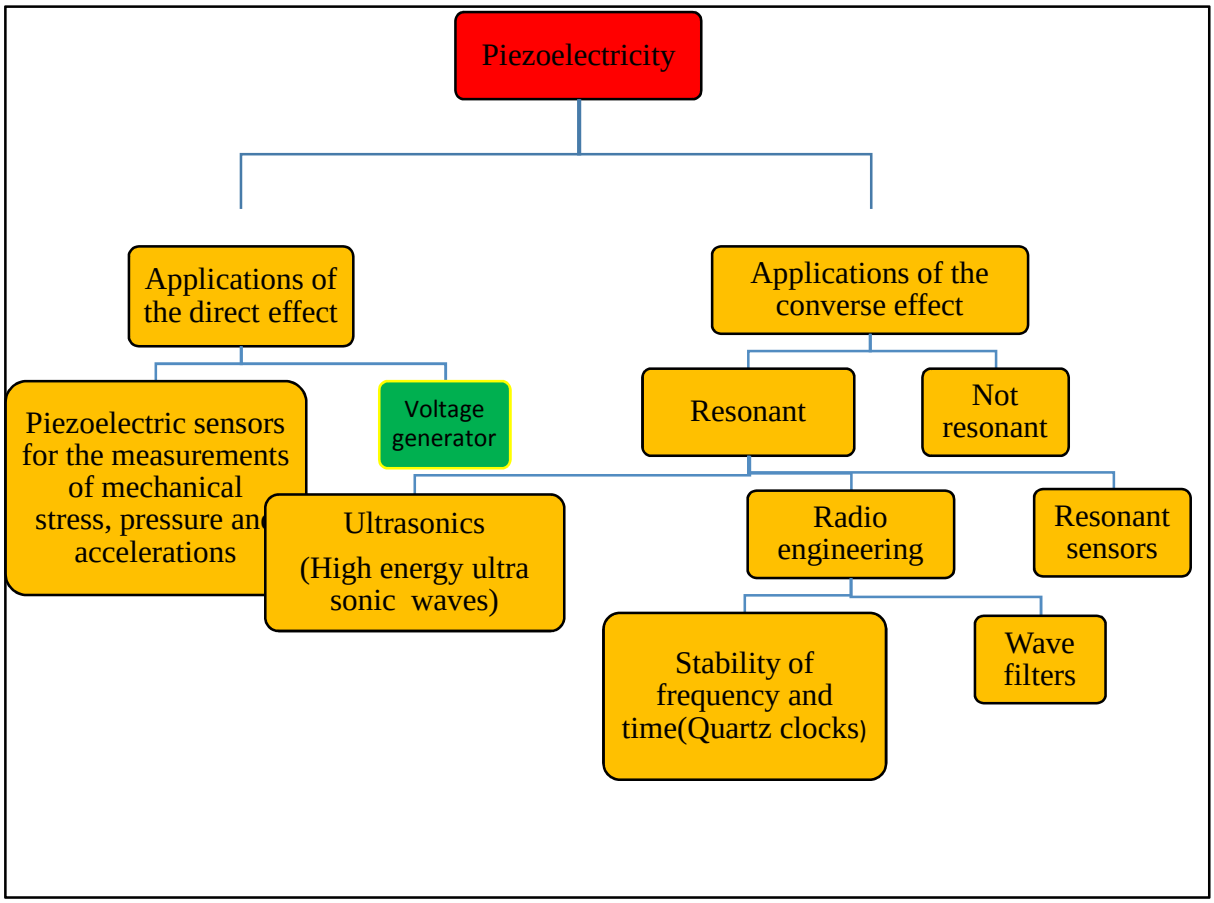

Fig.1.2 Applications of piezoelectricity

1.7 Linear constitutive equations of piezoelectricity

The four categories of linear piezoelectric constitutive equations are mentioned below(Equations 1.1 -1.8) [55].

Strain-Charge Form:

$$[S]=[s][\pm]+[d][E] \qquad (1.1)$$

$$[D]=[d][\pm]+[£][E] \quad (1.2)$$

Stress-Charge Form:

$$[\pm]=[k][S]-[e][E] \quad (1.3)$$

$$[D]=[e][S]+[£][E] \quad (1.4)$$

Strain-Voltage Form:

$$[S]=[s][\pm]+[g][D] \quad (1.5)$$

$$[E]=[-g][\pm]+[£]^{-1}[D] \quad (1.6)$$

Stress-Voltage Form:

$$[\pm]=[k][S]-[q][D] \quad (1.7)$$

$$[E]=[-q][S]+[£]^{-1}[D] \quad (1.8)$$

1.7.1 Electrical impedance of PZT disc type actuator

The impedance is a distinctive property for piezoelectric disc type actuators. For calculating the electrical power from output voltage the property of impedance is essential .It is very important property for vibration based piezoelectric disc type energy harvesters .Electrical impedance is well-defined as the voltage developed from piezoelectric disc type actuator divided by the current through the piezoelectric disc type actuator. Fig.3.3 shows the variation of impedance over a frequency range for non-piezoelectric dielectric elements. The behaviour of Impedance over a Frequency is quadratic non-linear. It follows the equation of $y=0.3405x^2-64.103x+4940.2$. Correlation is 98.32%.

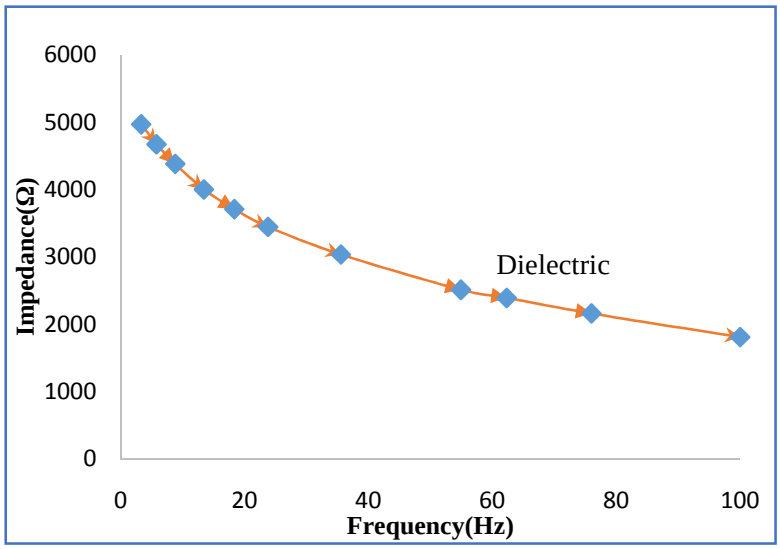

Fig.1.3 Electrical impedance over a frequency for a dielectric material

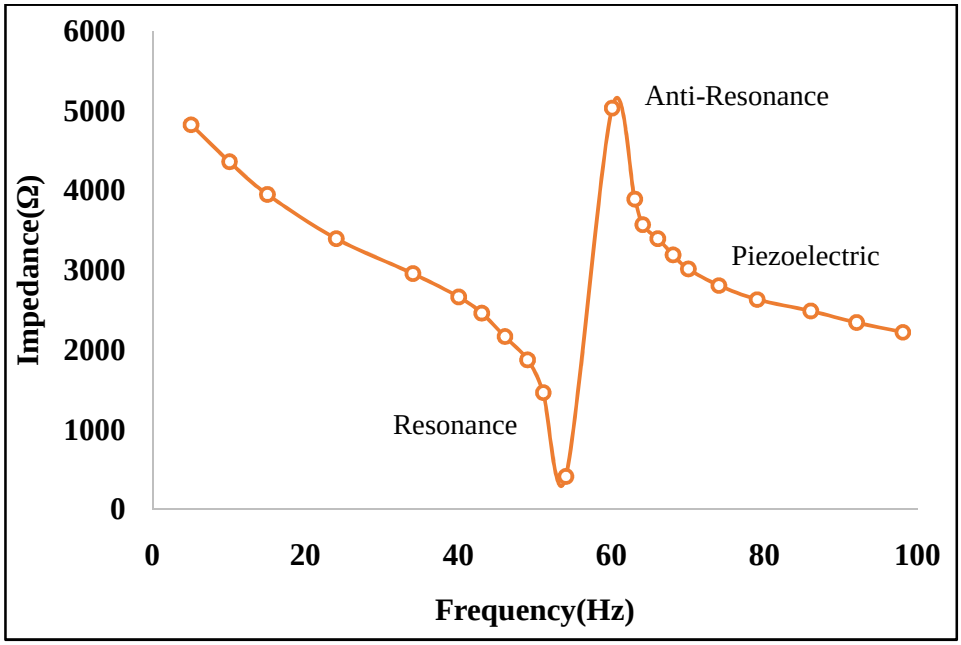

Fig.1.4 Electrical impedance over a frequency for piezoelectric material

Fig 1.4 shows the response of electrical impedance over a range of frequency for piezoelectric material under both resonance and anti- resonance conditions. For the resonance condition, electrical impedance is decreasing with the frequency and for the anti-resonance condition electrical impedance is increasing with the frequency. At the frequency range of 54Hz to 60 Hz there is a peak ascent in electrical impedance. It reflects the beginning of the zone of anti-resonance frequencies of piezoelectric material. The various operated frequencies effects the impedance of piezoelectric disc type actuator. Every natural frequency causes to create resonance and non-resonances in the impedance.

1.7.2. Equivalent Electrical Circuit of Piezoelectric disc type actuator

To study the behaviour of impedance, an equivalent electrical circuit is modeled. Fig.1.5 shows the equivalent electrical circuit of piezoelectric disc type actuator. It consists of L, R,C and Cp. This circuit is mainly to study the simulation of piezoelectric resonance behavior. The following assumptions are considered for accurate simulation.

i. The value of C must be smaller than Cp.
ii. C and Cp must be in parallel connection but not in series connection.

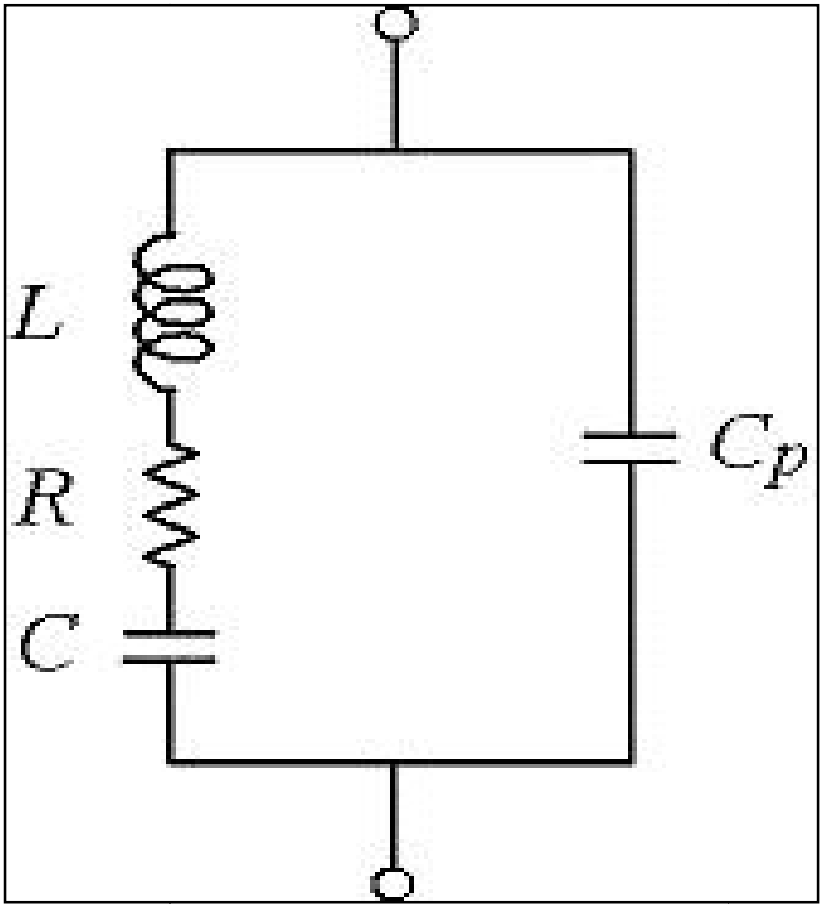

Fig.1.5. Equivalent electric circuit of piezoelectric disc

The unit of frequency is in Hz. The natural frequencies for resonance and anti-resonance can be calculated by using equations 1.9 & 1.10.

$$f_{resonance} = \frac{1}{2\pi\sqrt{LC}} \qquad (1.9)$$

$$f_{anti-resonance} = \frac{1}{2\pi\sqrt{L\dfrac{CC_p}{C+C_p}}} \qquad (1.10)$$

1.8 Piezoelectric effect

Direct Piezoelectric Effect:

When the compressive load (F) is applied on the piezoelectric disc type actuator, a dynamic strain will be induced and thereby generates voltage across the terminals, which can be measured by the voltmeter. Here the force is input, sample is piezoelectric material and the output is voltage.Fig.1.6 shows the schematic representation of principle of direct piezoelectric effect under the application of compressive load.

Inverse Piezoelectric Effect:

When the voltage is supplied to piezoelectric disc type actuator, mechanical deformation takes place, then this principle is called as inverse piezoelectric effect. This inverse piezoelectric effect is used for increasing the damping factor and isolation purposes of vibration systems.

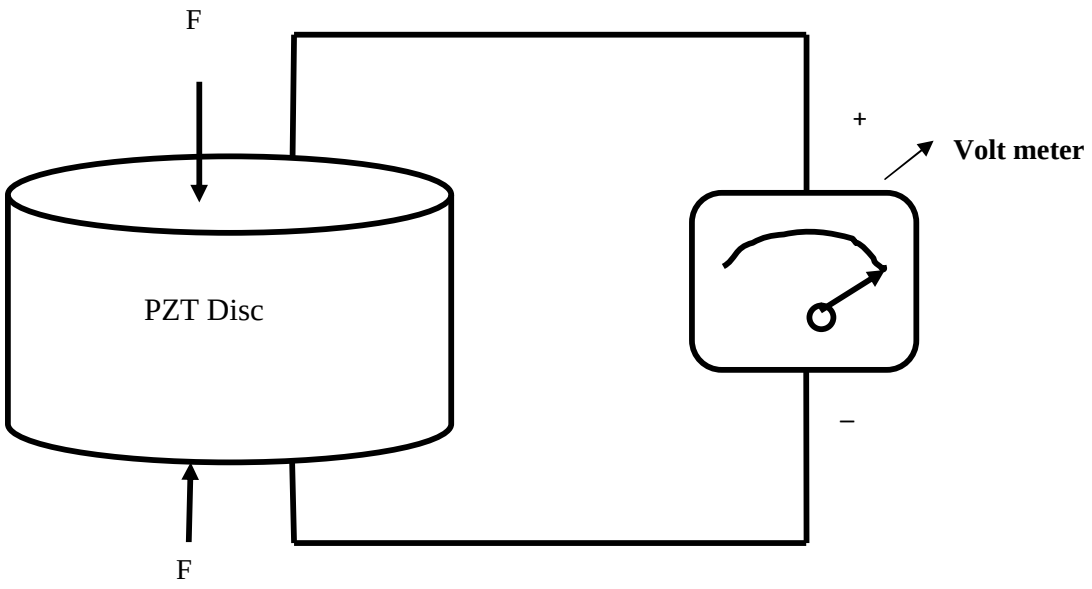

Fig.1.6 Principle of direct piezoelectric effect

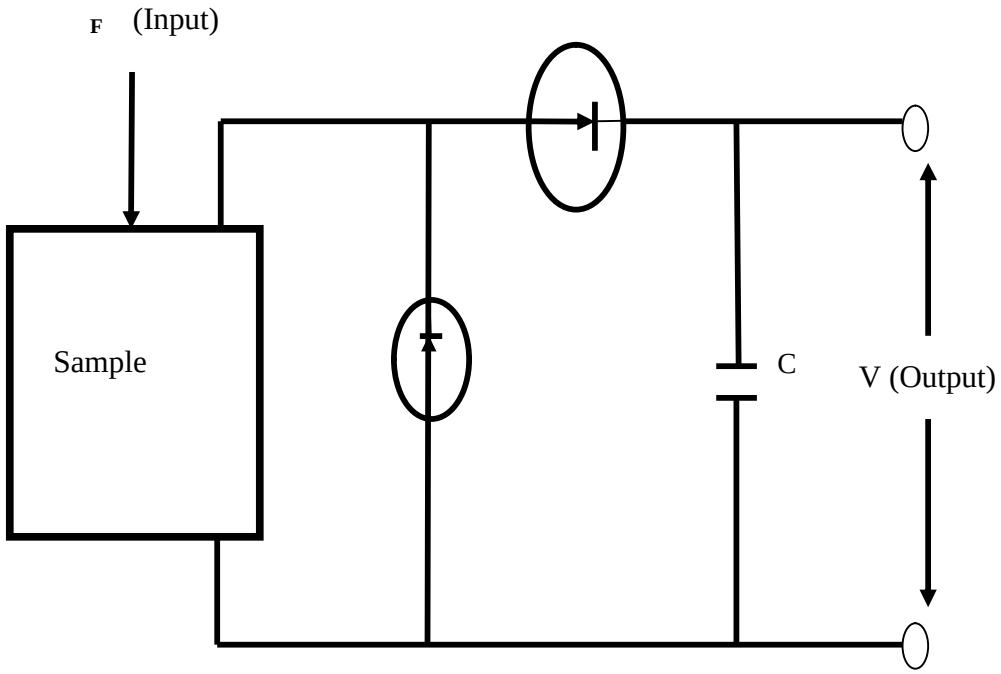

Fig.1.7 Direct piezoelectric effect with electrical circuit

Fig 1.7 represents the electrical circuit of the principle of direct piezoelectric effect. Half wave rectifier is used to convert AC to DC. A Capacitor (C) is meant for storing the DC Voltage for continuous supply of voltage.

1.8.1 Selection of PZT-5H

PZT-5H type disc type actuators are selected by considering the various parameters such as piezoelectric constant , permittivity and compliance for generating the maximum voltage and power. In this research direct piezoelectric effect is used for generating the maximum power. In order to gain maximum power piezoelectric constant should be high for the piezoelectric actuators, therefore PZT 5H is having high piezoelectric constant in comparison to PZT-2, PZT-4 and Ceramic B. These parameters are mentioned in table 1.3.

Table 1.5 Comparison of PZT-5H in relation to other materials [61]

	Ceramic B	PZT-2	PZT-4	PZT-5A	PZT-5H
Piezoelectric constant	26	26	50	64	100
Permittivity	35	13	38	50	100
Compliance	52	71	75	100	100

1.9 Introduction to COMSOL Multi-physics

In this dissertation COMSOL5.0 Multiphysics was used for studying the frequency responses, acceleration dependence and load dependence of energy harvester, therefore COMSOL 5.0 introduction has been mentioned.

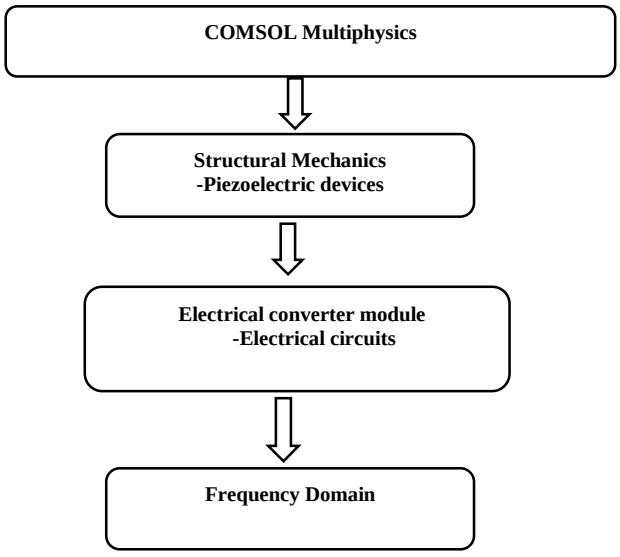

Fig 1.8 Flow chart presentation of overall view of COMSOL 5.0 Multiphysics tool

The overall view of COMSOL is shown in Fig 1.8. In this dissertation COMSOL is employed for simulating the piezoelectric disc type actuator at various accelerations from 20g to 100g under various frequencies of 25 Hz to 100 Hz. The analytical results which are obtained from COMSOL are validated with experimental results. In the past, many researchers were worked on energy harvesting by electrostatic and electromagnetic transduction mechanisms but the output power was not enough to operate certain micro electromechanical systems; therefore, piezoelectric transduction mechanism fulfilled that need. High power density is observed in relation to electro static and electromagnetic mechanisms. Many researchers were also worked in piezoelectric transduction mechanism, though power density is high, but requirement of power and voltage could not be achieved. It is observed that the design aspects of energy harvester may be considered; therefore, in this dissertation an attempt is made to maximize the voltage by fabricating the prototype model of piezoelectric energy harvester .Simulation studies are done and these results are validated with experimental data. The output obtain from piezoelectric transduction mechanism is AC but the application of DC is very much required for operating wireless sensor nodes and low powered electronic devices. MATLAB Simulink Toolbox is used for conversion and maximizing the power. Based on literature survey, it is observed that piezoelectric transduction mechanism may be used for controlling the vibrations apart from generating the electricity.

Chapter 2

LITERATURE REVIEW

In this chapter presented the literature survey starting from the pioneer work done by Hua-Bin Fanga & Jing-Quan Liu in 2006, several researchers have done commendable work in the various aspects of piezoelectric energy harvesting. Most of the work is grouped into piezoelectric generation using cantilever beams, human powered piezoelectric generation, micro-scale implementation and impact coupled devices. The present chapter summarizes the work performed by several researchers on the various aspects of piezoelectric energy harvesting. References 1-16 represents the research related to the voltage generation from cantilever beam type energy harvester, references 17-20 represents the research related to the electricity generation from human powered category, references from 21-28 represents the category of impact coupled devices, references from 29-37 represents the category of micro level voltage generation and the remaining represents the category of vibration based energy harvesters.

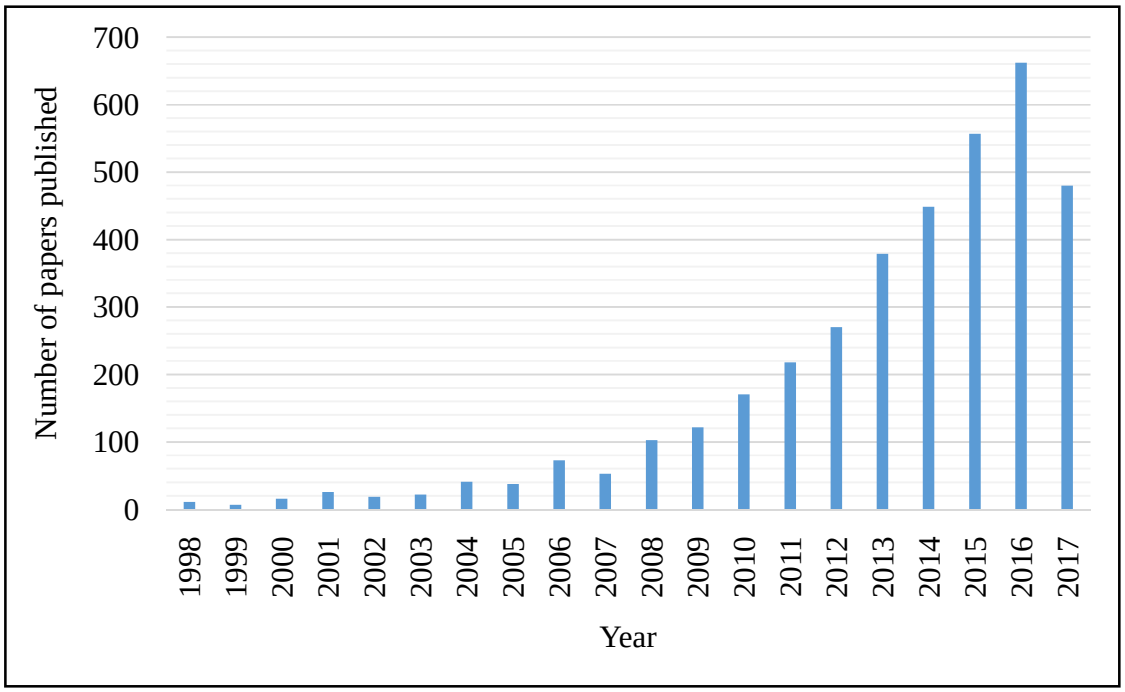

Fig.2.1 Number of papers published per year in piezoelectric energy harvesting

Fig.2.1 discusses about the number of papers published since January 1998 to May 2017. It shows the growth of research in the field of piezoelectric energy harvesting. Since 1998 to 2007,

the number of papers published per year in piezoelectric energy harvesting is less than hundred. The maximum papers were published in 2016.

2.1 Piezoelectric generation using cantilever beam

The research of piezoelectric energy harvesting is started with cantilever beam based. Many researchers have done and still doing their research on cantilever beam type in parallel to the category of human powered, impact coupled, micro scale level and application oriented vibration based energy harvesting.

In the year of 2006, cantilevered type piezoelectric micro power generator is proposed by Bin Fanga & Jing-Quan Liu. In their work composite based cantilever with nickel mass is used. It can be operated at low frequencies of 600 Hz to 610 Hz and 2.16 «W power and voltage is 0.89 V AC peak to peak are generated [1]. Hu brothers designed a cantilever beam based energy harvester by attaching a fixed mass at the free end and concluded that the power density can be increased from 200 to 300 « W/cm^3 by varying the inductance from 1x10^{-4} to 2x10^{-5} under fixed end mass [2]. Marco Ferrari demonstrated experimentally in 2009 that the more dynamic strain can be created by coupling the piezoelectric converter to permanent magnets. The added nonlinearity to cantilever beam was studied by using a MATLAB Stochastic Differential Equation (SDE) tool box [3]. Instead of single cantilever beam, bulk cantilever PZT thin films are used by Huicong Liu to optimize the voltage and power from micro watts level to milli watts level. He experimented parallel and series connections and concluded that the parallel connections of PZT thin films generates the maximum output of 90 mV which is three times more than the power generated in series connections at the load resistance of 800 kΩ [4]. Analytical models are demonstrated with high tip mass in relation to the applications of structural health monitoring and for wireless sensor nodes [5]. After that by using magneto electric transducers, unimorph piezoelectric transducers and comb shaped piezoelectric cantilever beam are used for increasing the power density from 100 « W/cm^3 to 10 m W/cm^3 by using ambient vibrations. Electro-mechanical coupled equations are developed to predict the responses of the piezoelectric cantilevers [6-8]. More electrical energy conversion can be taken place in proportion to the induced strain in the piezoelectric cantilevers, therefore by giving the radio frequency signal , strain is induced in the cantilevers. Instead of using unimorph cantilevers, bimorph cantilevers are manufactured and kept in array and used for producing more electrical energy under ambient vibrations. Three times more power is reached in comparison to

single unimorph piezoelectric cantilever [9-16]. The similarities are found from references 1 to 16 is that all were used piezoelectric cantilevers and the power generated was in micro watts. Even though the generated voltage is 1 V which is low but the exceptional work was done by Marco Ferrari in 2009 by using magnet developed a strain in the piezoelectric material.

2.2 Human powered piezoelectric generation

Jon etal used a PVDF film and unimorph piezoelectric composite patch which were inserted into a shoe, demonstrated a model for generation of electricity while walking; even though it is soothing to hear and very fascinating for scientists and researchers to develop their confidence levels in the applications of piezoelectric energy harvesting. The drawback is that if the person is having Plantar fasciitis and Achilles tendinitis, that shoe cannot be useful and also the maximum power of more than 2 mW cannot be generated by the health human beings [17]. Even though John etal work is not applicable everywhere but the developed power is in milli watts. In comparing the works of references [1-16], reference [17] is done the better work and developed a power of 10 mW. Jose et al also worked on generating electricity by four various human motions where as John et al used only one human motion that is walking. Jose et al used four different motions such as breathing, walking, typing and upper limbs motion. The maximum power is generated during walking i.e 900 mW at the load of 650 N under the frequency of 1 Hz. He has generated more power than reference [17]. Even though the mechanical power loss is high for walking motion but the generated power is also high. Jose et al mainly focused on to supply the power for audio and computation functions and for replacing the lithium ion batteries [18].

So far studied that maximum power can be generated only by giving the human motion through walking but Jamaludin et al demonstrated that by giving the motion via hand on the piezoelectric disc type actuator the electrical power can be generated. Jamaludin presented the complete steps for designing and developing an innovative piezoelectric generator prototype by using 4-axis machine including the factors considered for the best design. The process consist of designing the model refer to generator working principal and some new fabrication methods for the small thickness plate to be used for the piezoelectric generator. This alternative method of fabricating the 8mm thickness nylon plates by using 4-axis Modula Machine exposed the ability of that machine to operate such thin work piece. This innovation prototyping methodology can be applied for other similar project. A rapid prototyping machine was used for fabricating the nylon

device. The maximum voltage developed was 19.65 V [19]. The draw back from hand operation is that the power generated is not continuous. Therefore for supplying the continuous power, the power storage devices should be used.

M. Loreto also worked on human power by walking. Piezoelectric patches were inserted in the sole of the shoe. The maximum generated power is 6.08 V. Bimorph patches were used The advances made from this research build the framework for further experimentation with the tools necessary to use the piezoelectric fibber composite bimorph (PFCB) effectively in numerous applications [20].

2.3 Micro-scale implementations

Chao et al demonstrated the energy harvesting in micro level by considering various devices such as photovoltaic, thermo electric generator, vibration energy transducer, fuel cell and electro-magnetic generator. Various power densities were described in their research work. Power density for piezoelectric materials is high in comparison to other sources. Therefore in this dissertation piezoelectric disc type actuators are used for gaining maximum power output [29]. S.P.Beepy also worked on micro level energy scavenging and compared the output generation three conversion mechanisms by analytical approach. Equations of motion with damping for the mechanisms are also presented [30]. In the references 1-30 used PZT material was used for doing research to generate electricity, whereas Huan et al worked on zinc oxide crystal to generate electricity. Analytical studies were done and results are validated with experimental values of two years old research paper. The generated voltage was 10 mV [31]. Ahmedreza et al mainly worked on how to regulate the power which was generated from the piezoelectric element when it was under excitation, for that full bridge rectifier was developed and dc to DC converters were also used to optimize the power, mainly focused on power optimization. On the design of piezoelectric discs or design of energy harvesters were not explained. Already worked experimentation was used such as cantilever beam with piezoelectric patches. Although efficiency in output was improved but the generated output power was very low i.e. in micro watts. Ahmedreza et al work was addition to references 1-16 [32]. Fain et al also worked on cantilever piezoelectric beam model with tip mass in multiples. The source of vibratory motion to cantilever beams was riding by cycle, car, train or during walking. A case was fabricated such a way to keep the laptop inside and which was surrounded by piezoelectric cantilevers. When the people were riding a car with this laptop case, the oscillatory motion was given to laptop which

leads to the displacement of cantilevers thus electric power was generated. The power was generated by this method was still in micro level and was not continuous supply. For experimentation this work was good but the main drawback was laptop may be get damaged [33].

Manu Pallapa compared the Piezoelectric Micro-Power Generators (PMPG) modelling and simulation results obtained using four different approaches; (i) COMSOL Multiphysics 3.5a, (ii) Coventor, (iii) ANSYS and (iv) Lumped element analysis. It is found that the four approaches closely agree with each other. They indicate that while the nominal design of the PMPG is sound, it is quite conservative and inefficient. The simulations provide the basis for optimal design and fabrication of the PMPG [34]. Brijesh Kumar used zinc oxide material for developing electrical power. His work was similar to reference 31. Reference 31 used only nano crystals but Brijesh used various nano sized zinc oxide geometrical structures. Zinc oxide is ecofriendly material but the output power generated was in micro level. The importance of zinc oxide was mentioned in their research that this material can be used for gaining electricity from sun rays because of having semi-conductivity and at the same time it can be used for piezoelectricity due piezoelectric nature, therefore zinc oxide may be used for hybrid purposes to maximize the power generation. The limitation of their research that inverse piezoelectric effect and specific applications were not discussed [35]. In the field of micro level energy harvesting Jiyoung et al studied the literature from 2008 to 2012 on nano fiber energy harvesting and it's applications for supplying the power for electrical, electronic , mechatronic devices and wireless sensor nodes. Piezoelectric nano generators which were made of PVDF and PZT were used for study. Nano fibers characterization was studied by using various experimental setups such as x-ray diffraction, Fourier transform infrared, second harmonic generation, piezo-response force microscopy and Raman spectroscopy and also presented the prerequisites which were required to understand the nano fiber energy harvesting. In reference 31, zinc oxide was used for nano fibers but Jiyoung et al reviewed on the nano generators made of PVDF and PZT [36]. Jiyoung et al worked on piezoelectric nano fibers where Xudong worked on zinc oxide nano wires for extracting the power. The maximum power predicted is as same as reference 36. The difference between Jiyoung et al and Xudong was the materials for nano generators. The draw backs for this research was very less power generation and may not be applicable for the devices which functions on the platform of milli watts power [37]. Microstructural evaluation of piezoelectric

ceramic was done by Ching Chang Chung [62]. At morphotropic phase boundary piezoelectric response is high for the lead zirconate titanate material. At various ‘x’ values, lattice parameters were found by using x ray diffraction tests. The detailed lattice parameters of PZT [64] are presented under the section of 1.6.1.

2.4 Power generators for broadband vibration energy harvesting

The cantilever beam piezoelectric generators and nano fiber PVDF, PZT and Zinc oxide nano generators are studied so far for generating the electric power. The limitation was that the generated power was in micro and milli watts. Now broad band vibration energy harvesting is considered which includes electromagnetic, electrostatic and piezoelectric mechanisms. Jin Yang et al worked on electro magnetic mechanism and extracted electrical power. Cantilever beam was used which was made up of beryllium bronze. The design was complicated. It works on the principle that when the current carrying the conductor the magnetic flux produces electricity. Here, the cantilever beam moves within the magnetic field generates electricity. The conductor is the cantilever beam based on the movement of cantilever beam between the magnets the current depends on that. The maximum displacement was used is 4.2 mm and demonstrated the maximum power. Experimentation was done within the 1g acceleration and within the frequencies of 10 Hz [38].

Mao et al also worked on the electromagnetic energy harvesting and demonstrated that when the magnet moves between two magnets the electricity can be generated. The power was produced by using less than 1 Hz frequency. The vibration source was car riding vibrations. The device was fitted at the back place of car inside the cabin. The generated power was very low which was less than 1.5 micro watts. This power may not be used for all the devices and the limitations were very high. It seems that this experimentation was done for the sake of writing a paper but the application were very limited. The sensitive capability was 1Hz to 1 kHz [39]. L Tang et al worked on broad band electromagnetic energy harvesting by using vibrations. Cantilever beam with tip mass was used between the two permanent magnets. The tip was placed at the bottom surface of free end. Cantilever beam was made of piezoelectric material and the tip mass made of magnet. The whole set up was excited by the shaker [40]. Louis demonstrated a energy harvester working on ambient vibrations as the source. Tow piezoelectric patches were used for experimentation; mostly cantilever beam model was used. The conclusion was under chaotic vibrations maximum power can be generated but it was not true. Factually under the resonance

conditions the maximum power can be generated [41]. Challa et al also worked on vibration energy harvesting by using magnetic forces. His work is similar to references 39 to 41 but the difference was status of frequencies. References 39 to 41 worked on non-resonance frequencies but Challa et al worked on resonance frequencies. Energy harvesting device was designed. The cantilevered beam geometry was used as similar to L tang et al. At the frequency of 26 Hz the maximum power generated was maximum of 280 micro watts. The work was not novel in taking the geometry and experimentation [42].

2.5 Piezoelectric sensor applications

So far studied the cantilever beam based generating electrical energy under excitation of different frequencies from 1 Hz to 10 Hz. Micro power was generated by nano generators made up of PVDF, PZT and Zinc oxide. Some of the researchers worked on piezoelectric materials when subjected to impact forces such a way electricity can be generated. Burger et al gave the method of measuring the impact forces. There was no electricity generated. Multiple piezoelectric sensors were used for experimentation. It can be found out by accelerometer but it was not used [21]. Similar to Burger et al Kevin et al also worked on piezoelectric sensors application. Impact detection was measured by using piezoelectric sensors. It is completely sensing the impact load not for generating the electricity. The method of Kevin et al work can also be used for detecting the enemy's submarines, missiles by using piezoelectric sensors. His work is not energy harvesting by using vibrations [22]. Marco et al also had done research in the application of piezoelectric sensors in similar to Burger and Kevin et al. Impact load was measured by using piezoelectric accelerometers. The characterization method of piezoelectric sensors was discussed in the range of high frequencies. In Marco et al focused mainly on calibration of the piezoelectric sensor for measuring the impact loads but no power was generated. The concept of engineering mechanics was used in their work [23]. Renaud et al proposed the energy harvester in a prototype model by giving the motion to cubic ball which having the weight of sixty grams but did not mention the material of the ball. Missile impact on piezoelectric unimorphs was considered but how much impact was given could not be measured. By applying the work of Marco et al in addition to Renaud et al work would have been better. The weight of impact cubic missile was very low. No exciter and no accelerometers were used for experimentation. The source of vibration for their work was human hand operation with the frequency of ten Hertz and micro watts power was developed. The power in micro watts can be

used for charging the devices in limited [24]. Jacquelin et al used the two cantilever beams and measured the power when it was impacted by a seismic mass. His work was similar to references 6-8 but the difference was the method of creating dynamic strains in the piezoelectric cantilevers. The existing work of Renaud et al was considered as the base for this work. Mechanical design parameters were considered to optimize the output power. Electrical design parameters were not considered in their work. Two unimorphs were used but did not mention the geometry of sliding impact mass [25]. Janphuang et al also worked on piezoelectric cantilever beam but the dynamic strain was created by the motion of rotating gear. A novel idea was applied to give displacement to cantilever beam. A small mass was attached at the bottom of the free end of the cantilever beam and fixed such a way that that mass was always in touch with the tooth of the gear. The touching of the mass was not obstruct the rotating motion of the gear. The developed power was in micro watts. FEM analysis was done. The mode of applying load is not d_{33} mode but it was d_{31}[26]. Ferrari et al used bimorph cantilever beam was used. Steel was used as the substrut material. Vibration source was exciter and optimum power was gained at the frequency of 20Hz. There was no impact mass in experimentation [27]. Ki et al used the number of sticks to give impact load on the piezoelectric materials. These sticks were operated by an electric motor. There was no vibration source such as exciter. Impact load was given on the array of static piezoelectric modules. The output voltage was observed at the various phase differences with and without rectifiers. Their work was mainly focused on electrical aspects but not mechanical design aspects [28].

The research work going on in the field of piezoelectricity in India is significant. Balpande presented modelling and comparative evaluation of RF and PZT micro-power harvester for wireless sensors network He presented the design considerations and practical comparison of RF and in house power harvesting system. The results demonstrated the best choice for power harvesting depending upon the situation [47].

S. Zhao worked on the piezoelectric stacks to get maximum power. This work was similar to the reference of 38. Cantilever beam model was not used but the geometry of stack was in millimeter size. The maximum power was developed in microwatts. At various pressures and resistances, power density was calculated. Main drawback was power was very low [54]. So far the researchers worked on lead piezoelectric materials and demonstrated the method of generating power but Anshul et al presented a work on cantilever beam made up of lead free

piezoelectric material; mainly focused on the finite element analysis of cantilever beam energy harvester. The novelty of the work was only material i.e lead free piezoelectric material. In finite element analysis the formulation remains the same for the both the lead piezoelectric materials and lead free piezoelectric materials and proved that lead free piezoelectric materials generated maximum power in relation to lead piezoelectric materials [55]. In before sub headings studied the energy harvesting by using vibrations of the piezoelectric cantilever beams and generated the power in micro level of 100 to 500 « W. Hu et al studied the Eigen analysis on piezoelectric disc type actuators by keeping mass at the center of the discs and also studied the frequency behaviour of discs without mass. This work was not related to energy harvesting rather to vibration analysis. This work can be considered as the prerequisite for energy harvesting [59]. Many researchers worked on to generate maximum power either by using piezoelectric cantilevers by initiating dynamic strain through exciter, manually and electromagnetic forces. Nan et al proposed the novel idea in establishing the dynamic strain in the piezoelectric cantilevers during riding in vehicles, the mechanism was made such that cantilever beam was moved by lever and was given impact at the free end of the piezoelectric cantilever. At various speeds of the vehicle impact load was generated [60].

2.6. Research gaps and the scope for study

- In recent past, though piezoelectric elements are tested to generate voltage under vibrations (bags, shoes, floors etc.), the potentiality of these experimentations is not upto the level of fabricating the working devices.
- It is observed from the piezoelectric constitutive equations that the effect of piezoelectric coupling coefficients provides low voltage , there the evaluation of the effect of piezoelectric coefficients is required to achieve more power.
- The piezoelectric reliability studies of those elements to suit as energy harvesting devices under different loadings and different environments are not studied in the literature.
- Energy harvesting circuits were developed on clamped free beams for storing the energy which comes as an output, however ,enhancement of power output for charging high voltage devices is not yet done and the also the effect of temperature on the devices of energy harvester is also awaiting for research.

A piezoelectric energy harvester is proposed in this report. The innovation here is to take advantage of impact made by hitting masses on PZT elements and it causes to produce voltage. The generated voltage can be used for operating the portable electronic devices.

Chapter 3

Characterization of Piezoelectric Disc Type Actuators

In the recent years, many scientists and researchers are using PZT transducers for vibration based energy harvesting. While experimenting the energy harvesters especially impact loaded type, the knowledge of electromechanical characteristics of PZT disc types actuators are quintessential. Experimentation for effective energy harvesting conducted within the limiting conditions will lead to development of consistent devices, therefore, in this chapter described the importance of electromechanical characterization of piezoelectric disc type actuators by testing them under compressive strength test rig, fatigue test rig, hardness test rig and electrochemical impedance analyzer.

3.1 Importance of electromechanical characterization

i) For yielding the maximum voltage of energy harvester.

ii) For protecting the energy harvester from the applied mechanical and electrical loads.

iii) For protecting the energy harvester from creep and fatigue failures.

iv) For increasing the life of the energy harvester.

3.1.1 Compression strength of PZT transducer

Compressive strength of piezoelectric disc type actuator is found out for anticipating the applied loading conditions. In order to design the energy harvester (EH) by using PZT disc type actuators, according to the norms of product design one must know the properties of PZT discs. PZT discs are manufactured by APC International limited, PZT material density(ρ) is 7.6 g/cm^3 , Piezoelectric voltage constant(g_{33}) is 24.8 x10^{-3} m^2/C, relative dielectric constant (K^T) is 3300, modulus of elasticity (Y_3) is 6.3x10^{10} N/m^2 , curie temperature(t) is 320^{0}C and Piezoelectric charge constant(d_{33}) is 630x10^{-12} m/V. Even though the manufacturers of PZT have provided the values of above properties but not the values compressive strength, hardness and impedance of PZT which are required data for the design of energy harvester. Therefore the compressive test hardness test and impedance tests are conducted to design the energy harvester. The schematic

representation piezoelectric disc type actuator is shown in Fig 3.1. In this dissertation, unimorph piezoelectric disc type actuator is used. The PZT disc is made of two materials. One is brass disc (35 mm diameter) and the PZT material (28 mm diameter) is coated on the brass disc. The total thickness of the disc is 0.2 mm.

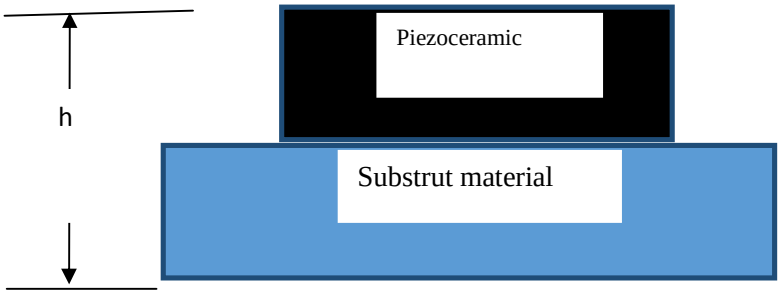

Fig.3.1. Schematic representation of piezoelectric circular disc

Table 3.1: Electro-mechanical properties of piezoelectric material

S.NO	Property	Notation	Value
1	Density in kg/m^3	°	7600
2	Piezoelectric Voltage Constant (10^{-3} V m/N or 10^{-3} m^2/C)	g_{33}	24.8
3	Relative Dielectric constant	K^T	1900
4	Young's modulus in Pa	E	$6.3x10^{10}$
5	Piezoelectric Charge Constant(10^{-12}C/N or10^{-12}m/V)	d_{33}	630

In this dissertation the piezoelectric disc type actuator is subjected to compressive load, for that the stress strain behaviour of the piezoelectric disc is much needed, therefore , the PZT disc is tested under electromechanical universal testing machine (model WDW-S20) which is shown in

Fig.3.2. It consists of movable jaw, fixed jaw and data acquisition system. Movable jaw is used to apply the load on the component and the data acquisition system is used for measuring the load under different deflections, failure load under the function of time and failure load under the deflection in transverse directions. The maximum load of 20 kN can be applied by this machine with load accuracy of less than or equal to 0.5 % and deformation accuracy of less than or equal to 0.5% of the real value. The diameter of piezoelectric disc type actuator is 35 mm, there is no vice for holding for fixing the testing component, and therefore, a customized support is made to support the component. A method of gradually applied loading is followed in order to measure the ultimate compressive strength of the piezoelectric disc type actuator. The observed maximum compressive strength of PZT disc type actuator is 13.4 kN. Fig 3.3 shows the stress strain curve of piezoelectric disc type actuator. In this figure stresses are intrigued on the Y-axis and corresponding strains are intrigued along X- axis. As mentioned in Fig 3.1, piezoelectric disc type actuator consists of two layers, top layer (ceramic) is having the property of brittle nature and the bottom layer (brass) is having the property of ductile nature, therefore, this stress strain curve is the combination of brittle and ductile curves. The curve from **o** to **b** is for ceramic material and from **b** to **g** is for brass material.

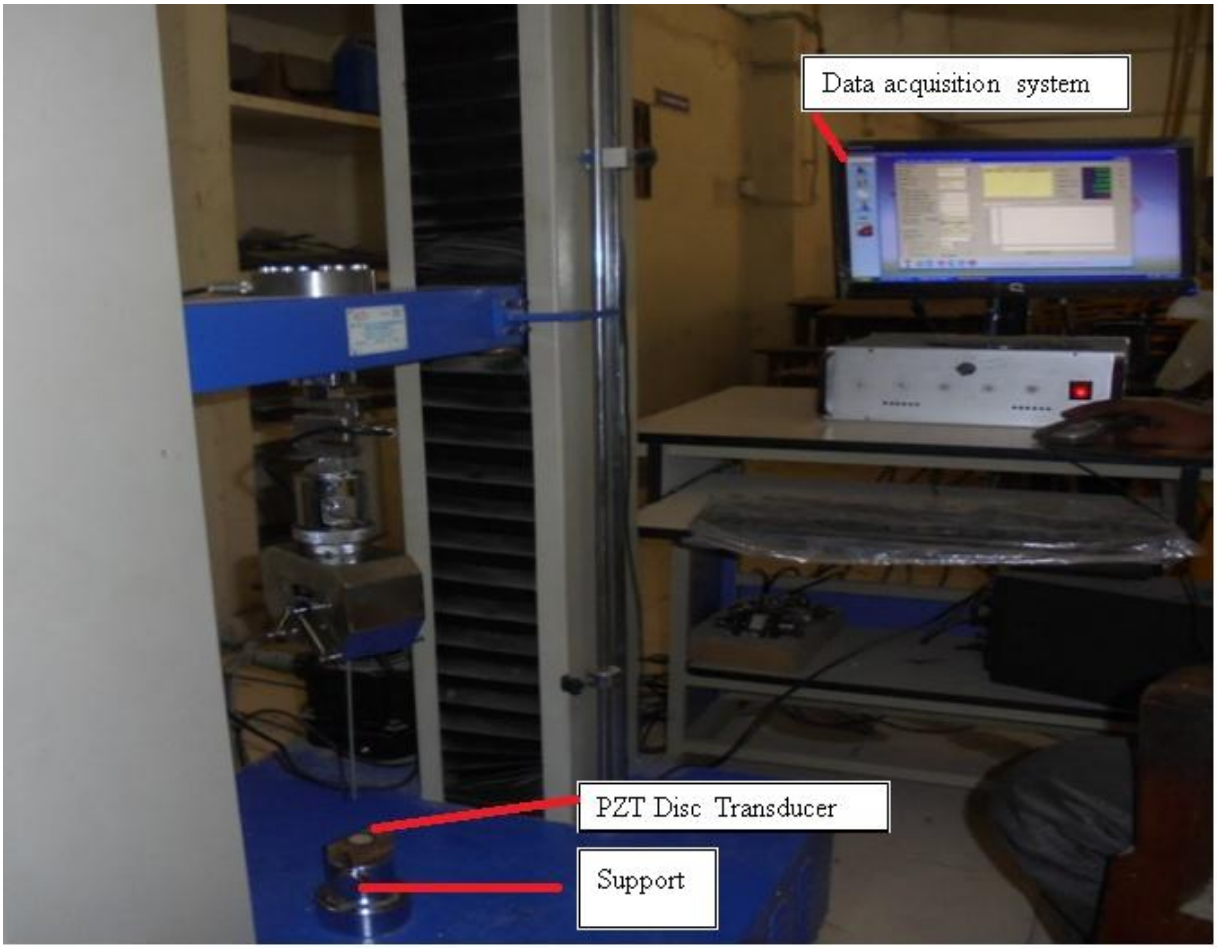

Fig.3.2. Electro-mechanical universal testing machine with PZT disc transducer

Different mark points can be seen on the stress strain diagram. When the piezoelectric disc type actuator is experimented under compressive test rig, it goes through different stages before reaching rupture stage. There is no yielding point for the ceramic materials due to its brittle nature. The stress strain curve of piezoceramic is from **o** to **b**. The stress train curve for substrut (brass) material is from **b** to **g** is shown in Fig 3.3 which includes proportionality state, yielding state, ultimate stress state and breaking state. The strength at the proportional state of the substrut material is 2400 N/mm^2. The strength at the yielding state of the substrut material is 2300 N/mm^2. The strength at the ultimate stress state of the substrut material is 4300 N/mm^2. The strength at the breaking stress state of the substrut material is less than 4300 N/mm^2. During the experimentation of the pzt disc type actuator, the PZT is followed initially by linear trend line,

non-linear trend and again linearity. This might be the cause of brittle and ductile natures of both main and substrut materials.

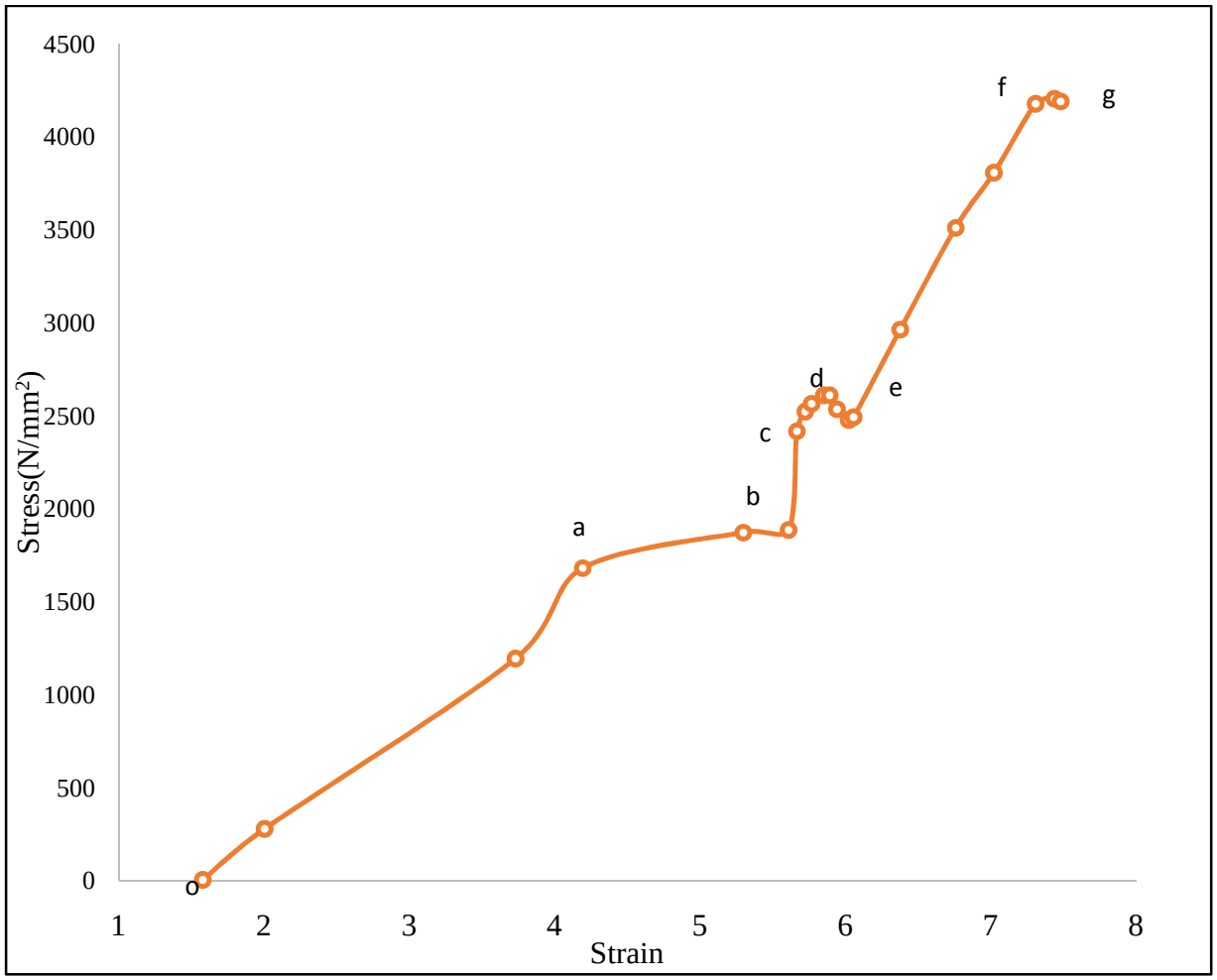

Fig.3.3. Stress-Strain curve of PZT disc

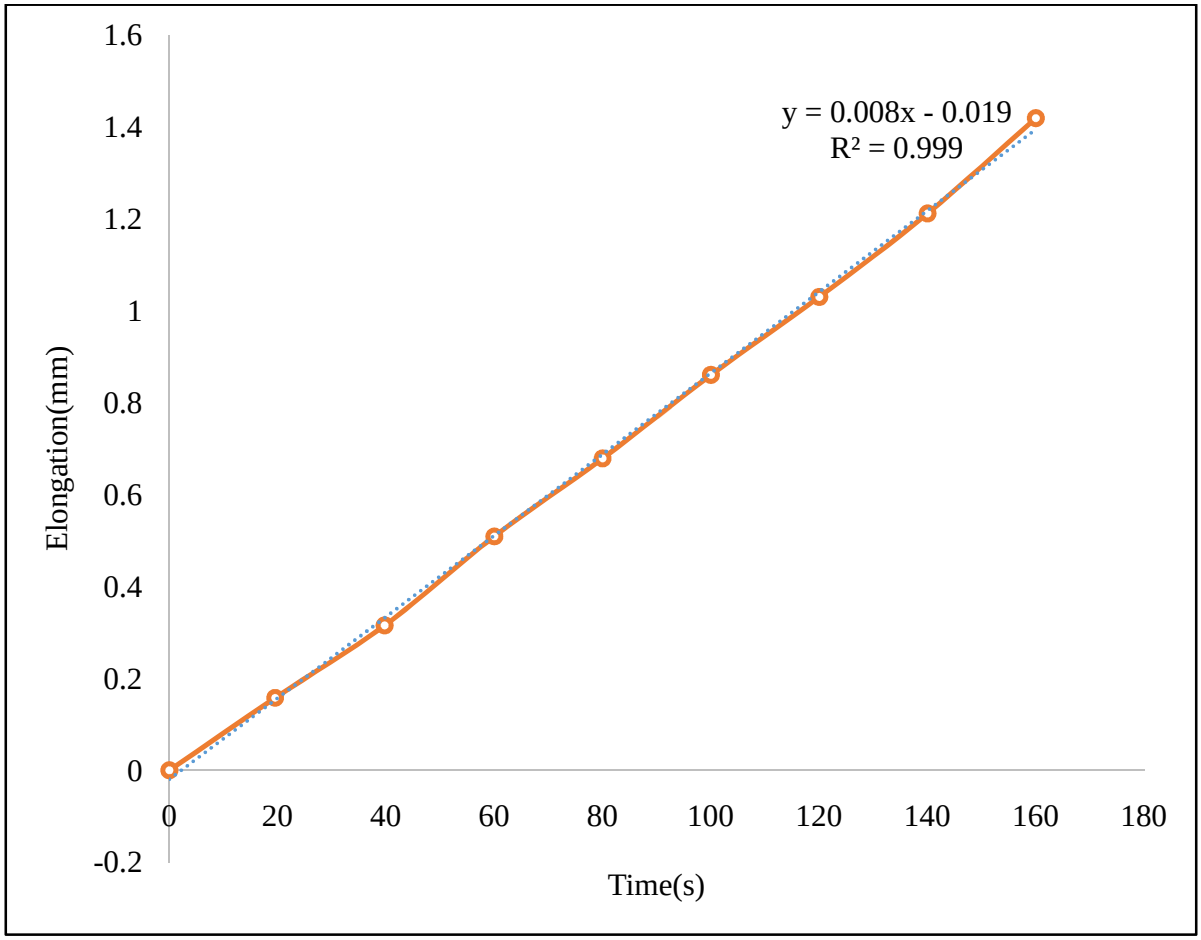

Fig.3.4. Deformation of PZT disc under the Time consideration

During the experimentation of energy harvester under excitation, maximum elongation of piezoelectric disc under different loads with the function of time is required. Therefore, deformation of piezoelectric disc with the time consideration is studied and is shown in Fig 3.4. Elongation is taken on the vertical axis and Time on X-axis. A linear behavior is observed between the elongation and time. The observed maximum deflection may be 1.4 mm at the time of 160 sec. The equation of trend line is y= 0.0088x – 0.0194. A non-inverse relationship can be observed between two variables.

3.2 Fatigue strength of PZT material

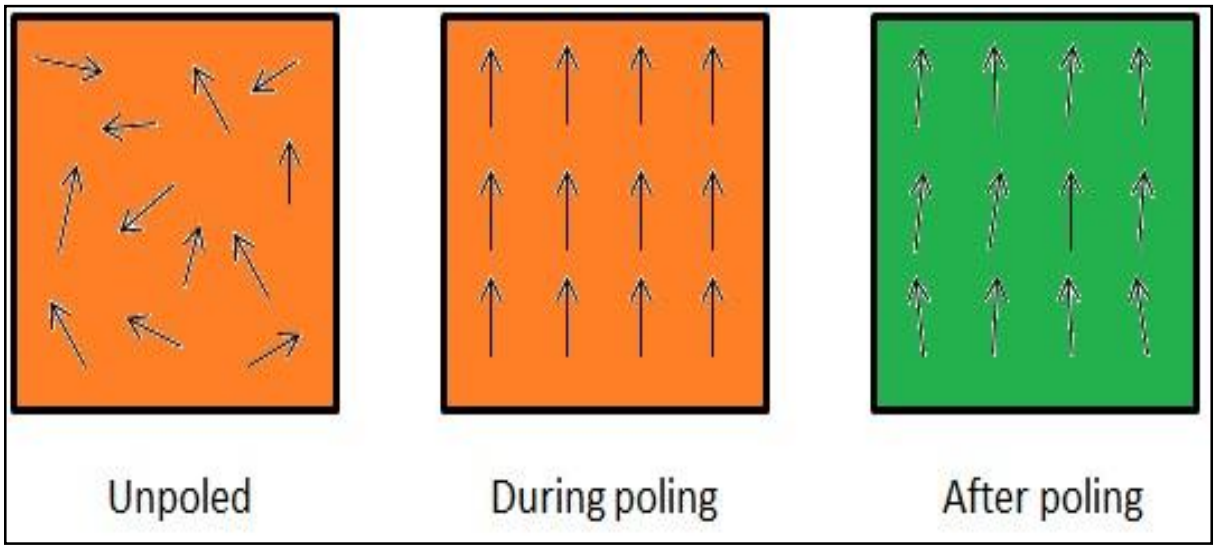

Fig.3.5Principle of Poling of PZT disc

The knowledge of the direction of polarization is essential to apply the loads on the PZT disc before going to use them for the better results otherwise results. The process of poling is shown in Fig.3.5.

3.2.1Experimental setup of Fatigue test

The schematic presentation of three point bending test machine is shown in Fig 3.6. It consists of top bracket, moving crosshead, machine base and the data acquisition system. Piezoelectric disc is located on the customized support. Cyclic bending load is applied on the PZT disc. Any etching technique is not conducted for studying the domain structure of PZT material. A fatigue test is conducted to know how much force the lead ball should execute on the unimorph PZT disc such a way that the dynamic strain can be occurred in the PZT thus energy transduction can be taken place.

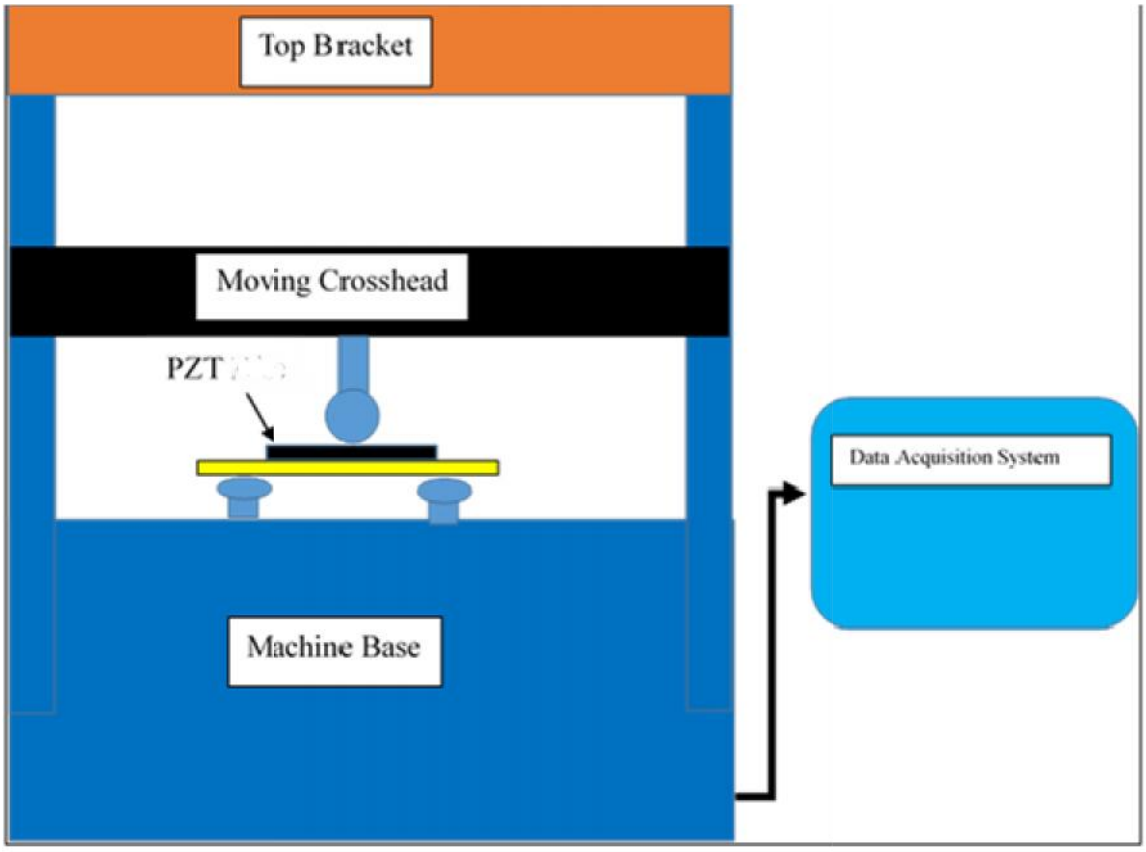

Fig.3.6Three point bending test with PZT on the support

The specimen for fatigue test is made by ASTM standards i.e, 40 mm x 3mm x 3mm. The numbers of samples used are 25. The bending fatigue test is also conducted at the frequency of 0.03 Hz and r_a = 0.02. The maximum cyclic load, *f*max, is determined on the basis of the bending strength (f_b), where f_{max} is designed to be less than 90% of f_b. The bending stress is calculated using the simple formula $f = 3M/2rt^2$, where M is the bending moment, and r and t are the PZT radius and thickness. The cyclic loading is applied along the direction of the normal to the surface of the PZT disc as shown in Fig 3.6. In the past some researchers had done experimentation of using the etching techniques with electron back scatter diffraction for seeing the domain structures of Piezoceramics and also used a scanning electron microscope for their studies. Nowadays piezo ceramics are readily available in the market therefore no need to go for studying the domain structure unless we require for optimization of properties by adding different dopents. The strength of PZT disc is 130 MPa at the strain of 0.004 mm/mm. It is observed that under three point bending test the life of the PZT disc is 10^7 cycles at a stress of

38 MPa and is shown in Fig 3.7. If the host structure is operated at 25 Hz per hour per day then the life of machine 18.26 years. A regression analysis is carried out for S-N curve of piezoelectric disc. An inverse relationship can be observed between the stress and the life cycles. The S-N curve is followed by linear model equation with a negative slope of 13.203 and an initial maximum stress of 143.67 MPa at zero load is y= -13.203 x+143.67. Coefficient correlation is 0.9643. The maximum stress can be observed at zero loading is 143.67MPa.

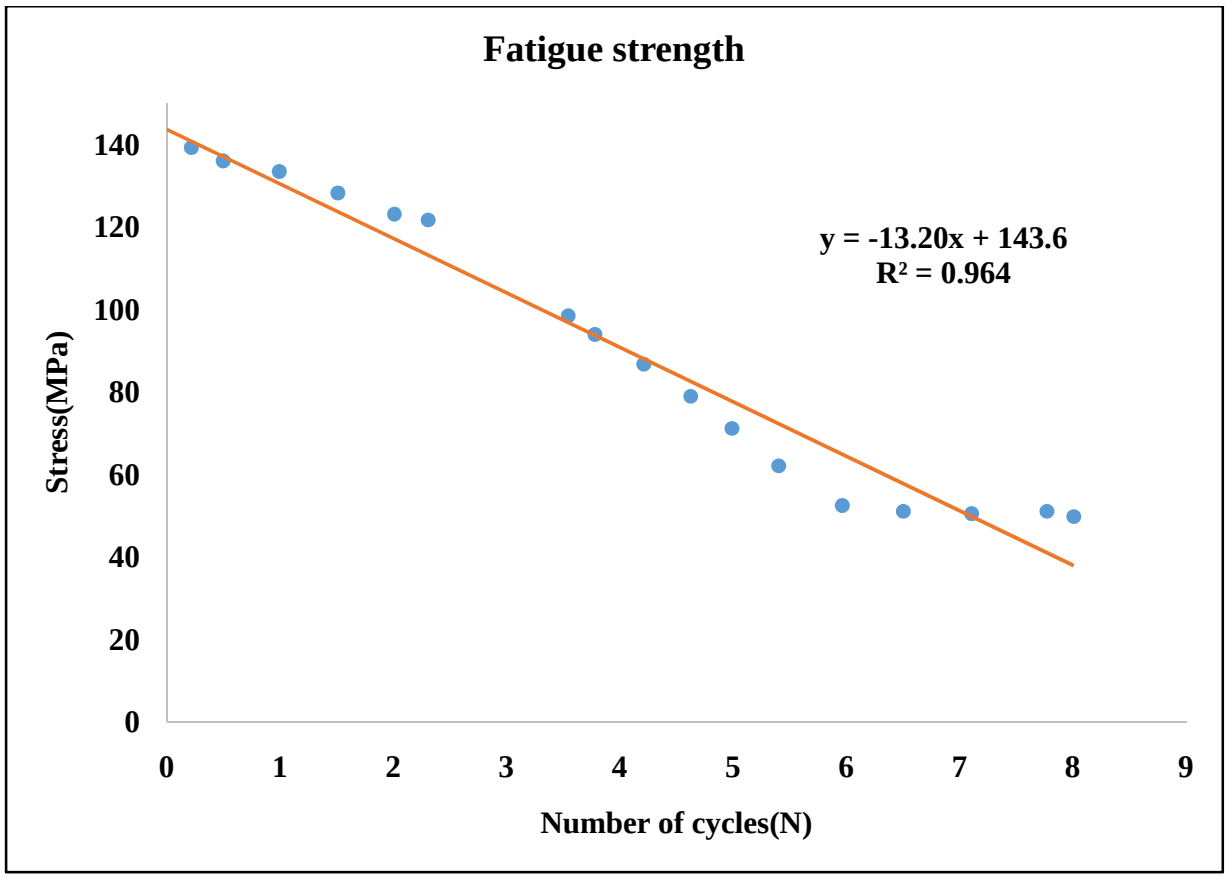

Fig 3.7 S-N curve for PZT disc

3.3 Contact stress analysis of PZT disc type actuator

Contact stress analysis is defined as the study of the analysis of stresses when the two bodies are in contact periodically. Certain assumptions are considered for doing the contact stress analysis which are mentioned below:

- The size of the contact area is small compared with the size of the curved bodies.

- Both contacting surfaces are smooth and frictionless.

- The gap, h between the un-deformed surfaces may be approximated by an expression of the form $h=Ax^2 +By$ (e.g. the contact between spheres, cylinders, and ellipsoids).

- The deformation is elastic and can be calculated by treating each body as an elastic half space2.

$$P_{max} = \frac{3\,W}{2\,®\,a\,b}$$

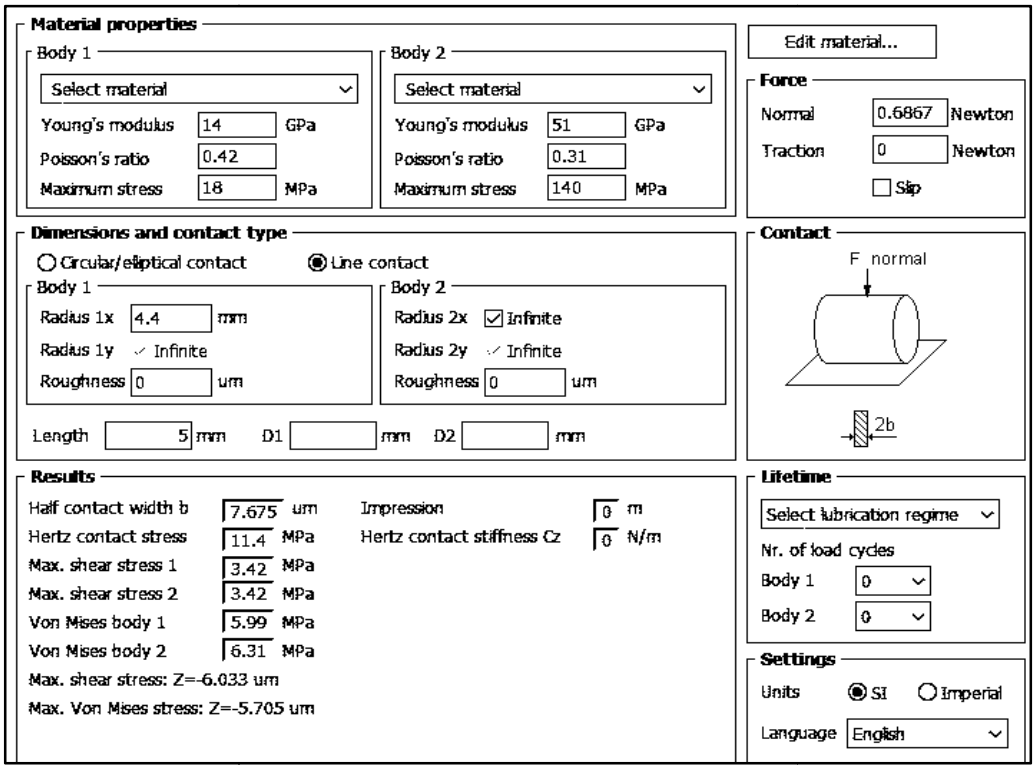

Fig 3.8 Parameters for contact stress analysis of PZT disc type actuator

Fig 3.8 describes the input parameters and output parameters during the contact of lead cylinder to piezoelectric disc type actuator. The lead cylinder is considered as body1 and the piezoelectric disc is considered as body2. The poison's ratio, modulus of elasticity and maximums stress of body1 are 0.42, 14 GPa and 18MPa. Whereas for body2 are 0.31, 51GPa and 140Mpa. The radius of lead cylinder is 4.4 mm and the applied normal force 0.6867N. The observed Hertz contact stress is 11.4MPa. These values are shown through the graph of normal deflection in Z-direction and the Hertz contact stress in Fig 3.9. The normal stress is plotted on X- axis and the

deflection in micrometer is plotted in negative Y- axis. The behaviour of contact stress in relation to applied load and deflection is non-linear.

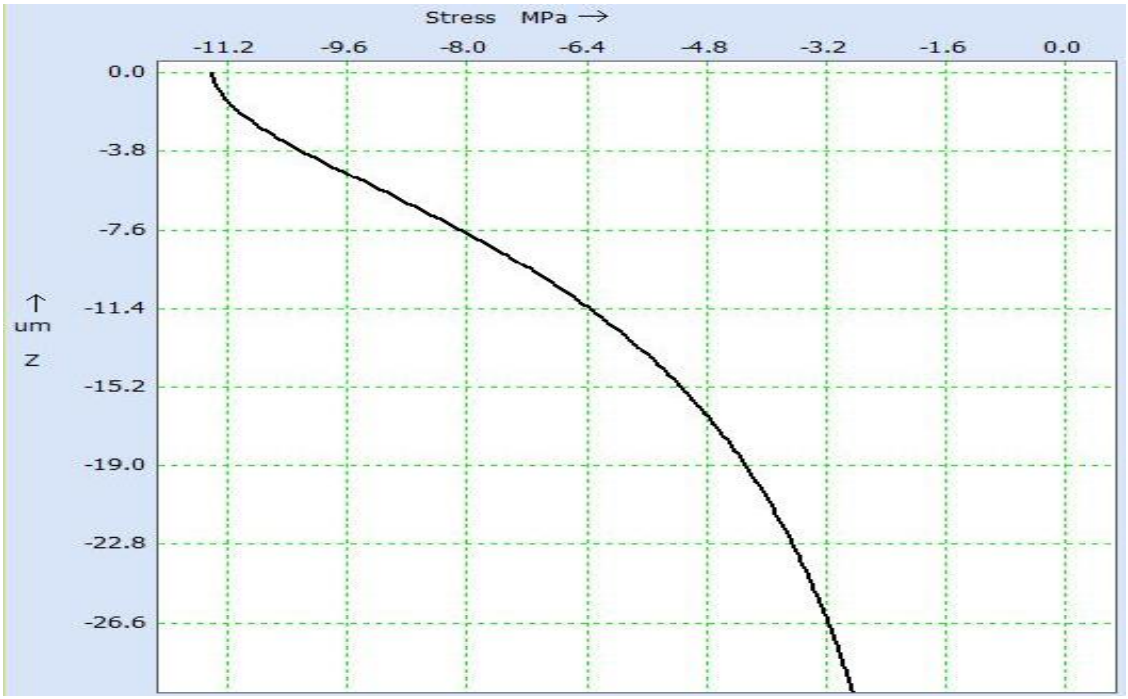

Fig 3.9 Hertz contact stress in z direction of PZT disc type actuator

3.4 Surface morphology studies of PZT disc type actuator

For effective voltage generation during the applied impact load on the piezoelectric disc type actuator, the piezoelectric disc should be crack free and damage free, therefore, surface morphology of piezoelectric disc type actuator is studied. These studies are done by scanning electron microscope. Figure 3.10 represents the base morphology of the surface of PZT disc.

Fig 3.11 and Fig 3.12 shows the morphology of the cross sections of PZT discs without crack and with crack. For obtaining the maximum voltage from piezoelectric disc type actuators cracked free ones are better.

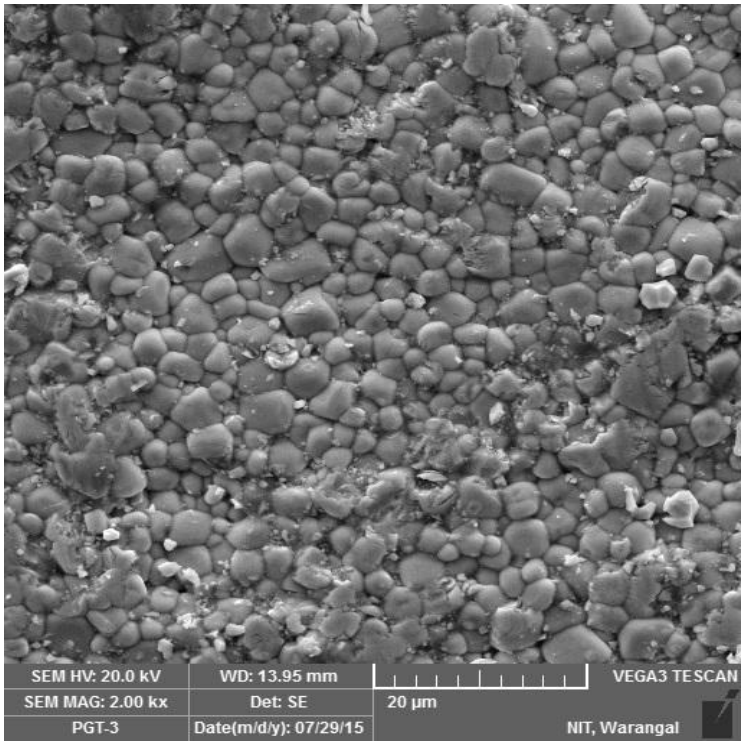

Fig 3.10 SEM image of PZT-5H

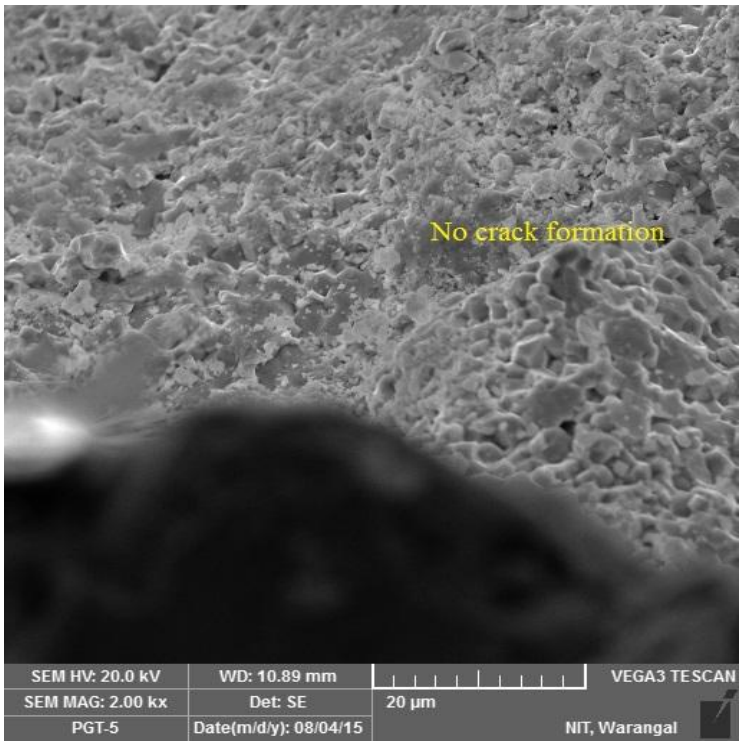

Fig 3.11 SEM image of PZT-5H cross section without crack

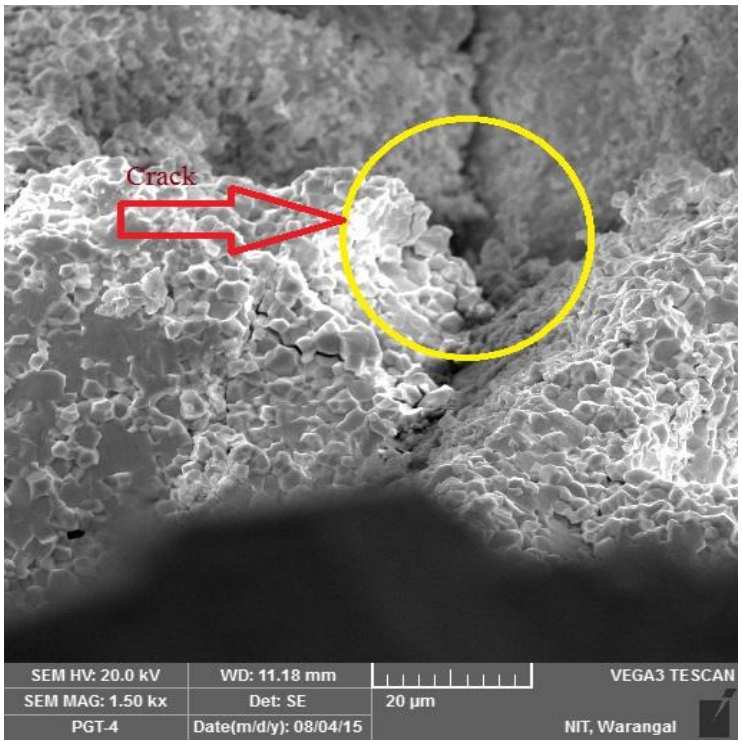

Fig 3.12 SEM image of PZT-5H cross section with crack

3.5 Impedance of PZT-5H disc type actuator

An AC voltage is an output of vibration based energy harvester. In order to calculate electric power the impedance property is very much needed. And also studying the influence of frequency on impedance of the piezoelectric disc type actuator needed to observe the performance of piezoelectric energy harvester, therefore, electrochemical impedance analyzer is used for measuring the impedance of PZT disc type actuator under various frequencies. Though electrochemical impedance analyzer can be used for characterizing and enhancing the performance of fuel cells but also it can be used for measuring the impedance of piezoelectric disc type actuators under different frequencies.

The experimental setup of electrochemical spectroscopy with the testing of PZT-5H disc type actuator is shown in Fig 3.13. It consists of frequency response analyzer, main leads, voltage sense leads, PZT-5H disc type actuator fitted between leads and the data acquisition system. The voltage is supplied at various frequencies and observed the impedance values at those frequencies. The impedance values are shown under various frequencies is shown in Fig.3.14. From Fig 3.14, it can be observed that at lower frequencies the impedance of PZT-disc is maximum i.e., at 100 mHz the impedance may be 30 kΩ and at the frequency of 100 kHz, the impedance value may be 30 Ω, therefore the PZT disc type actuator patch may be operated at higher frequencies for better results.

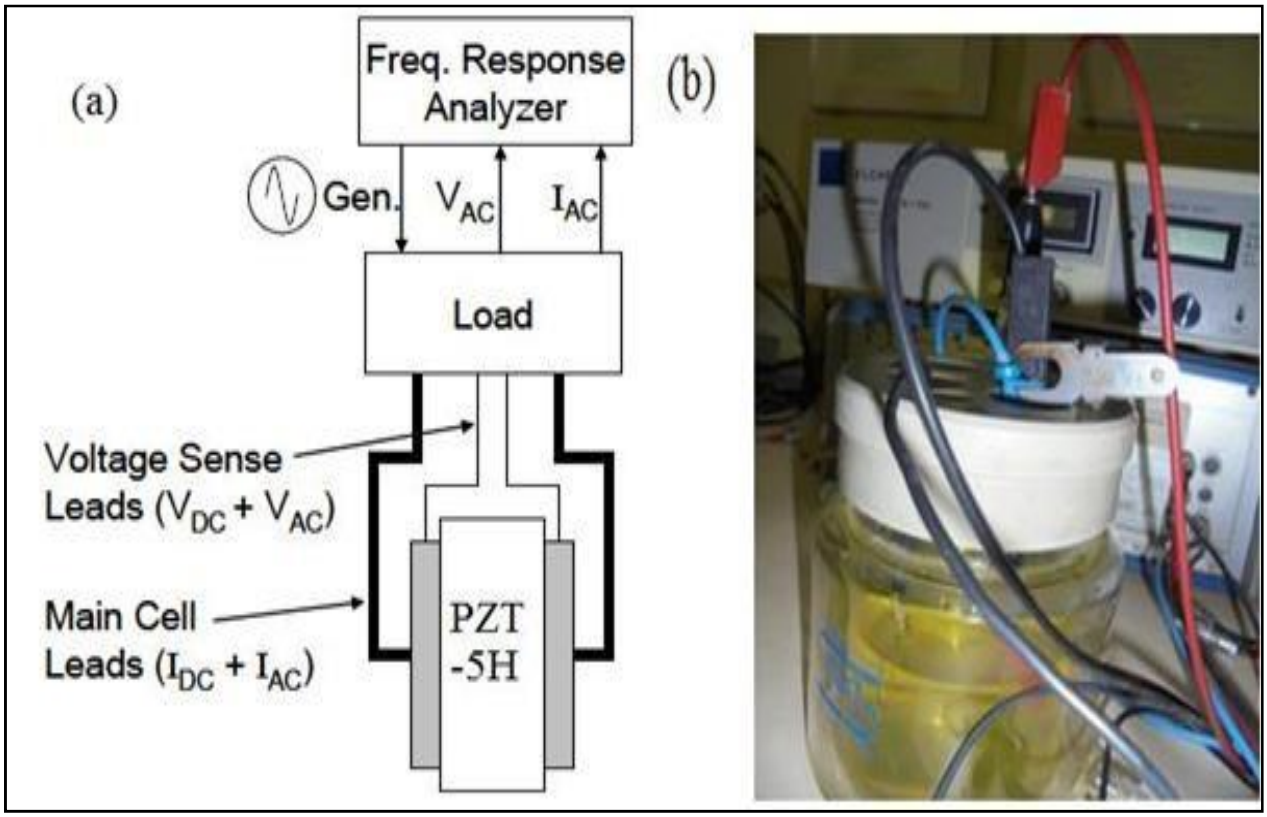

Fig 3.13 Testing of PZT disc (a) Schematic representation (b) Electrochemical impedance spectroscopy with PZT disc type actuator

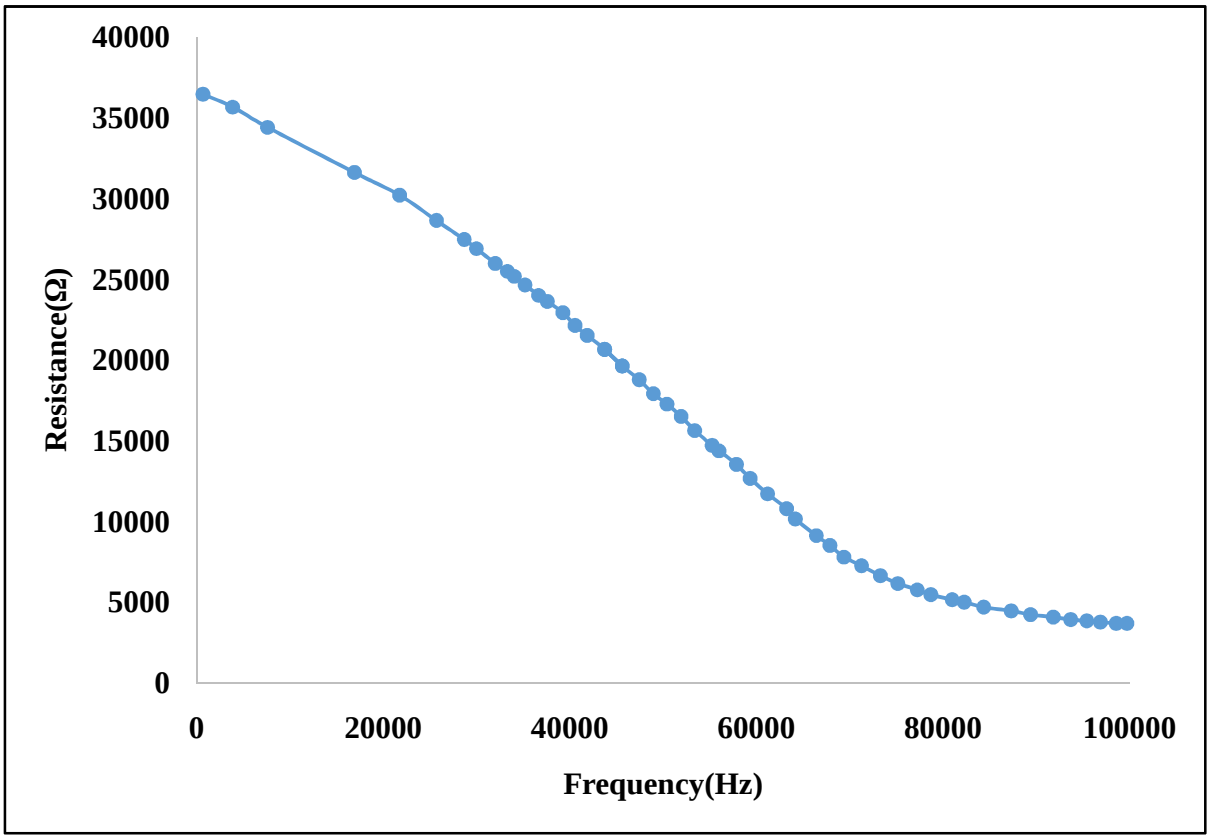

Fig 3.14 Impedance graph of PZT disc at various frequencies

3.6 Summary of the chapter

In this chapter mechanical and electrical properties of piezoelectric disc type actuator have been studied. The mechanical properties such as compressive strength, hardness, fatigue strength and surface morphology and electrical property such as electrical impedance at different frequencies and at different phase angles are studied. The compressive strength of PZT-5H disc is 4267.516 N/mm^2 and the BHN is 78 for PZT material. Thus, these properties are useful for operating the piezoelectric disc type actuator without causing damage. If the contact stress is beyond 11.4 MPa, crack formation takes place which is shown in Fig.3.12 and if the contact stress below 11.4 MPa, there is no crack formation which is shown in Fig.3.11. In Fig.3.14, at low frequencies contact stress is high because of the amplitude with which coming for contacting with body two is high. This chapter helps the designer to know the operating limiting loads for optimizing the output voltage and the energy harvesting device.

Chapter 4

Simulation Studies of Energy Harvester

This chapter describes the fabrication procedure of the uni-axial impact loaded energy harvester. Mathematical modelling has been done. Electric voltage is generated from the energy harvester by conducting the experiments on Syscon exciter at different frequencies. Simulation results are validated by experimental values. The Frequency responses, load dependence and acceleration dependences of the energy harvester are studied in COMSOL 5.0.

4.1 Mathematical modeling of energy harvester

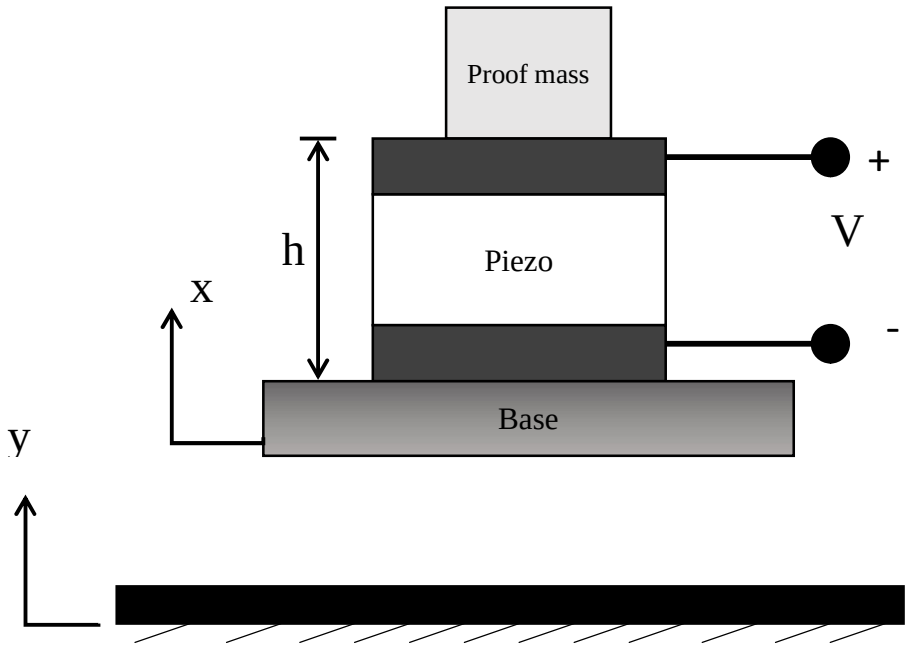

Fig. 4.1 Schematic diagram of energy harvester

A coupled electromechanical one dimensional model is proposed that informs the response of piezoelectric disc type vibration energy harvester. The schematic diagram is illustrated in Fig.4.1 and consists of piezoelectric disc excited by a base input 'y'. The thickness of piezoelectric disc type actuator is 'h', and is having a mass m_p and is connected to a full wave rectifying circuit for converting AC to DC. A proof mass, M, is considered. In this Figure the circuit is considered as

open circuit without bridge rectifier. Using the one dimensional configuration, the linear piezoelectric constitutive equations 4.1 to 4.2 are as followed.

$$[S] = [s][\pm] + [g][D] \quad (4.1)$$

$$[E] = [-g][\pm] + [\pounds]^{-1}[D] \quad (4.2)$$

m_{eff} = Effective mass = 0.305 kg

ξ = Damping factor =0.05

d_{33} = Piezoelectric coefficient = 630 x 10^{-12}

ω_n = Natural frequency of the harvester = 196,750 rad/s

$r = R_{eq}\, c_p\, \omega_n$

R_{eq} = 5 x 10^9 ohm

c_p = 0.457 x 10^{-9} farads

Ω = ratio of ω and ω_n

ω = Operated frequency

k_e = Coupling factor = 1.287

h=0.2 mm

The source of value of R_{eq} and k_e is collected [48]. ± , E, D and S are defined as the normal stress, Electric field, Electric displacement and normal strain, respectively. From a dynamic equilibrium analysis, the equations (4.3) to (4.4) can be found in terms of the energy harvesting device parameters defined in Fig.4.1 [48]:

$$\ddot{x} + 2\P\mu_n \dot{x} + \mu_n{}^2 x - \mu_n{}^2 d_{33} v = -\ddot{y} \quad (4.3)$$

$$R_{eq} c_p \dot{v} + v + m_{eff} R_{eq} d_{33} \mu_n{}^2 \dot{x} = 0 \quad (4.4)$$

$m_{eff} = M + \frac{m_p}{3}$ is the effective mass, x is the displacement, $\dot{x}$ is the time derivative x , $\ddot{x}$ is time derivative of $\dot{x}$. Using Laplace transforms, the equations of displacement, output voltage and power are evaluated. These equations (4.6) to (4.8) are normalized by the base input acceleration and modified from Dutoit et al [48]. The dimensionless parameters in the equations (5.6) to (5.8) are $r, k_e and \Omega$.

$$\left|\frac{x}{\ddot{y}}\right| = \frac{1/\mu_n{}^2\sqrt{1+(r\Omega)^2}}{\sqrt{\left[1-(1+2\P r)\Omega^2\right]^2+\left[(1+k_e{}^2)r\Omega+2\P\Omega-r\Omega^3\right]^2}} \quad (4.6)$$

$$\left|\frac{v}{\ddot{y}}\right| = \frac{m_{eff}R_{eq}d_{33}\mu_n\Omega}{\sqrt{\left[1-(1+2\P r)\Omega^2\right]^2+\left[(1+k_e{}^2)r\Omega+2\P\Omega-r\Omega^3\right]^2}} \quad (4.7)$$

$$\left|\frac{p_{out}}{(\ddot{y})^2}\right| = \frac{m_{eff}/\mu_n r k_e{}^2 R_{eq}/R_l\Omega^2}{\sqrt{\left[1-(1+2\P r)\Omega^2\right]^2+\left[(1+k_e{}^2)r\Omega+2\P\Omega-r\Omega^3\right]^2}} \quad (4.8)$$

4.2 Simulation studies of Energy harvester

4.2.1 Introduction to Comsol Multiphysics

In this research work, two modules of Comsol 5.0 such as structural mechanics and piezoelectricity were used for doing the simulation of energy harvester. There are different geometric shapes such as square, rectangle and disc type can be modeled in COMSOL. In this dissertation, based on the requirement, piezoelectric disc type actuator is modeled. A model of unimorph piezoelectric disc type actuator is shown in Fig. 4.2 and consists of piezoelectric material at the top and non-piezoelectric substrate material is in the bottom and is generated based on the defined geometric properties mentioned in Table 4.1.In COMSOL Multiphysics software, Frequency responses under Acceleration dependence and load dependence have been studied for the piezoelectric disc type actuator. In order to measure the voltage generation and electric power this actuator is simulated at various accelerations from 20g to 100g and at various frequencies from 25 Hz to 100 Hz. These results are illustrated in the Fig. 4.3 to 4.12 for 25 Hz frequency. These Figures indicate the responses of Voltage and electric power at various input accelerations.

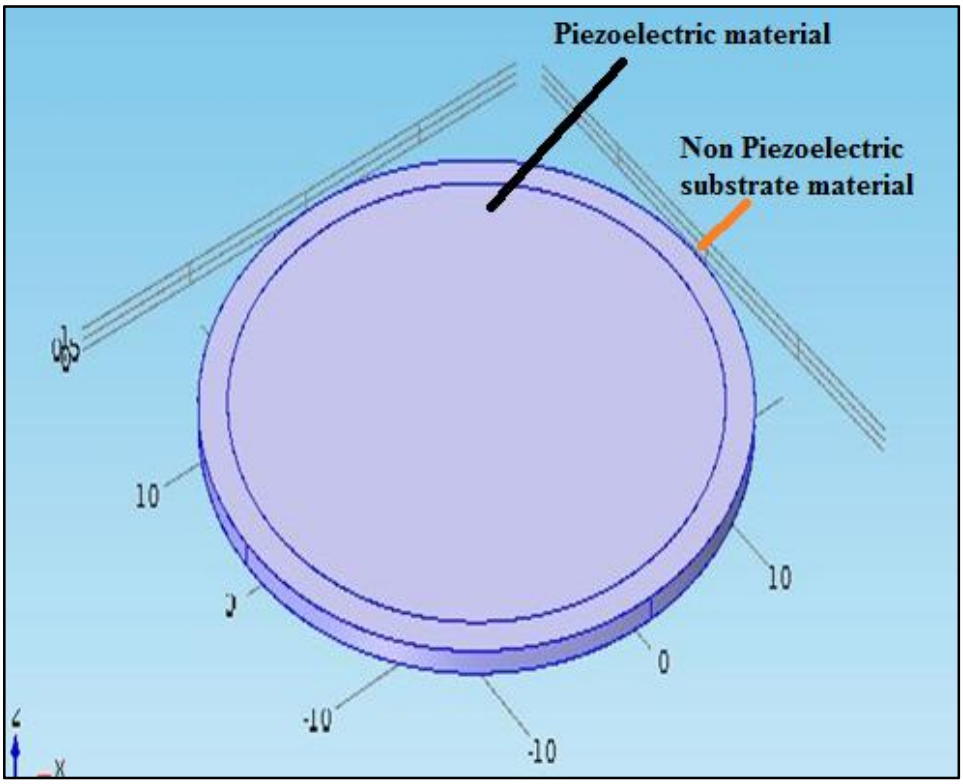

Fig. 4.2 Model of PZT disc type actuator

4.2.2 Acceleration dependence of EH at 25 Hz

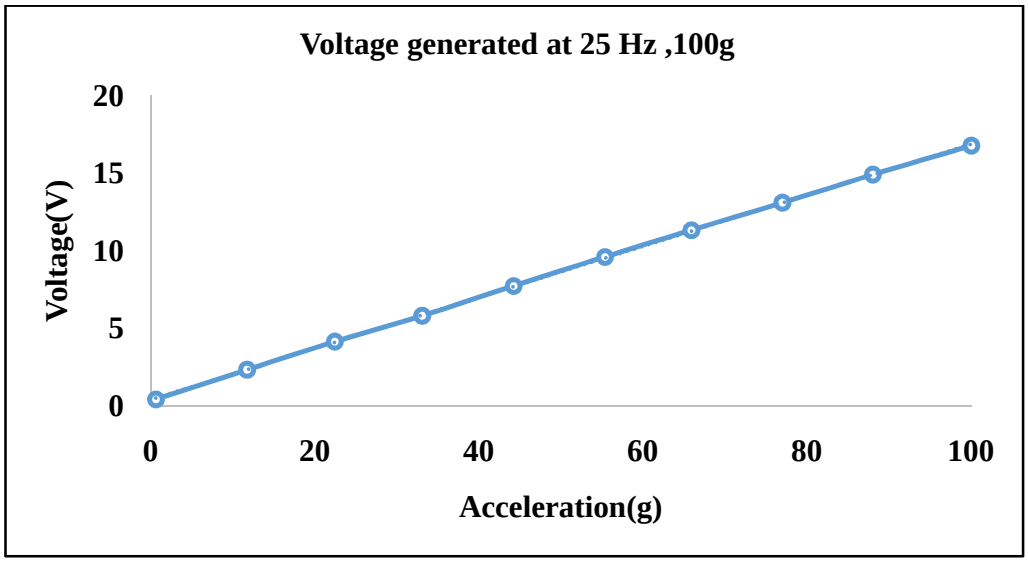

Fig. 4.3 Variation of voltage at 25 Hz with 0 to 100g acceleration

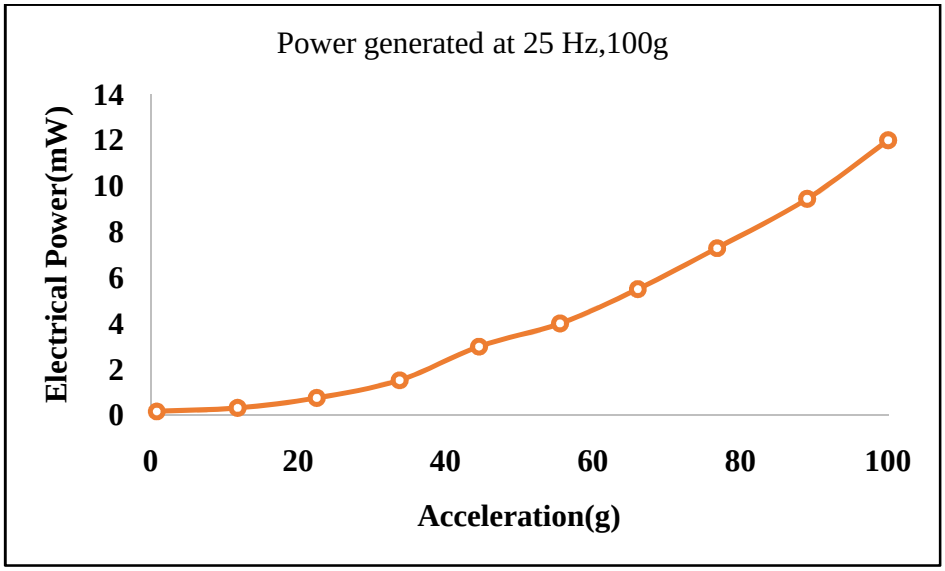

Fig. 4.4 Variation of power at 25 Hz with 0 to 100g acceleration

Fig.4.3 shows the variation of voltage under 0-100g input acceleration at the frequency of 25 Hz. The output voltage is varying linearly with the input Acceleration. The maximum voltage may be 16.77 V at the acceleration of 100g and at 25 Hz. The uncertainty error observed may be 4.36%.The variation of power under 0-100g input acceleration at the frequency of 25 Hz is shown in Fig.4.4. The output power is having quadratic non-linear relation with the input Acceleration. The maximum power may be 12 mW at the acceleration of 100g and 25 Hz. The uncertainty error may be 3.17%. Table 4.1 describes the values of voltage and power at various accelerations such as 20g, 40g, 60g, 80g and 100g.

Table 4.1 Voltage and Power at the frequency of 25 Hz under variable accelerations

Acceleration (g)	Voltage (V)	Power (mW)
20	3.8	0.583
40	7.22	2.04
60	9.9	4
80	14	7.76
100	16.77	12

4.2.3 Acceleration dependence of EH at 35 Hz

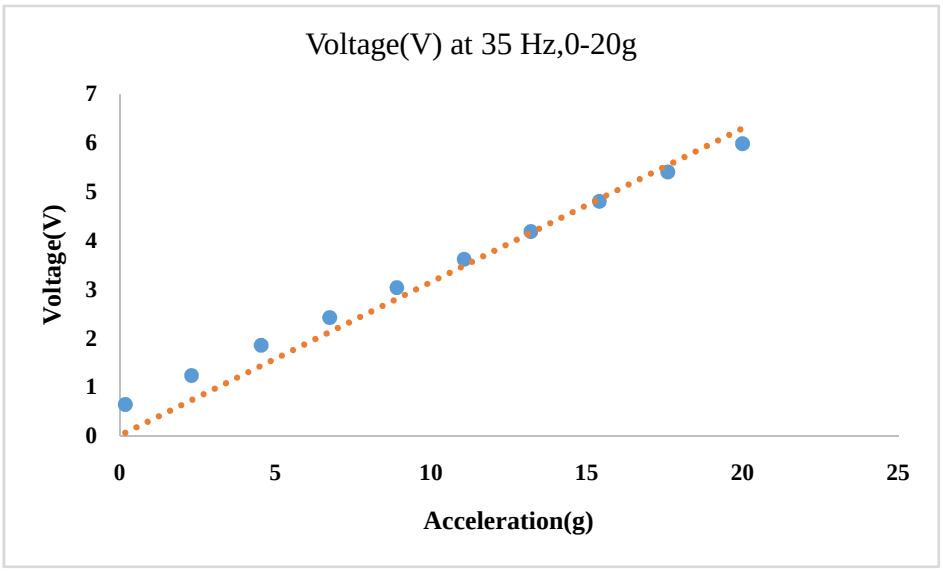

Fig. 4.5 Variation of voltage at 35 Hz with 0 to 20g acceleration

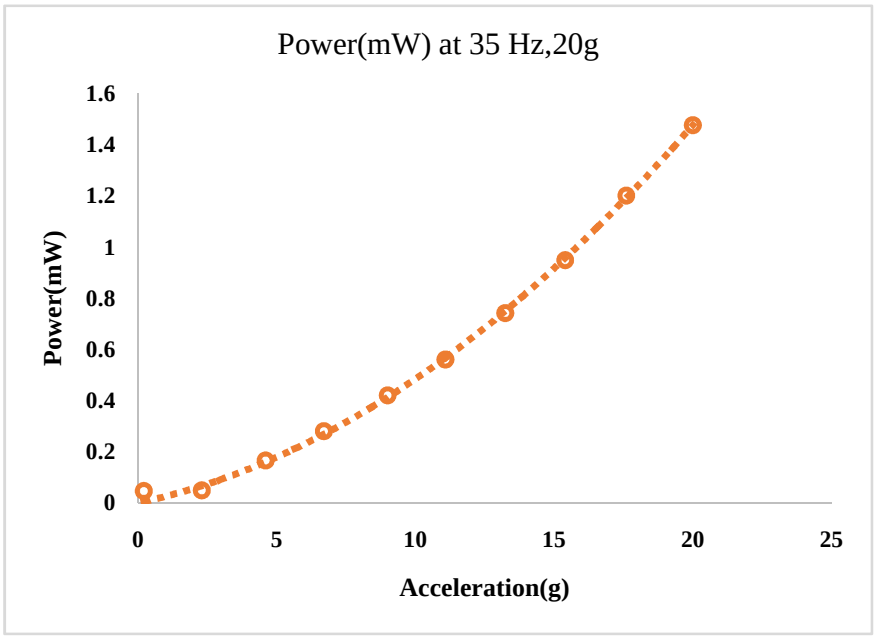

Fig. 4.6 Variation of power at 35 Hz with 0 to 20g acceleration

Fig.4.5 shows the variation of voltage under 0-20g input acceleration at the frequency of 35 Hz. The output voltage is varying linearly with the input Acceleration. The maximum voltage may be 5.98 V at the acceleration of 20g and at 35 Hz. The linear regression analysis is done. The

equation of linear regression is V=0.3144a and the R-squared value 0.9639. By following the regression equation the maximum voltage of 6.288 V is observed. The error observed is 4.89%. It may be uncertainty type of error. At the accelerations of 13g and 17g, the output voltage may be completely linear.

The variation of power under 0-20g input acceleration at the frequency of 35 Hz is shown in Fig.4.6. The output power is having quadratic non-linear relation with the input Acceleration. The maximum power may be 1.477 mW at the acceleration of 20g and 35 Hz. By following the polynomial regression equation i.e P= $0.0025a^2+0.023a$ the maximum voltage of 1.46 mW is observed. The uncertainty error observed is 1.1 %.If the coefficient determination is very closure to 1 (here it is 0.9989), the error can be very low.

4.2.4 Acceleration dependence of EH at 45 Hz

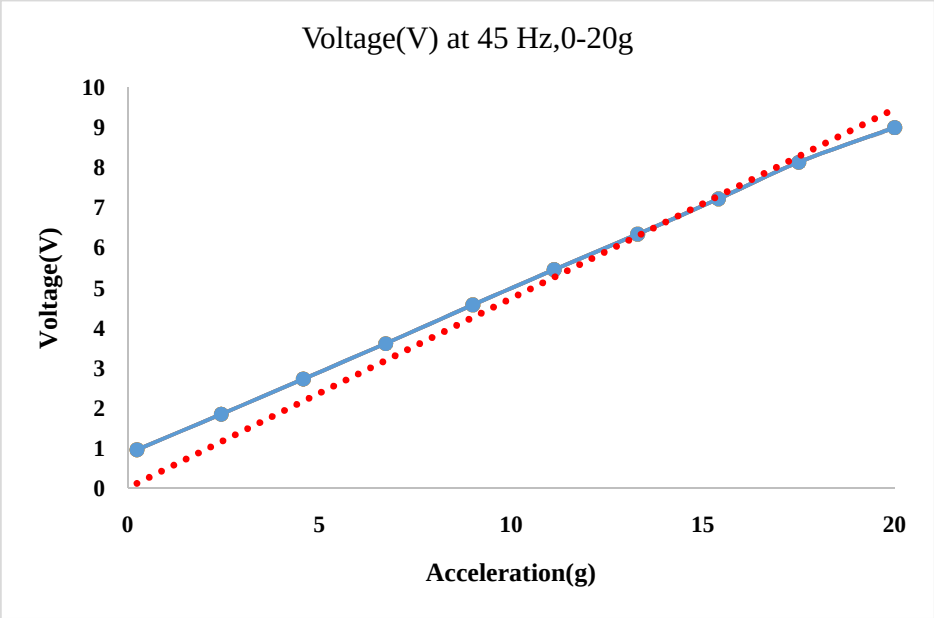

Fig. 4.7 Variation of voltage at 45 Hz under 0 to 20g acceleration

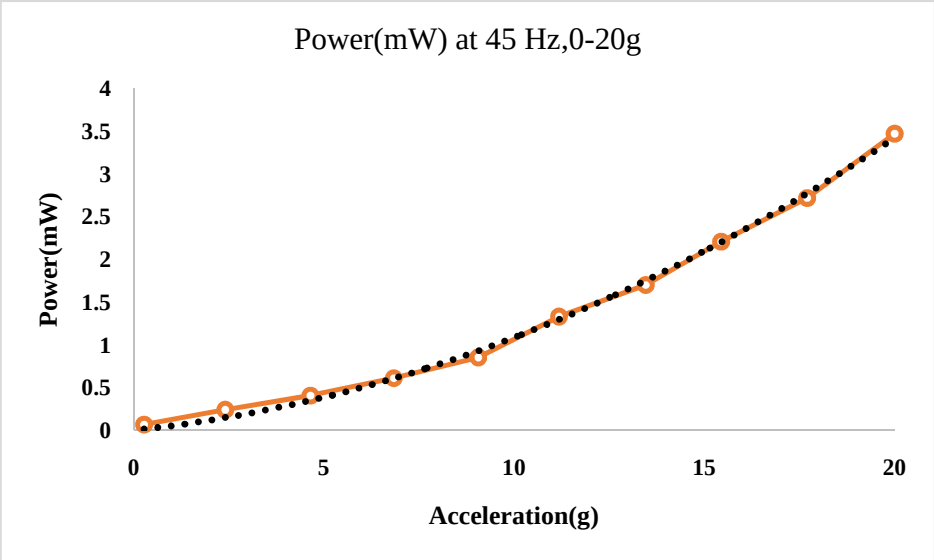

Fig. 4.8 Variation of power at 45 Hz under 0 to 20g acceleration

Fig.4.7 shows the variation of voltage under 0-20g input acceleration at the frequency of 45 Hz. The output voltage is varying linearly with the input Acceleration. The maximum voltage may be 9 Vat the acceleration of 20g and at 45 Hz. The linear regression analysis is done. The equation of linear regression is V=0.4732a and the R-squared value 0.9693. By following the regression equation the maximum voltage of 9.464 V is observed. The error observed is 4.9%. It may be uncertainty type of error. At the accelerations of 14g and 18g, the output voltage may be completely linear.

The variation of power under 0-20g input acceleration at the frequency of 45 Hz is shown in Fig.4.8. The output power is having quadratic non-linear relation with the input Acceleration. The measured maximum power may be 3.47 mW at the acceleration of 20g and 45 Hz. By following the polynomial regression equation i.e. $P= 0.0062a^2+0.0461a$ the maximum power of 3.402 mW is predicted. The uncertainty error observed is 1.9 %.If the coefficient determination is very closure to 1 (here it is 0.9974), the error can be very low.

4.2.5 Acceleration dependence of EH at 55 Hz

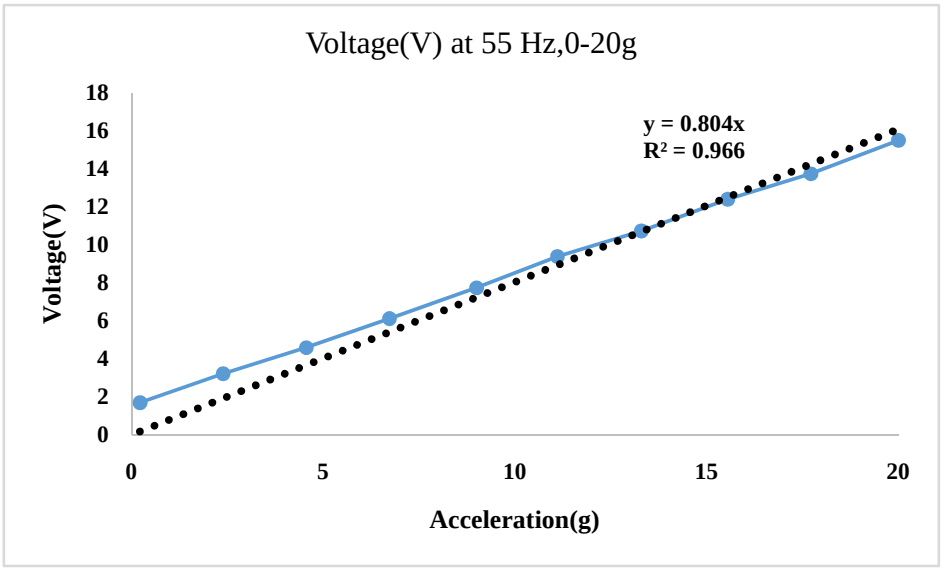

Fig. 4.9 Variation of voltage at 55 Hz with 0 to 20g acceleration

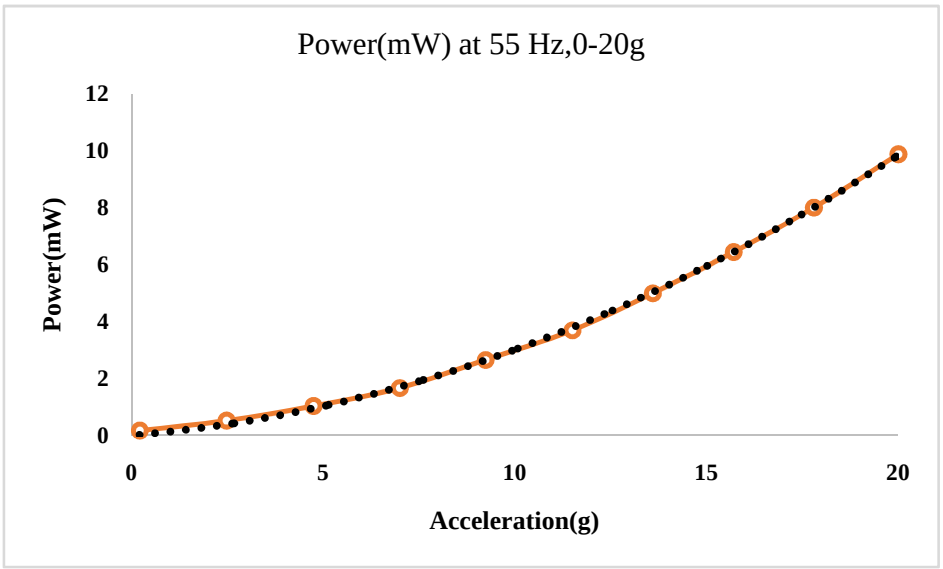

Fig. 4.10 Variation of power at 55 Hz with 0 to 20g acceleration

Fig.4.9 shows the variation of voltage under 0-20g input acceleration at the frequency of 50 Hz. The output voltage is varying linearly with the input Acceleration. The maximum voltage may be 15.5 Vat the acceleration of 20g and at 50 Hz. The linear regression analysis is done. The

equation of linear regression is V=0.8044a and the R-squared value 0.9667. By following the regression equation the maximum voltage of 16.088 V is observed. The error observed is 3.65%. It may not be phenomenon error. At the accelerations of 14g the output voltage may be completely linear. The variation of power under 0-20g input acceleration at the frequency of 50 Hz is shown in Fig.4.10. The output power is having quadratic non-linear relation with the input Acceleration. The maximum power may be 9.87 mW at the acceleration of 20g and 50 Hz. By following the polynomial regression equation i.e. $P= 0.0191a^2+0.1104a$ the maximum voltage of 9.848 mW is observed. The uncertainty error observed is 0.22 %.If the coefficient determination is very closure to 1 (here it is 0.9994), the error may be very low.

4.2.6 Acceleration dependence of EH at 60 Hz

It can be seen from Fig. 4.11, the variation of voltage under the acceleration of input excitation amplitude of 20g to 100g. The maximum measured voltage can be 103.9 V at the input 100g acceleration excitation. The minimum measured voltage can be 25 V at the input 20g acceleration excitation. The relationship is linear between response and predicted variables. Fig. 4.12 shows the variation of power with excited acceleration of 20g to 100g. The maximum power observed is 496.2 mW at 100g excitation and it is varying quadratic nonlinear with the input excitation. The quadratic non linearity in the power to acceleration graph is validated the ohm's law.

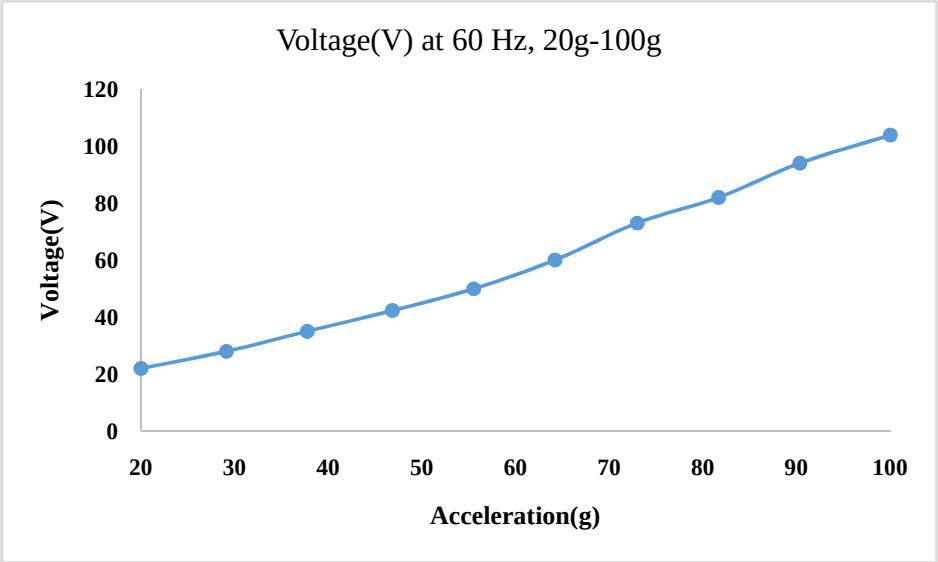

Fig. 4.11 Variation of voltage at 60 Hz with 20g-100g acceleration

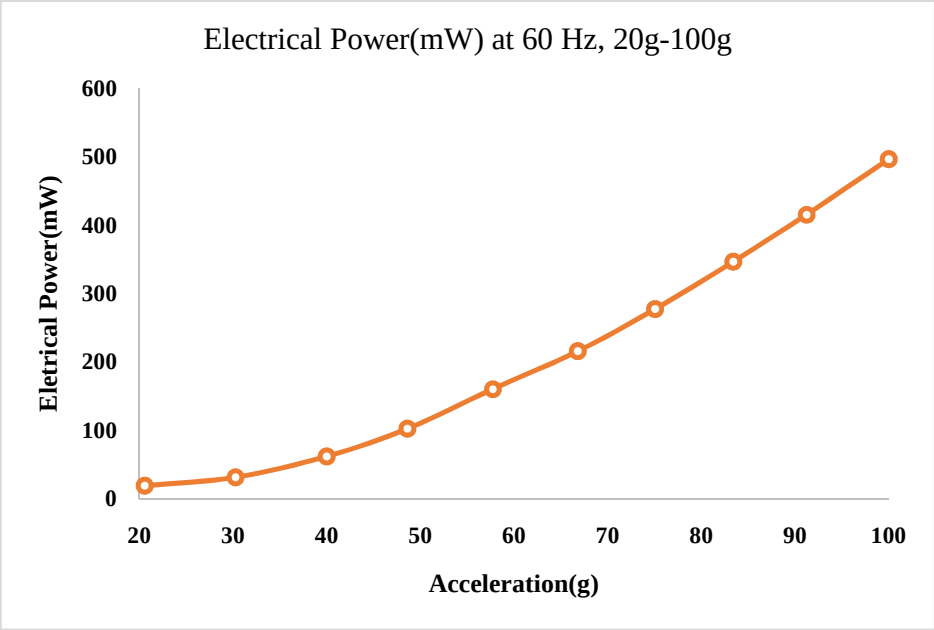

Fig. 4.12 Variation of power at 60 Hz with 20g-100g acceleration

According to ohm's law power is equal to square of voltage is divided by load resistance.Fig.4.13 and Fig.4.14 shows the voltage and power variation at the excited frequency 60 Hz under the excited acceleration of 0 to 20g. The maximum observed voltage at 20g is 25V and Power is 18.5 mW.

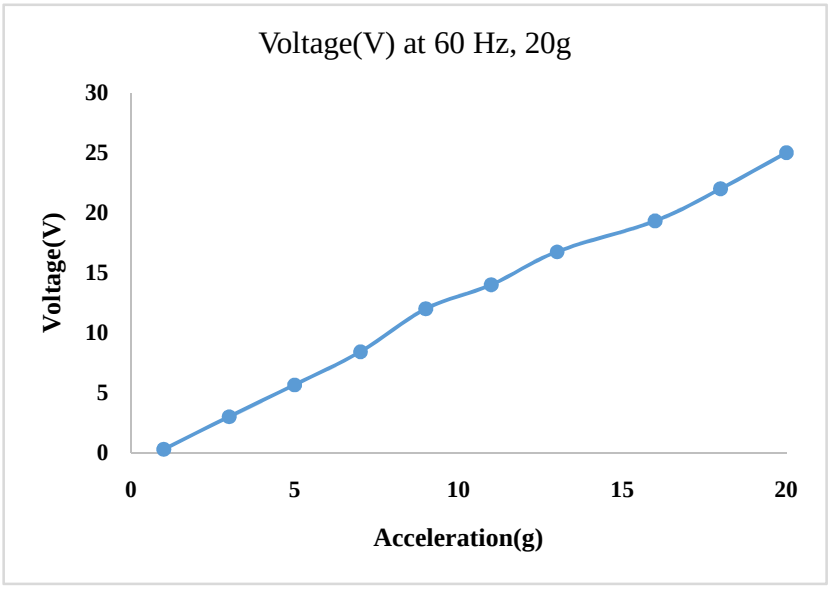

Fig. 4.13 Variation of voltage at 60 Hz with 0-20g acceleration

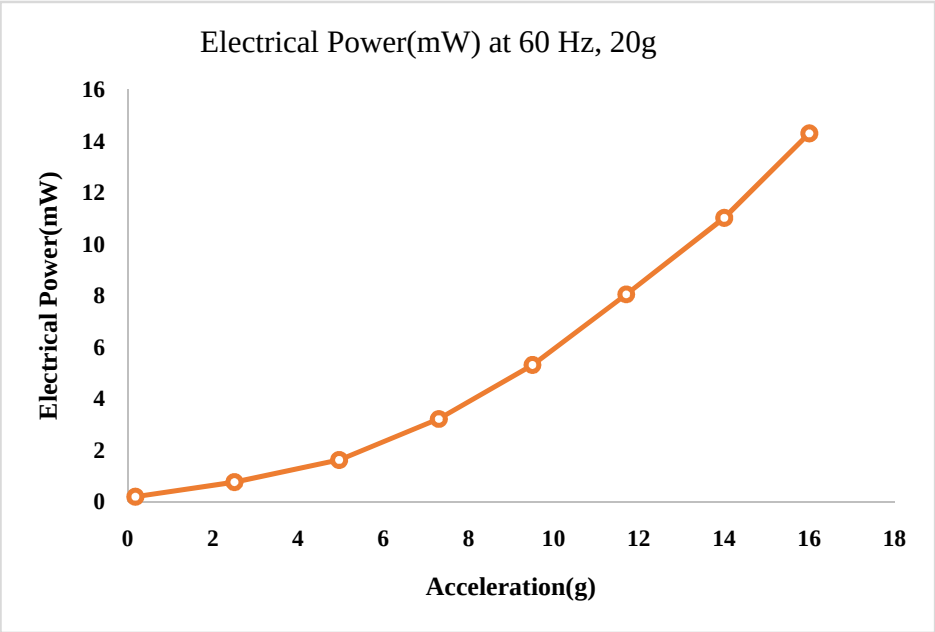

Fig. 4.14 Variation of power at 60 Hz with 0-20g acceleration

4.2.7 Acceleration dependence of EH at 65 Hz

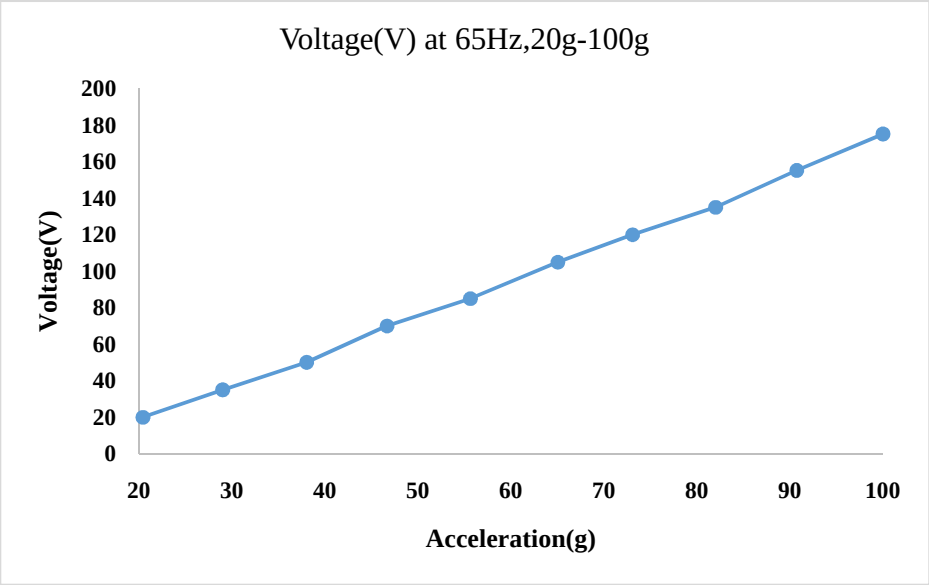

Fig. 4.15 Variation of voltage at 65 Hz under 20g-100g acceleration

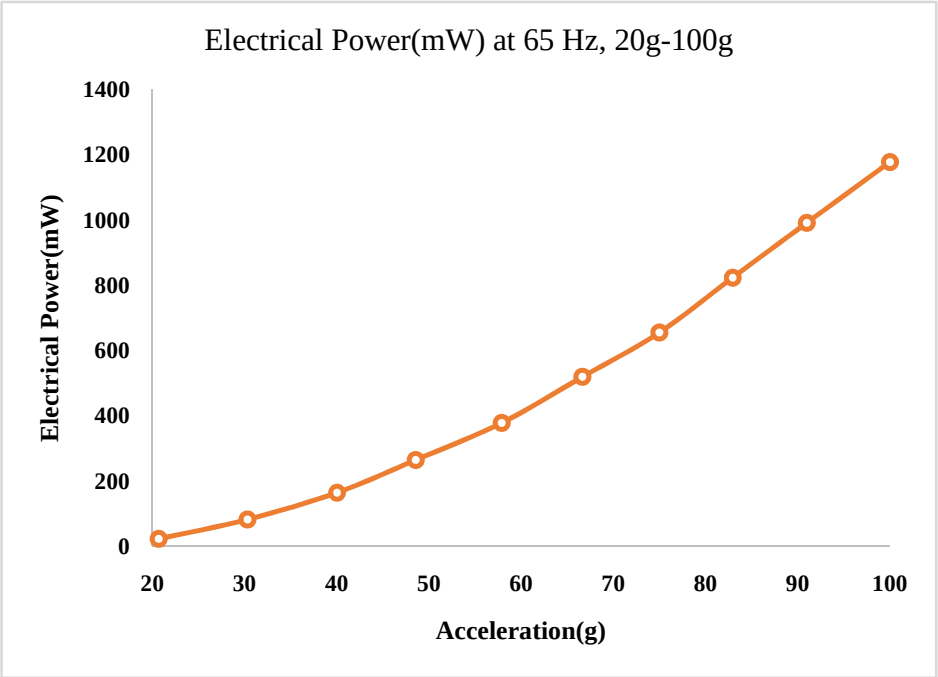

Fig.4.16 Variation of power at 65 Hz under 20g-100g acceleration

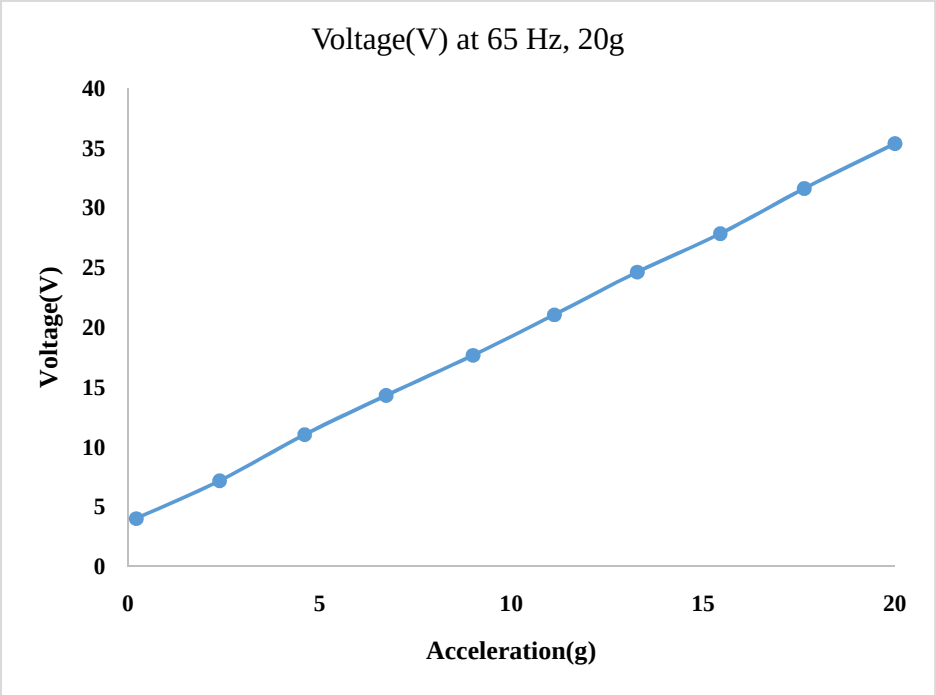

Fig. 4.17 Variation of voltage at 65 Hz under 0-20g acceleration

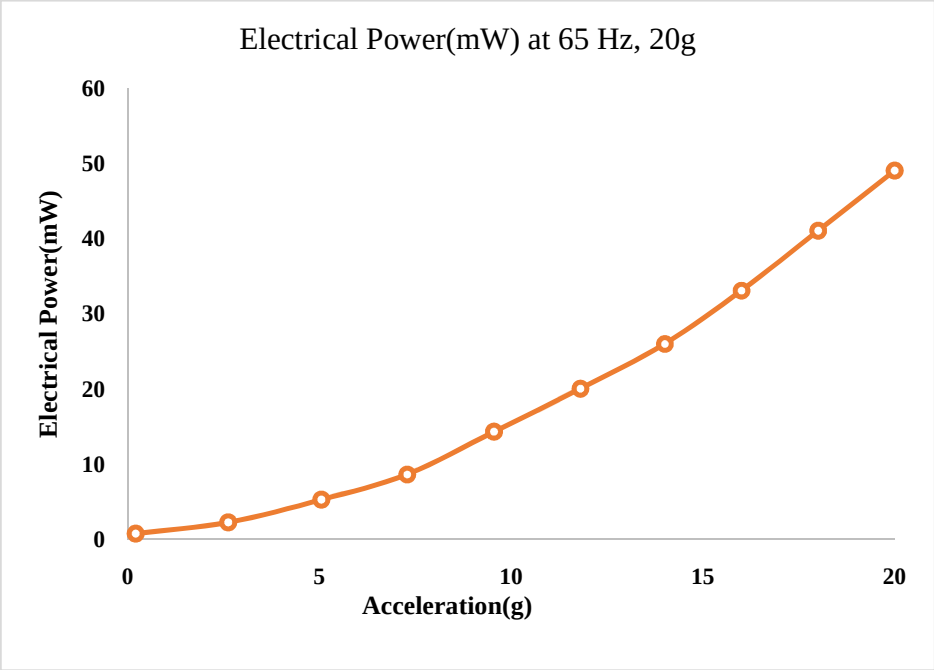

Fig. 4.18 Variation of power at 65 Hz under 0-20g acceleration

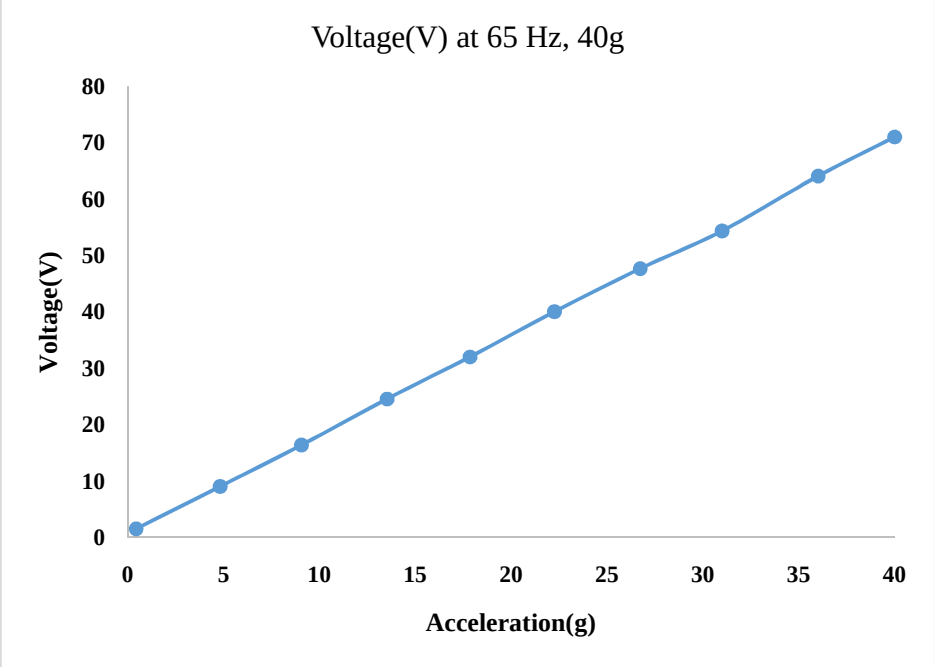

Fig. 4.19 Variation of voltage at 65 Hz under 0-40g acceleration

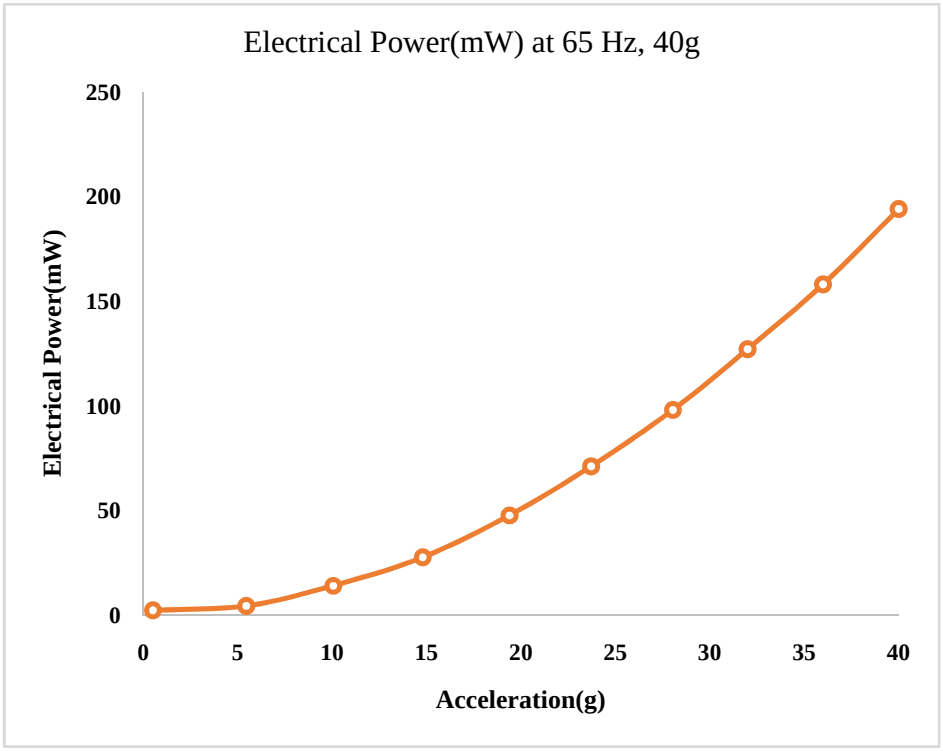

Fig. 4.20 Variation of power at 65 Hz under 0-40g acceleration

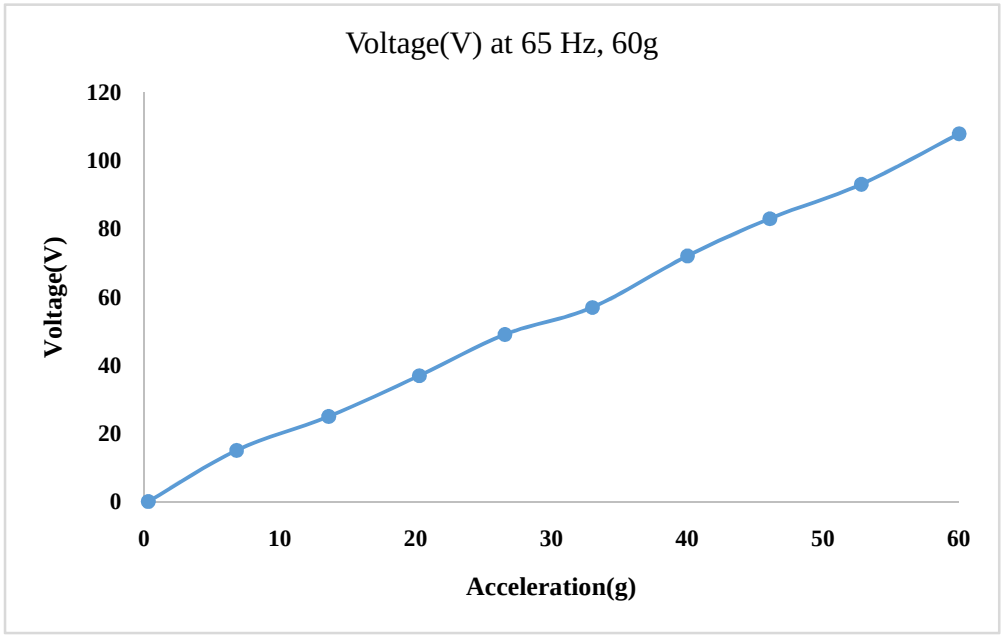

Fig. 4.21 Variation of voltage at 65 Hz under 0-60g acceleration

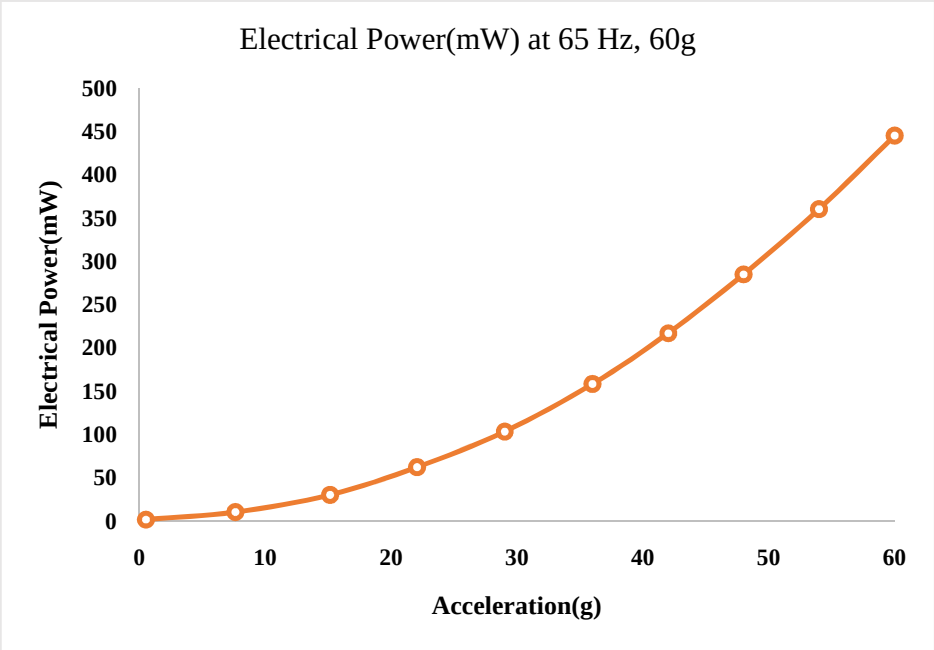

Fig. 4.22 Variation of power at 65 Hz under 0-60g acceleration

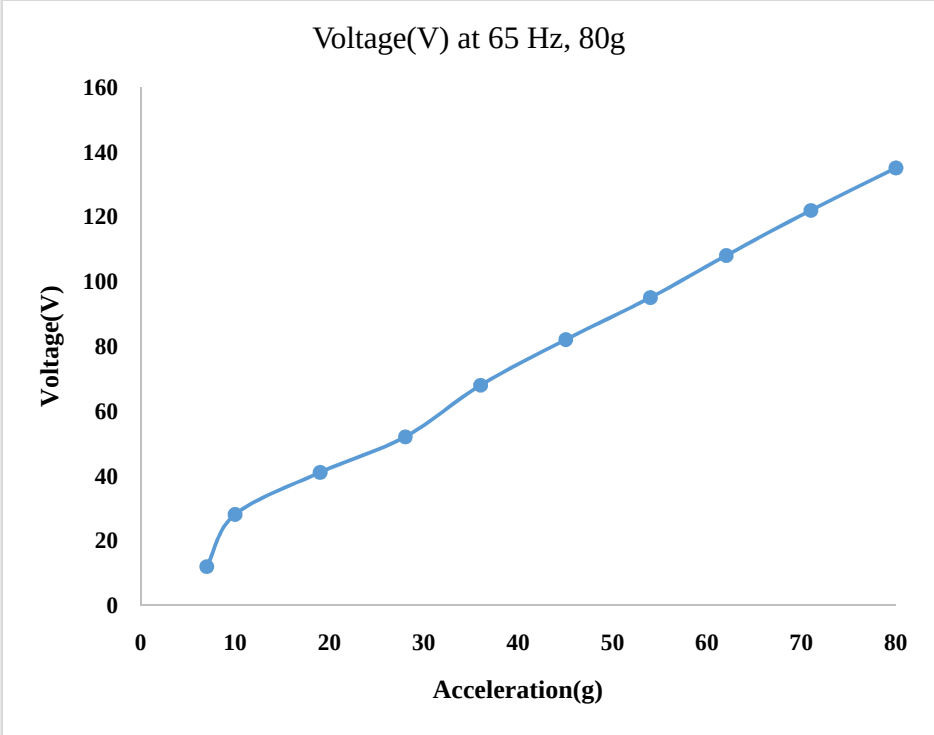

Fig. 4.23 Variation of voltage at 65 Hz under 0-80g acceleration

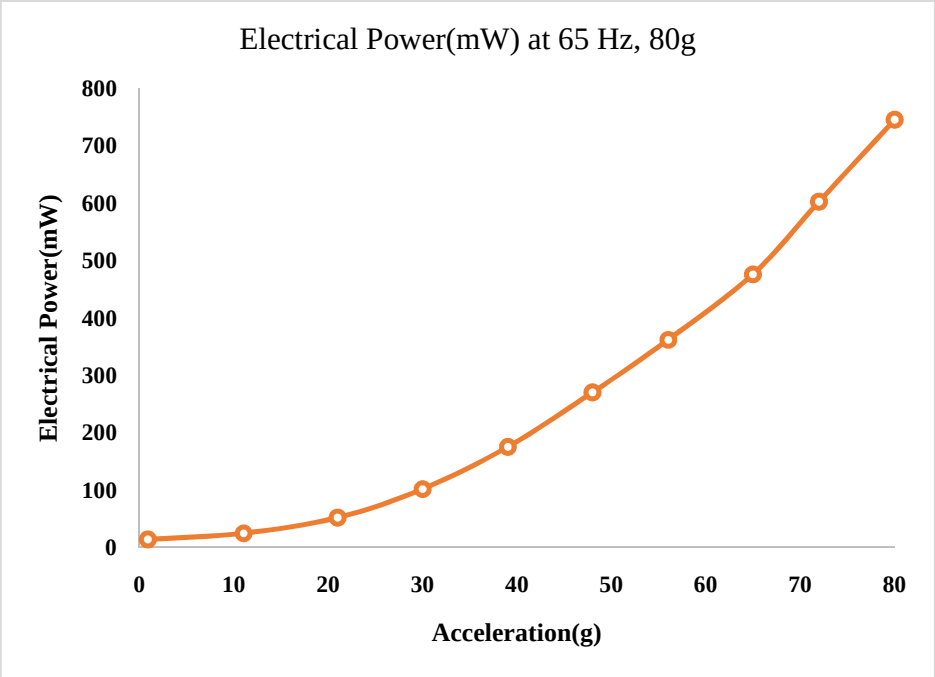

Fig. 4.24 Variation of power at 65 Hz under 0-80g acceleration

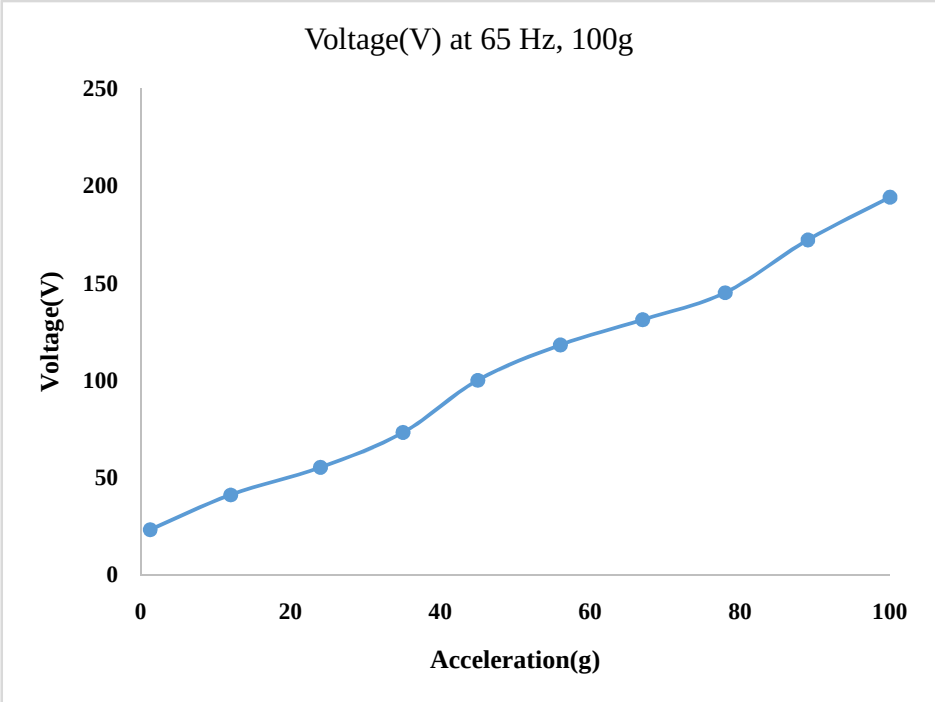

Fig. 4.25 Variation of voltage at 65 Hz under 0-100g acceleration

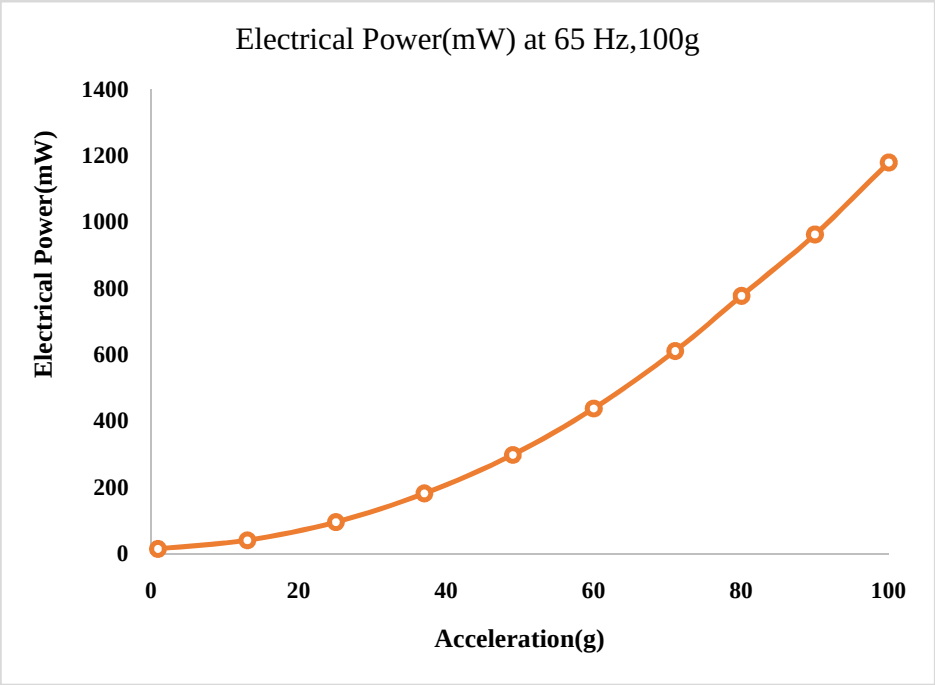

Fig. 4.26 Variation of power at 65 Hz under 0-100g acceleration

From Fig 4.15 to Fig.4.26 are shows the variation of voltage and power with respect to excited accelerations at 20g to 100g, 0-20g,0-40g,0-60g,0-80g and 0-100g under the operated frequency of 65Hz.

The following salient points are observed at the operated frequency of 65Hz and at various excited accelerations.

- At 20g excited acceleration maximum voltage observed is 35.34 V and Power is 49mW.
- At 40g excited acceleration maximum voltage observed is 71 V and Power is 194mW.
- At 60g excited acceleration maximum voltage observed is 107.8 V and Power is 445mW.
- At 80g excited acceleration maximum voltage observed is 135V and Power is 745mW.
- At 100gexcited acceleration maximum voltage observed is 194 V and Power is 1178mW.

The maximum voltage is observed at the maximum force of 100g acceleration. The variation of response voltages with input excited accelerations are linear. These are satisfying the linear constitutive equation of the direct piezoelectric effect. According to this equation the electrical displacement is directly proportional to the applied stress or pressure on the piezoelectric disc type actuator. The constant proportionality is called the piezoelectric coupled coefficient. This

coefficient is in times of 10^{-12} units, which plays a crucial role in the analytical calculations of output voltage and power which was discussed in chapter 3.

4.2.8 Acceleration dependence of EH at 70 Hz

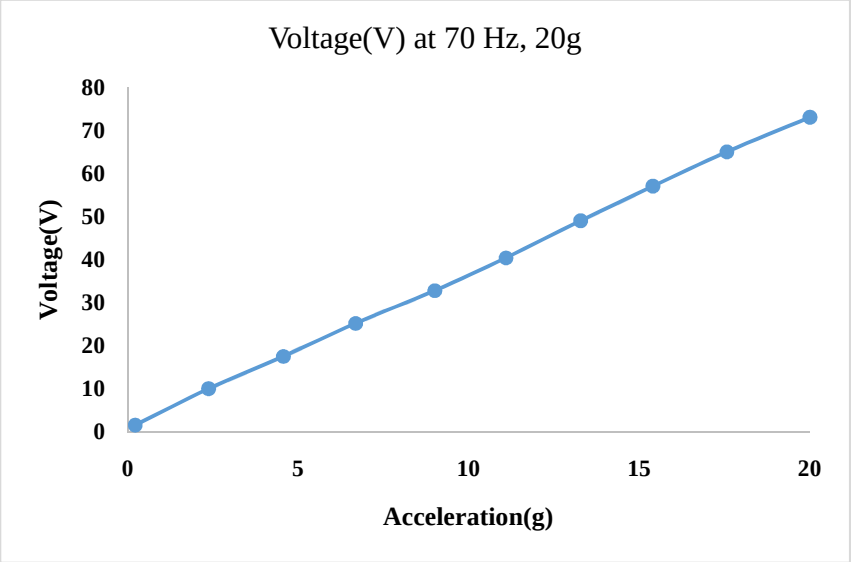

Fig. 4.27 Variation of voltage at 70 Hz under 0-20g acceleration

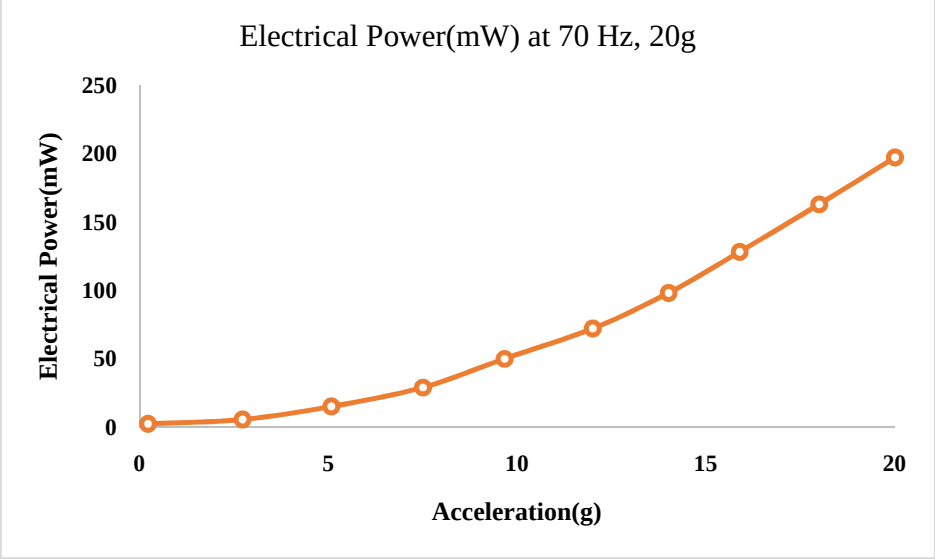

Fig. 4.28 Variation of power at 70 Hz under 0-20g acceleration

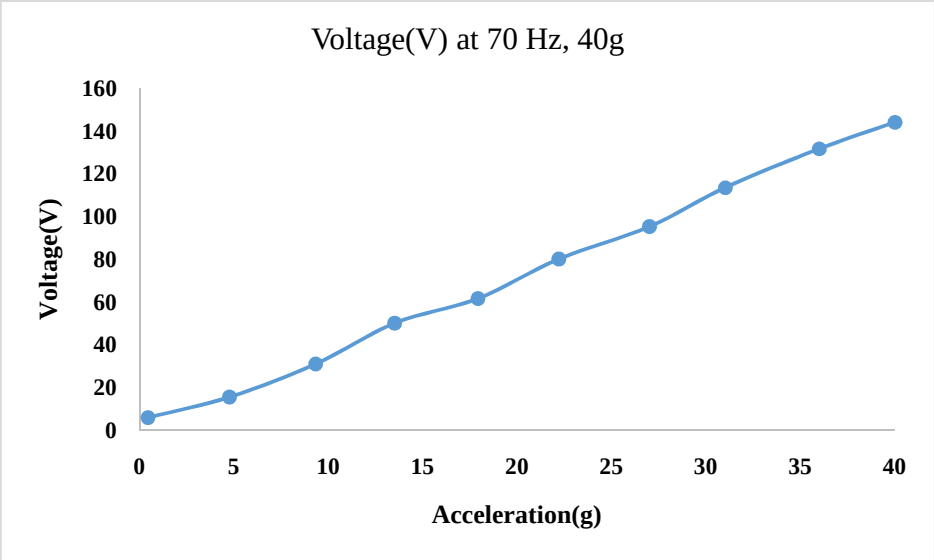

Fig. 4.29 Variation of power at 70 Hz under 0-40g acceleration

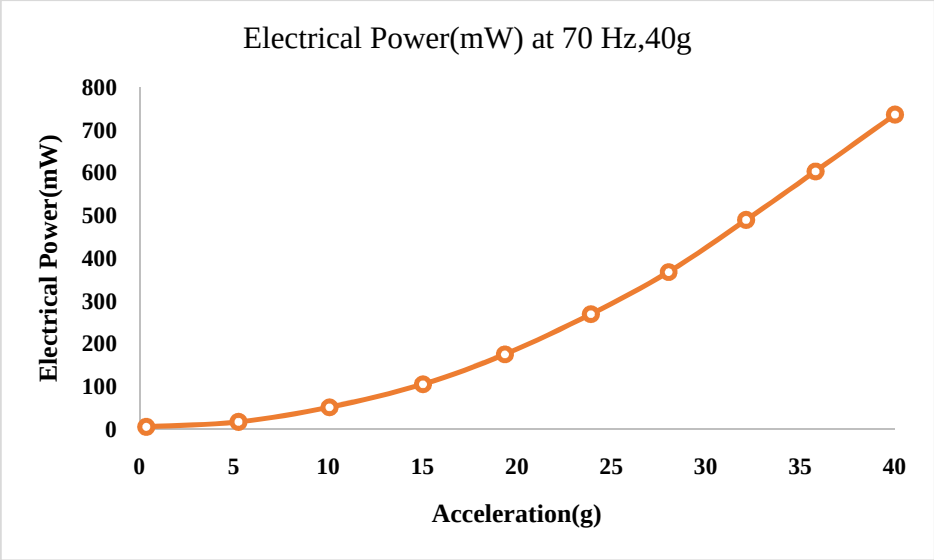

Fig. 4.30 Variation of power at 70 Hz under 0-40g acceleration

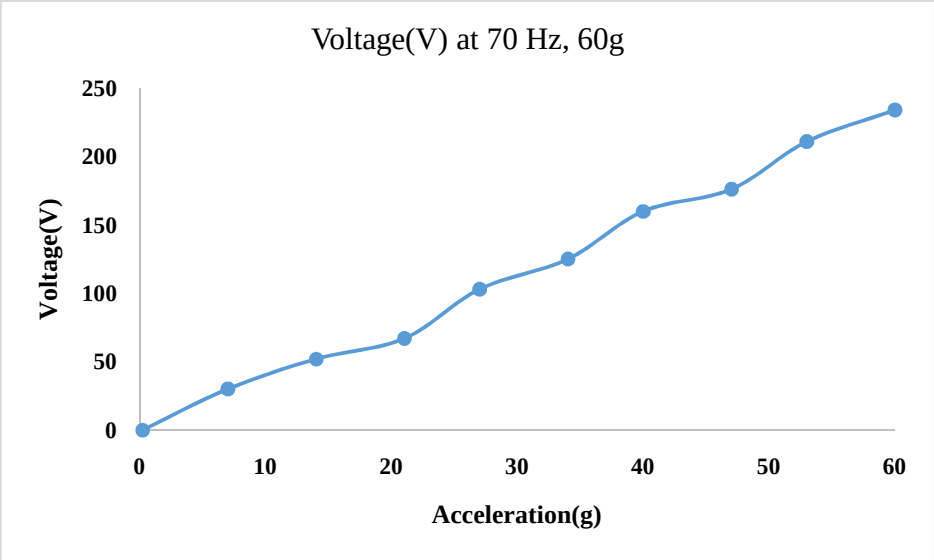

Fig. 4.31 Variation of voltage at 70 Hz under 0-60g acceleration

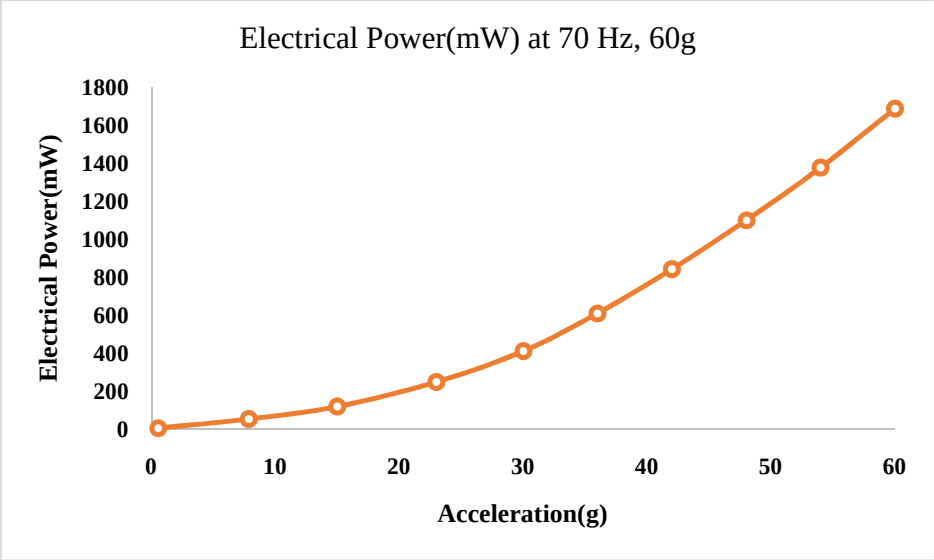

Fig. 4.32 Variation of power at 70 Hz under 0-60g acceleration

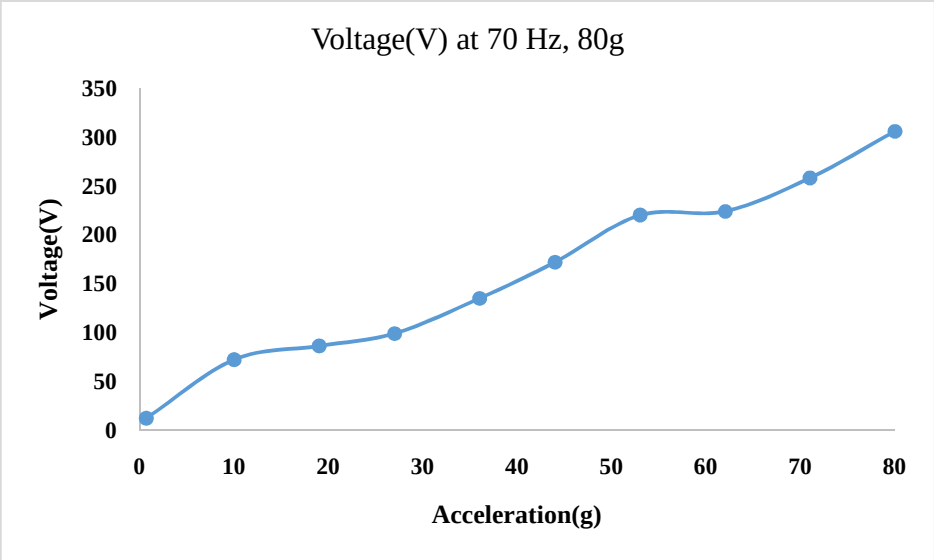

Fig. 4.33 Variation of power at 70 Hz under 0-80g acceleration

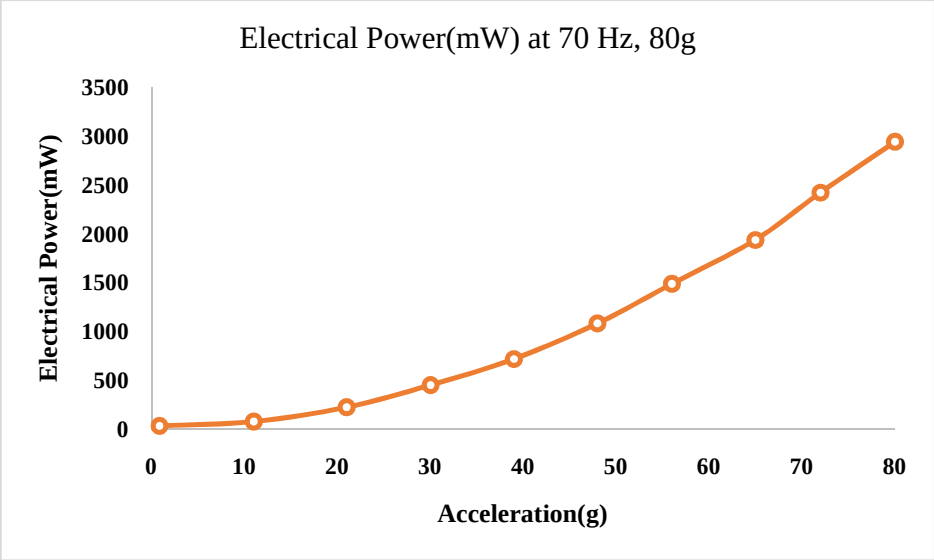

Fig. 4.34 Variation of power at 70 Hz under 0-80g acceleration

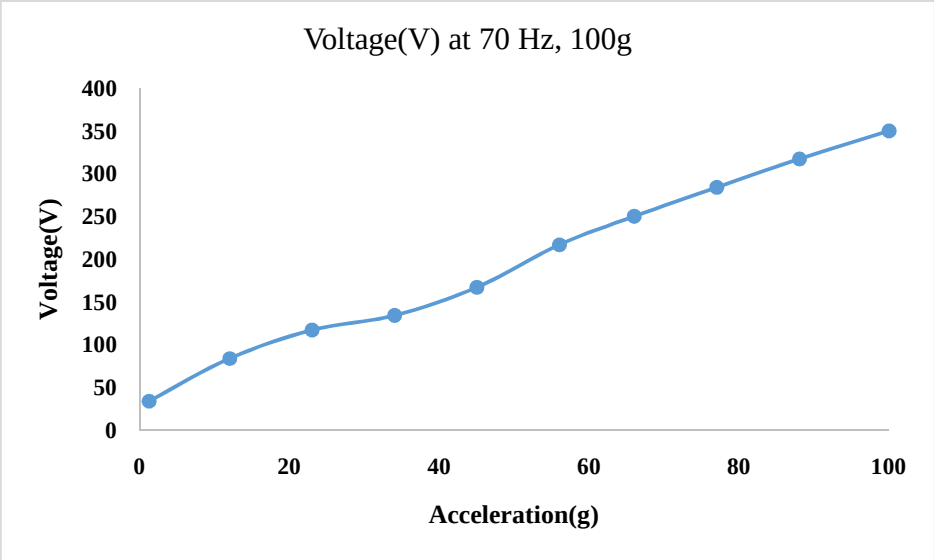

Fig. 4.35 Variation of voltage at 70 Hz under 0-100g acceleration

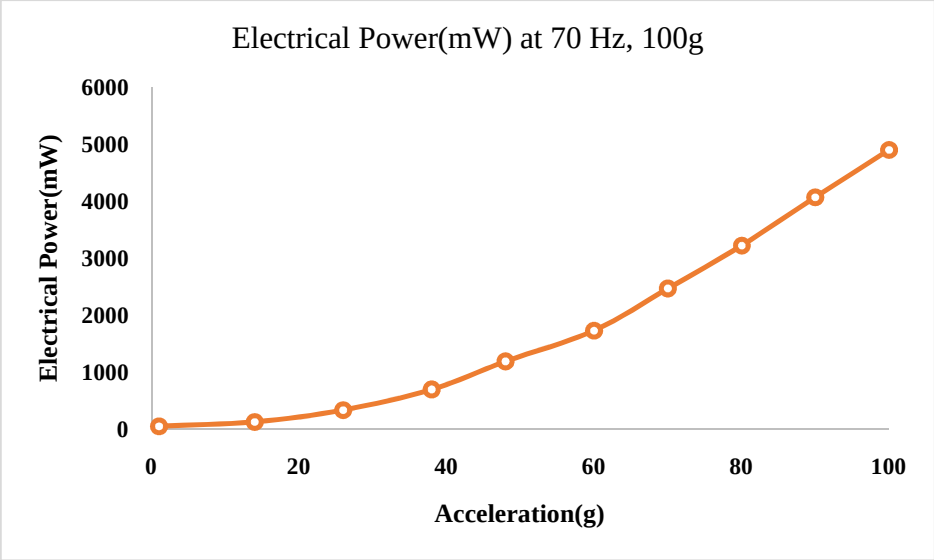

Fig. 4.36 Variation of power at 70 Hz under 0-100g acceleration

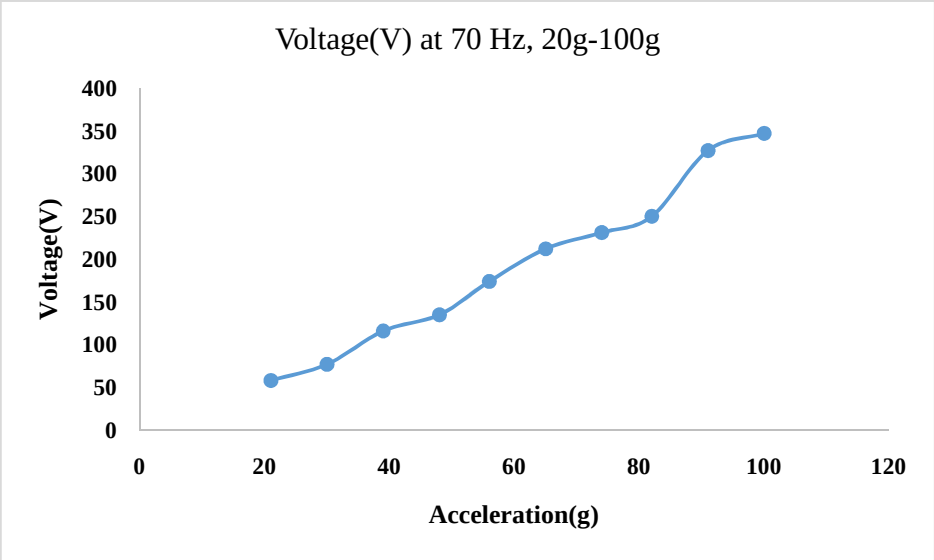

Fig. 4.37 Variation of voltage at 70 Hz under 20g-100g acceleration

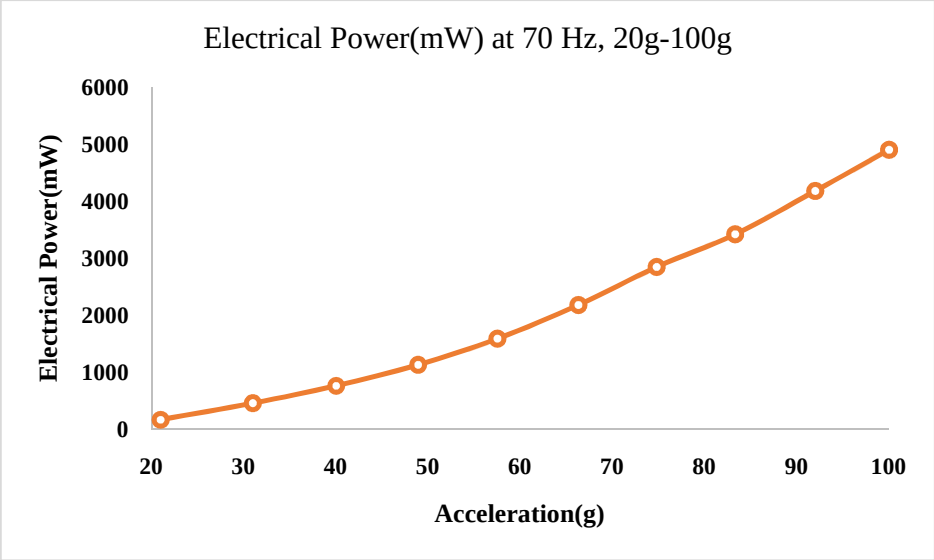

Fig. 4.38 Variation of power at 70 Hz under 20g-100g acceleration

From Fig 4.27 to Fig.4.38 are shows the variation of voltage and power with respect to excited accelerations at 20g to 100g, 0-20g,0-40g,0-60g,0-80g and 0-100g under the operated frequency of 70 Hz.

The following salient points are observed at the operated frequency of 70 Hz and at various excited accelerations.

- At 20g excited acceleration maximum voltage observed is 73 V and Power is 197 mW.

- At 40g excited acceleration maximum voltage observed is 144.13V and Power is 736 mW.
- At 60g excited acceleration maximum voltage observed is 234 V and Power is 1688mW.
- At 80g excited acceleration maximum voltage observed is 306V and Power is 2944mW.
- At 100gexcited acceleration maximum voltage observed is 350 V and Power is 4906mW.

The maximum voltage is observed at the maximum force of 100g acceleration i.e., 350 V. The variation of response voltages with input excited accelerations are linear. These are satisfying the linear constitutive equation of the direct piezoelectric effect which is mentioned in international standards of American piezoelectricity. According to this equation the electrical displacement is directly proportional to the applied stress or pressure on the piezoelectric disc type actuator. The constant proportionality is called the piezoelectric coupled coefficient. This coefficient is in times of 10^{-12} units, which plays a crucial role in the analytical calculations of output voltage and power.

4.2.9 Acceleration dependence of EH at 73.5 Hz

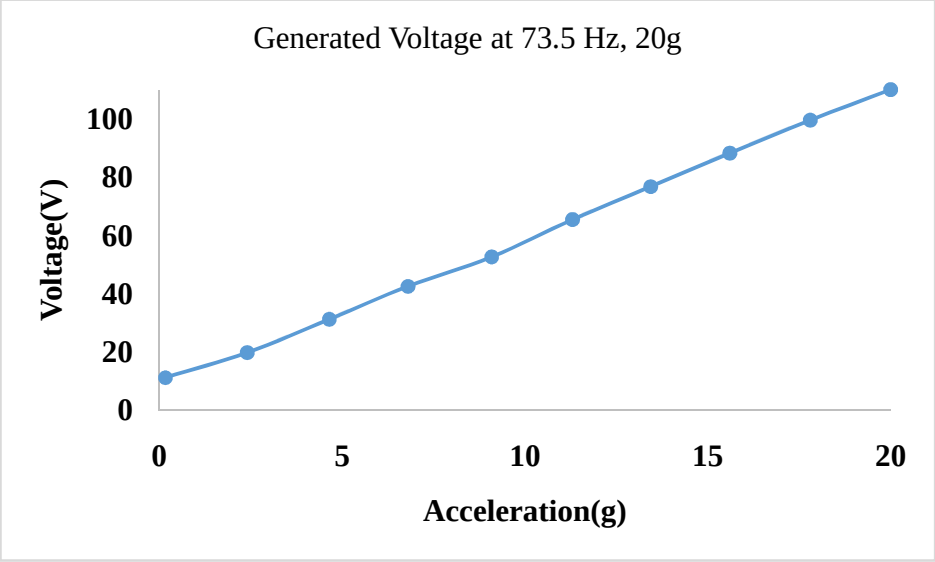

Fig. 4.39 Variation of voltage at 73.5 Hz under 0-20g acceleration

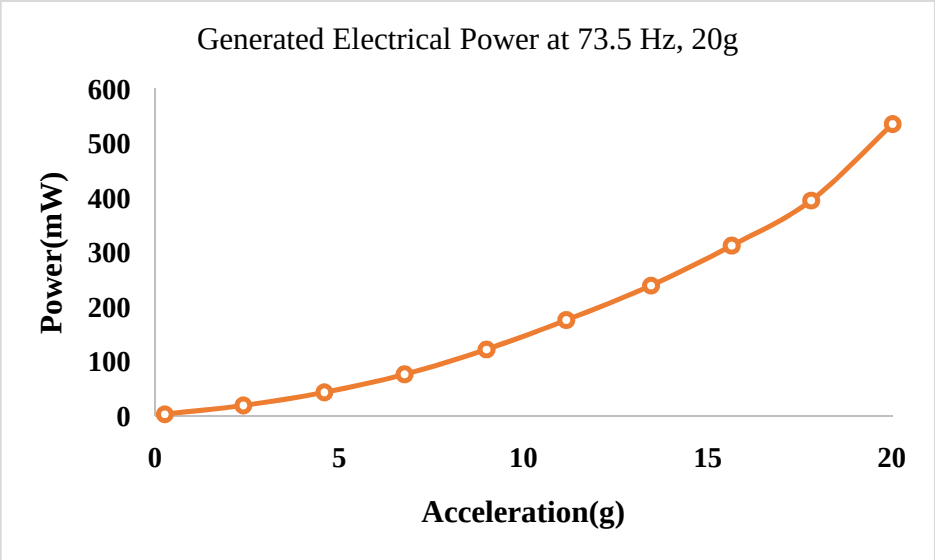

Fig. 4.40 Variation of power at 73.5 Hz under 0-20g acceleration

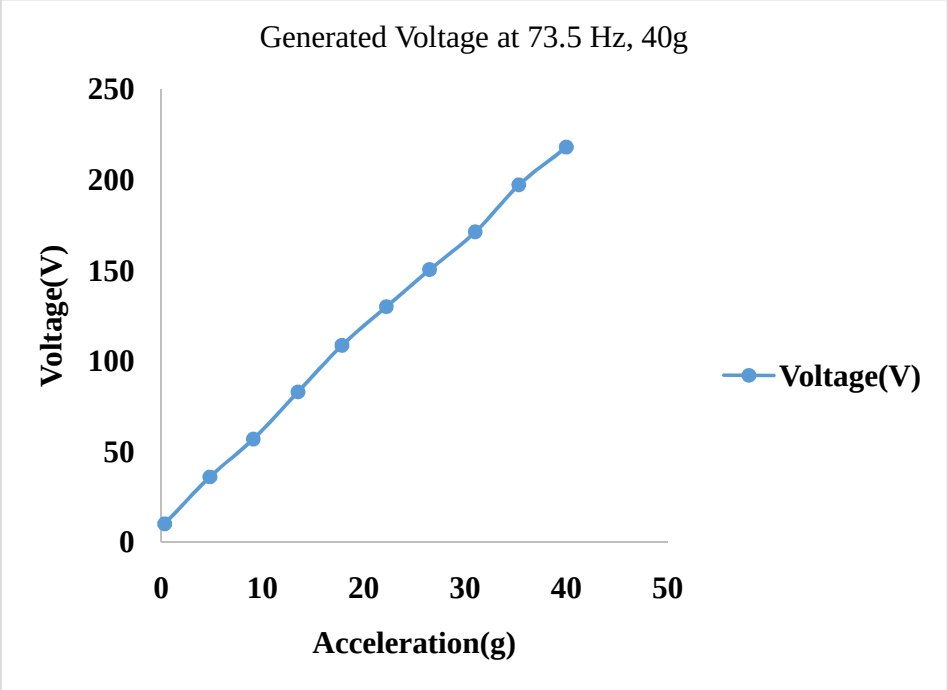

Fig. 4.41 Variation of voltage at 73.5 Hz under 0-40g acceleration

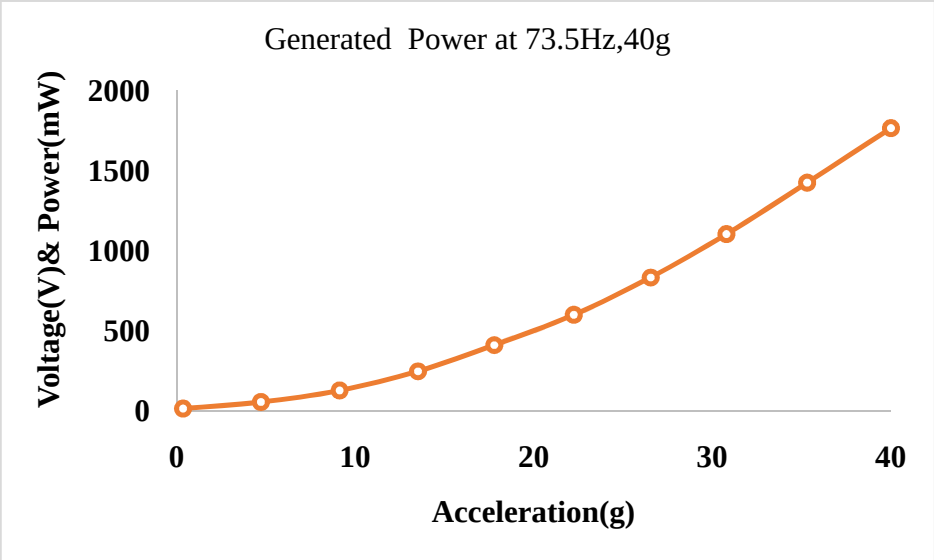

Fig. 4.42 Variation of power at 73.5 Hz under 0-40g acceleration

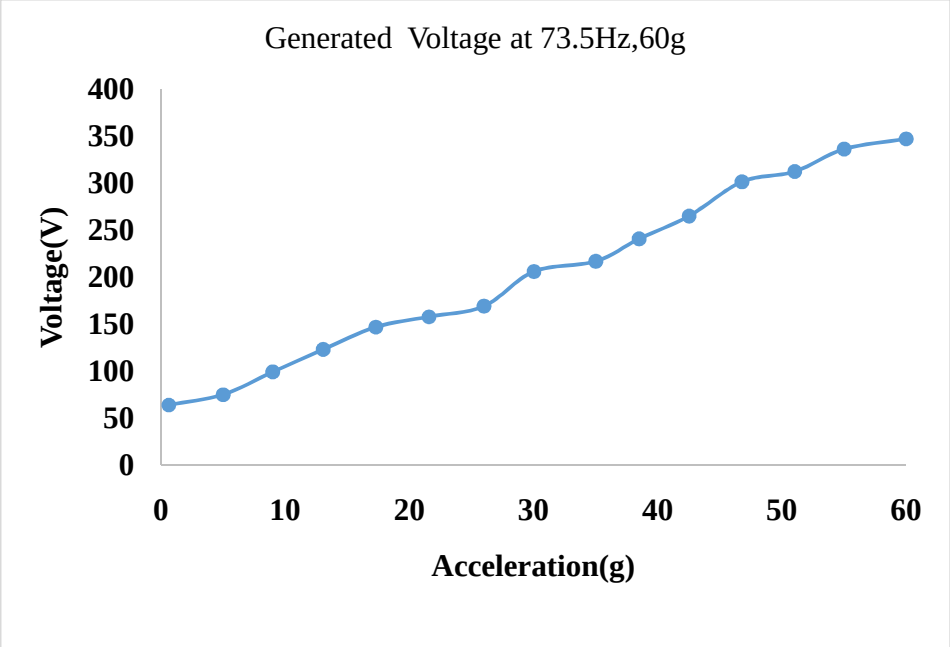

Fig. 4.43 Variation of voltage at 73.5 Hz under 0-60g acceleration

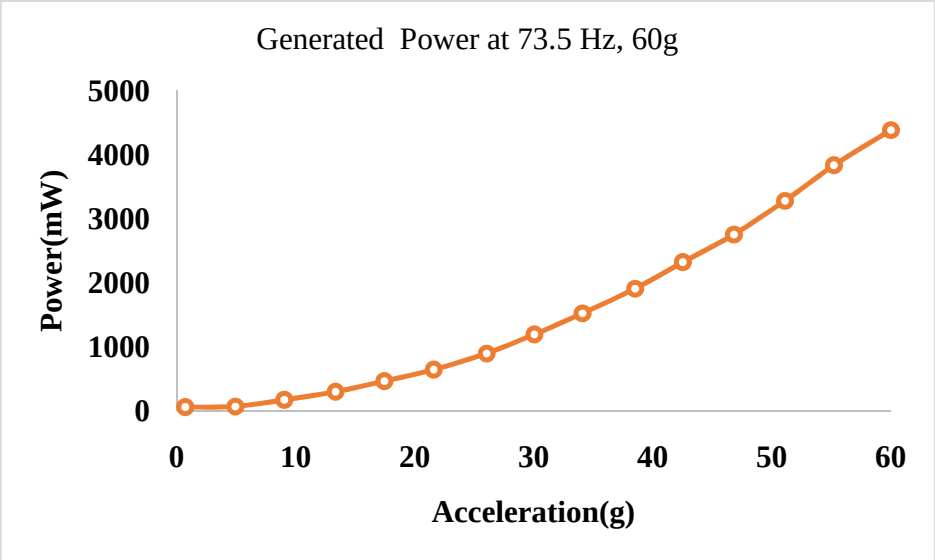

Fig. 4.44 Variation of power at 73.5 Hz under 0-60g acceleration

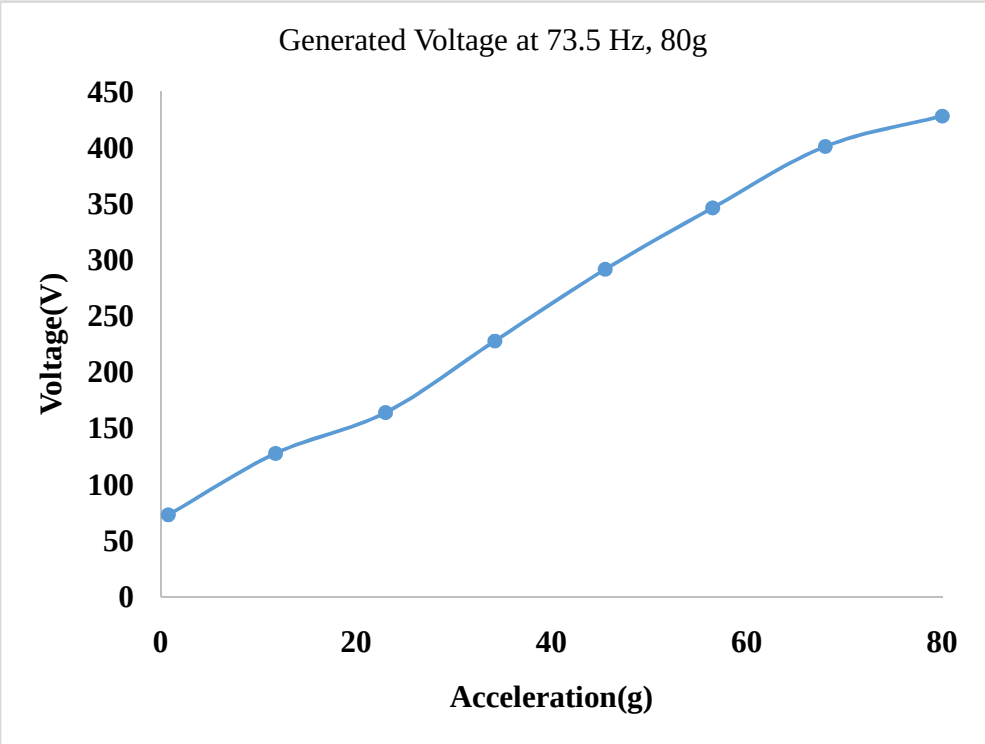

Fig. 4.45 Variation of voltage at 73.5 Hz under 0-80g acceleration

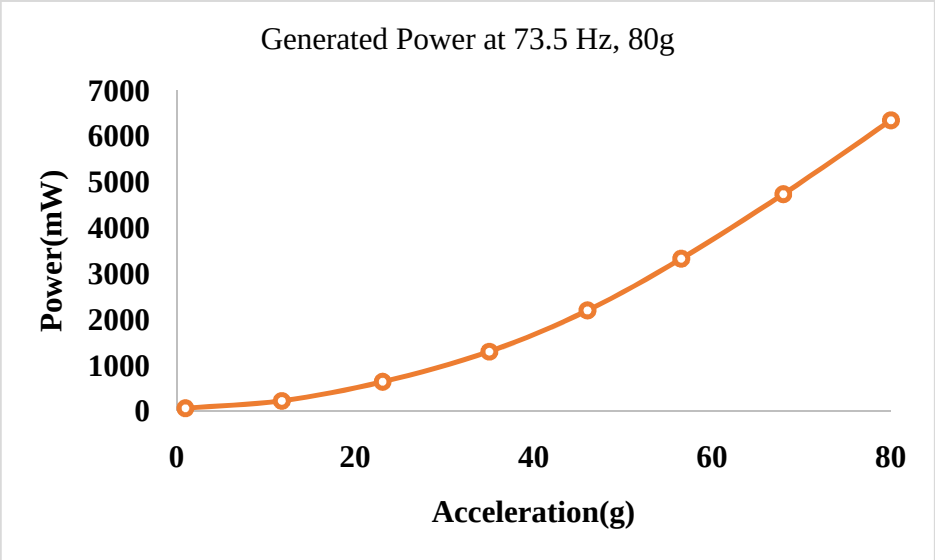

Fig. 4.46 Variation of power at 73.5 Hz under 0-80g acceleration

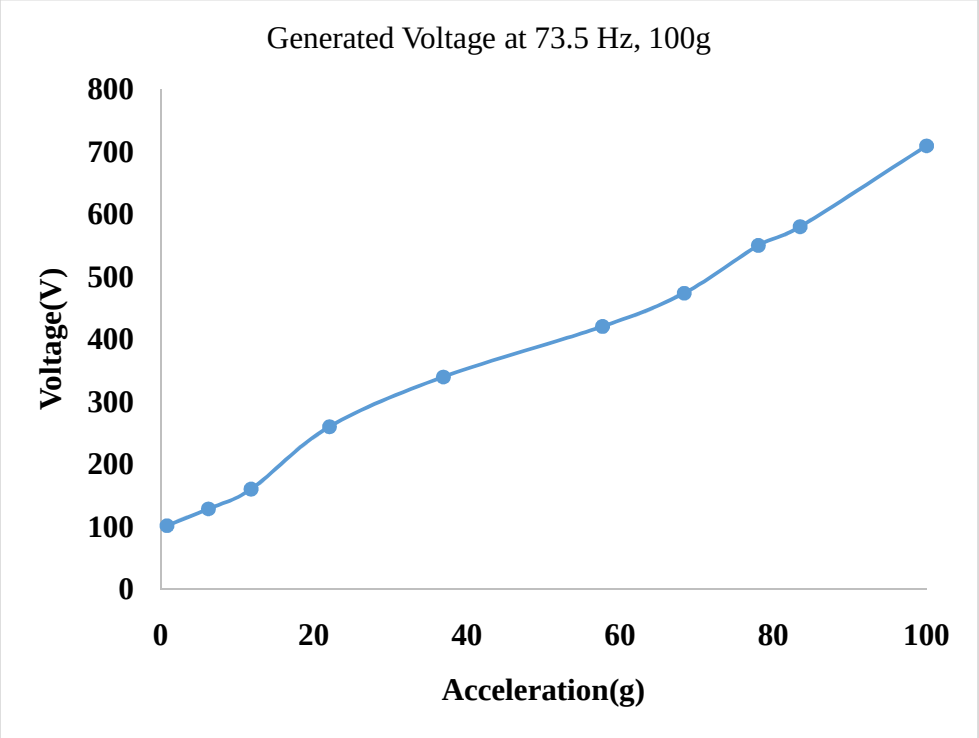

Fig. 4.47 Variation of voltage at 73.5 Hz under 0-100g acceleration

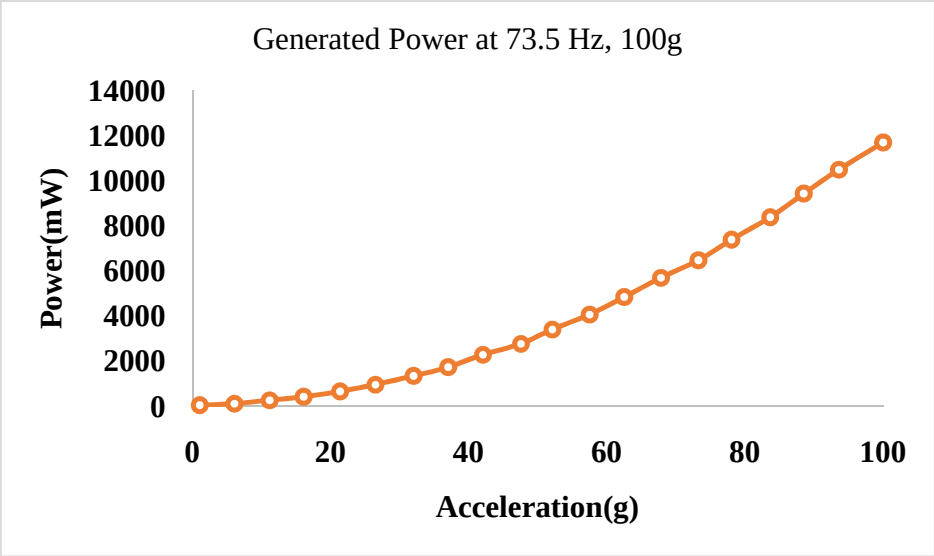

Fig. 4.48 Variation of power at 73.5 Hz under 0-100g acceleration

From Fig 4.39 to Fig.4.48 are shows the variation of voltage and power with respect to excited accelerations at 20g to 100g, 0-20g,0-40g,0-60g,0-80g and 0-100g under the operated frequency of 73.5 Hz.

The following salient points are observed at the operated frequency of 73.5 Hz and at various excited accelerations.

- At 20g excited acceleration maximum voltage observed is 110 V and Power is 535.6 mW.
- At 40g excited acceleration maximum voltage observed is 218V and Power is 1764.46 mW.
- At 60g excited acceleration maximum voltage observed is 347.4 V and Power is 4384.6 mW.
- At 80g excited acceleration maximum voltage observed is 428.5 V and Power is 6345.1 mW.
- At 100gexcited acceleration maximum voltage observed is 586 V and Power is 11694.3 mW.

The maximum voltage is observed at the maximum force of 100g acceleration i.e., 586 V. The variation of response voltages with input excited accelerations are linear. These are satisfying the linear constitutive equation of the direct piezoelectric effect which is mentioned in international standards of American piezoelectricity. Based on the linear constitutive equations, the electrical displacement is directly proportional to the applied stress or pressure on the piezoelectric disc type actuator. The constant proportionality is called the piezoelectric coupled coefficient. This coefficient is in times of 10^{-12} units, which plays a crucial role in the output generation. The role

of piezoelectric coupled coefficient is demonstrated by using Buckingham's pi theorem in Appendix A.

4.2.10 Acceleration dependence of EH at 75.5 Hz

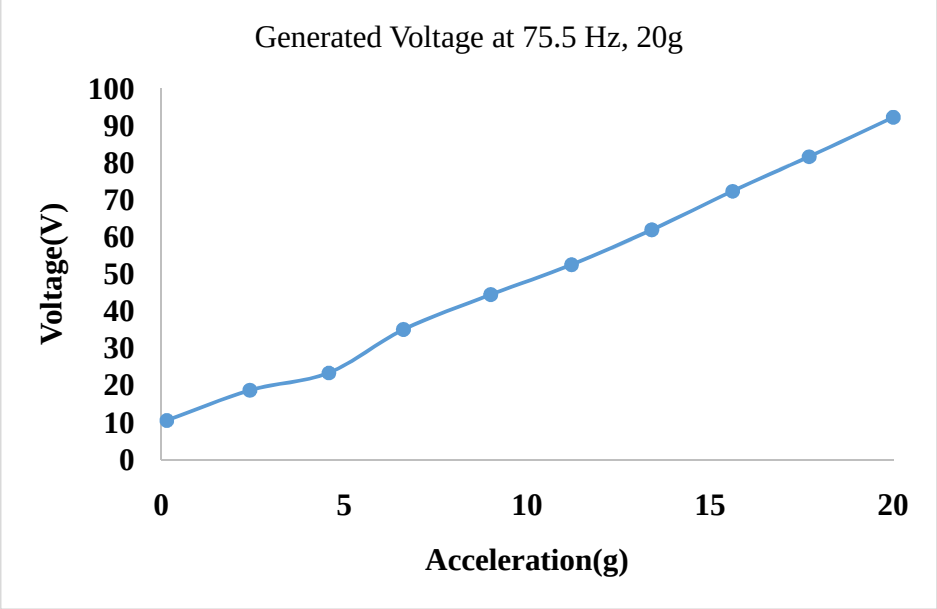

Fig. 4.49 Variation of voltage at 75.5 Hz under 0-20g acceleration

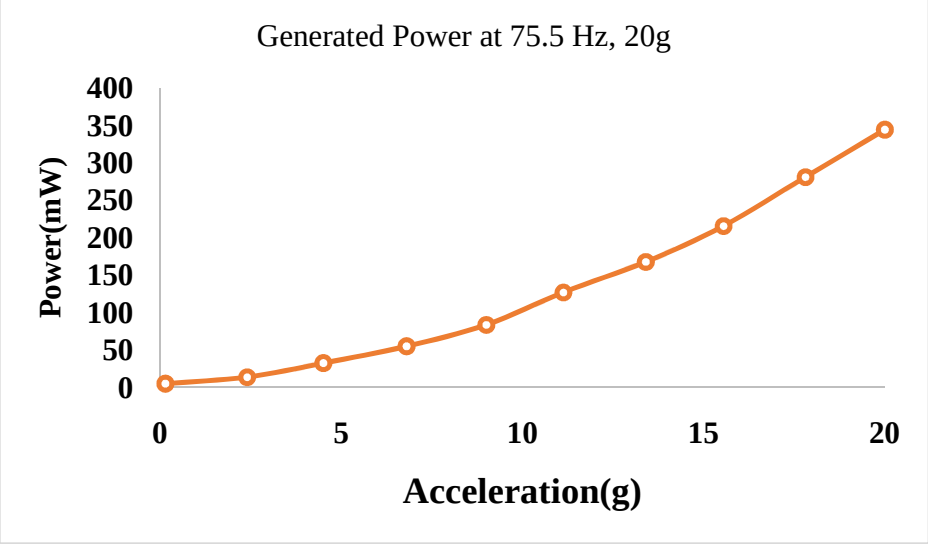

Fig. 4.50 Variation of power at 75.5 Hz under 0-20g acceleration

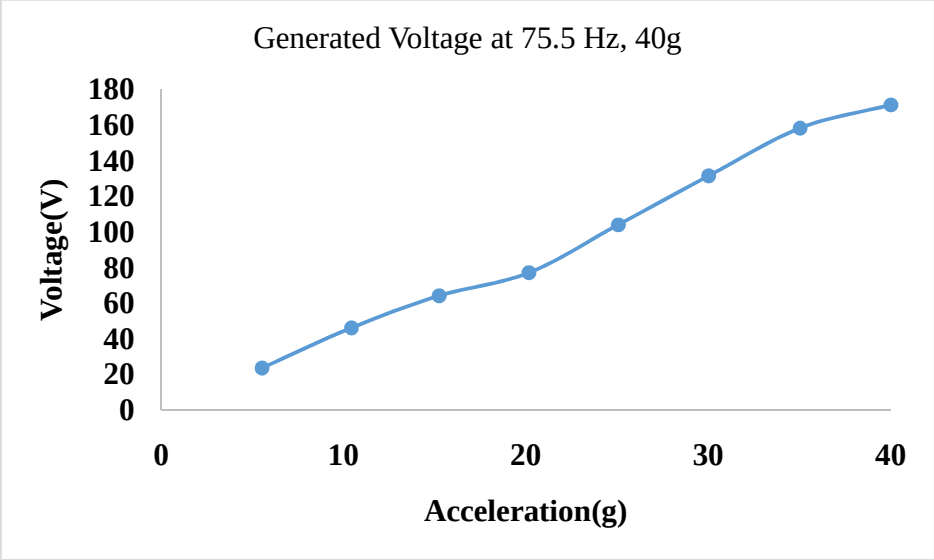

Fig. 4.51 Variation of voltage at 75.5 Hz under 0-40g acceleration

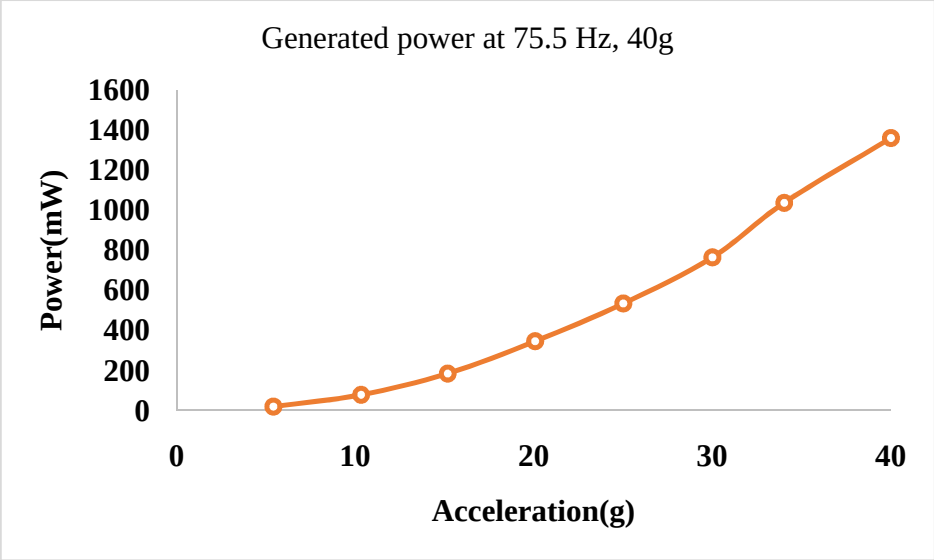

Fig. 4.52 Variation of power at 75.5 Hz under 0-40g acceleration

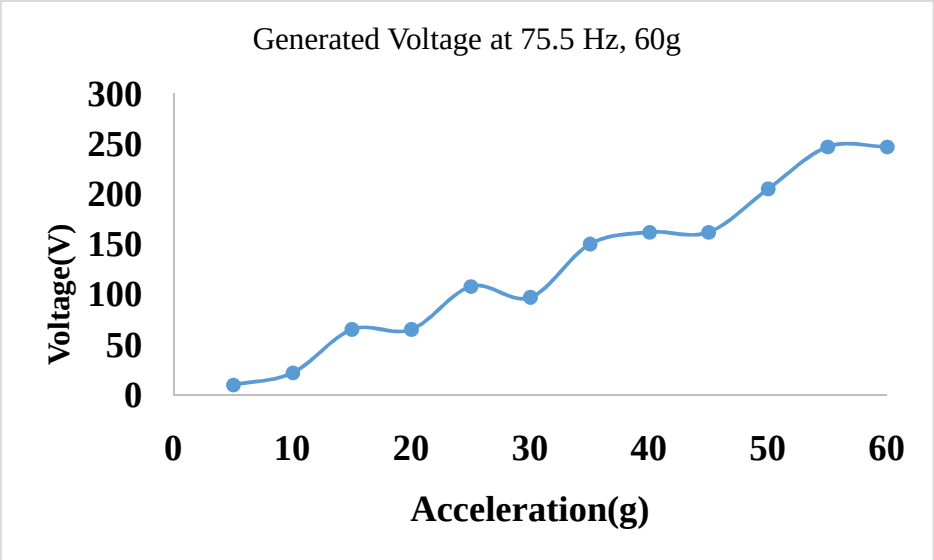

Fig. 4.53 Variation of voltage at 75.5 Hz under 0-60g acceleration

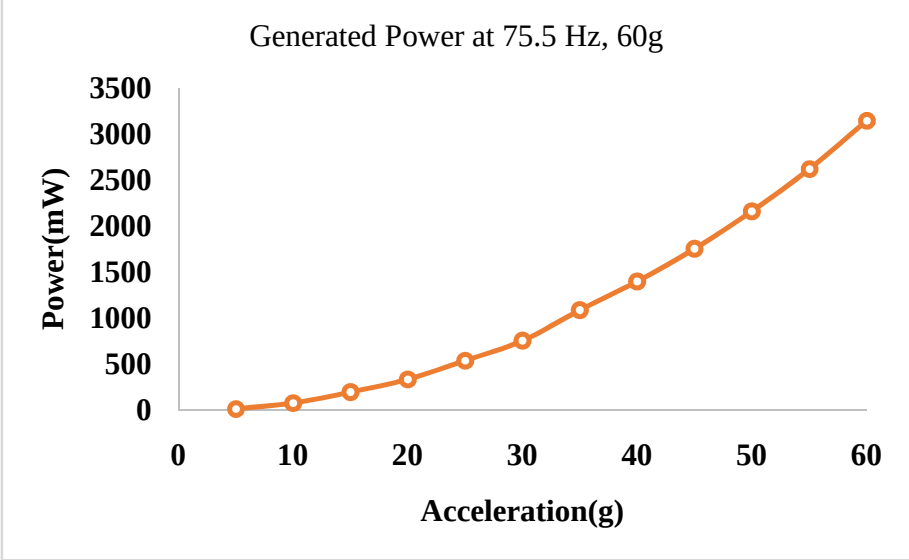

Fig. 4.54 Variation of power at 75.5 Hz under 0-60g acceleration

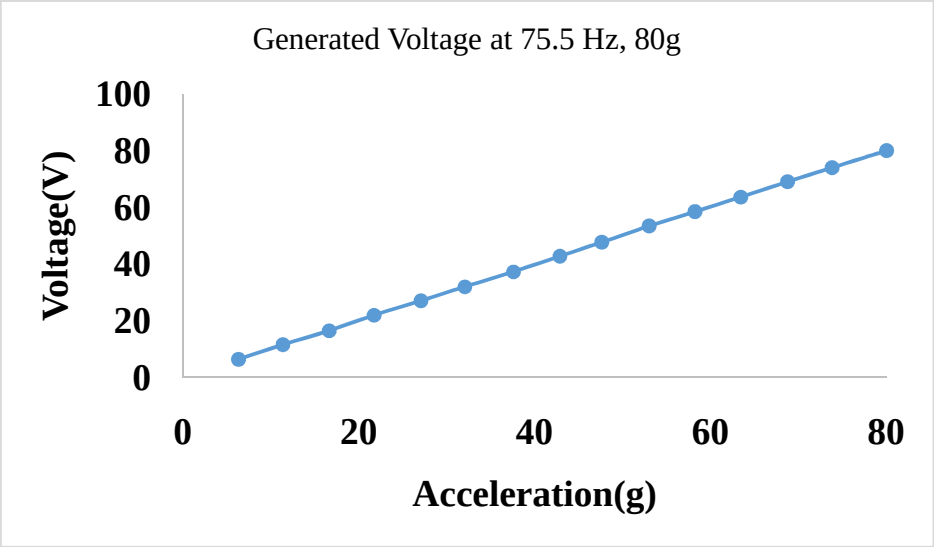

Fig. 4.55 Variation of voltage at 75.5 Hz under 0-80g acceleration

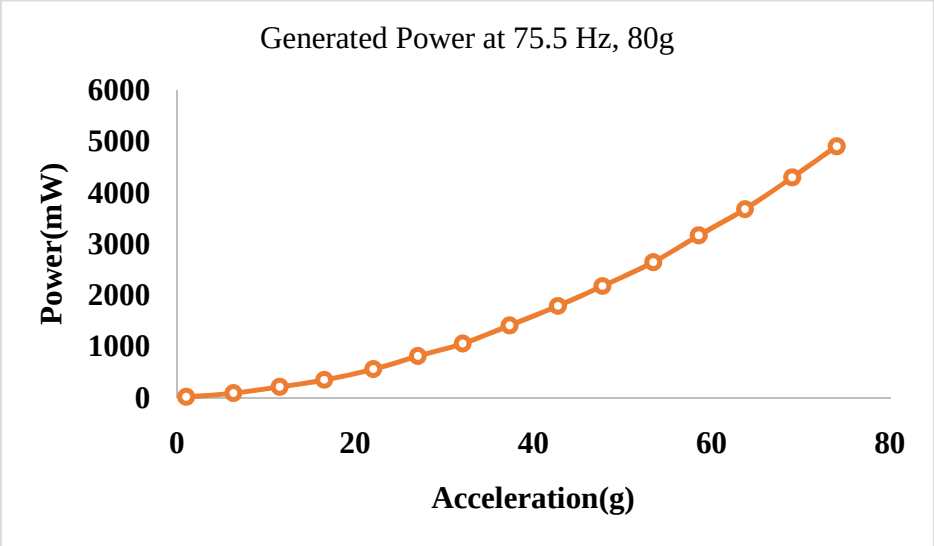

Fig. 4.56 Variation of power at 75.5 Hz under 0-80g acceleration

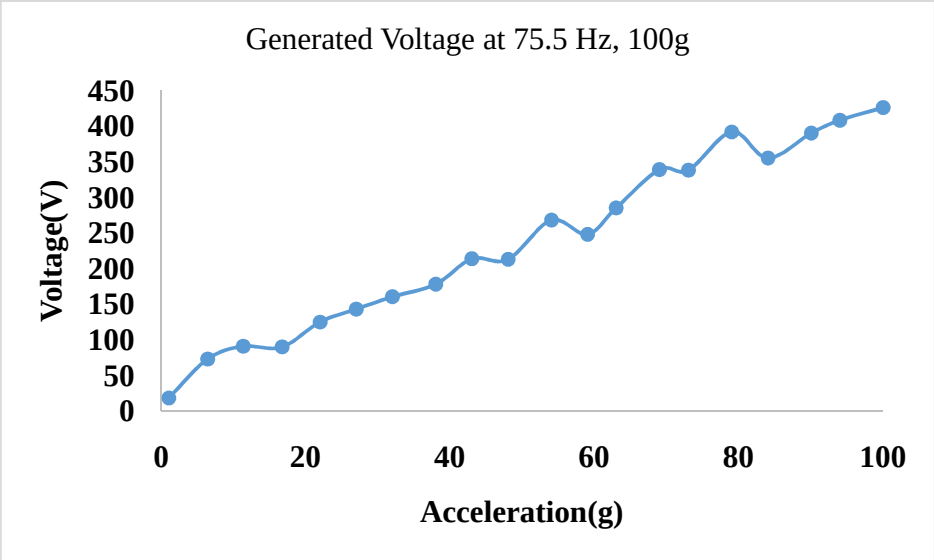

Fig. 4.57 Variation of voltage at 75.5 Hz under 0-100g acceleration

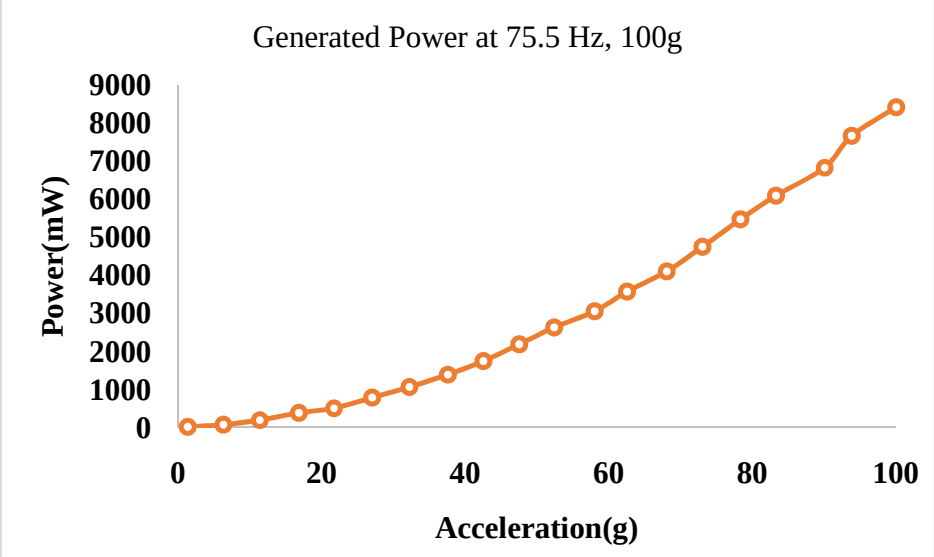

Fig. 4.58 Variation of power at 75.5 Hz under 0-100g acceleration

From Fig 4.49 to Fig.4.58 are shows the variation of voltage and power with respect to excited accelerations at 20g to 100g, 0-20g,0-40g,0-60g,0-80g and 0-100g under the operated frequency of 75.5 Hz.

The following salient points are observed at the operated frequency of 75.5 Hz and at various excited accelerations.

- At 20g excited acceleration maximum voltage observed is 92.17 V and Power is 344.17 mW.
- At 40g excited acceleration maximum voltage observed is 171.35V and Power is 1358.5 mW.
- At 60g excited acceleration maximum voltage observed is 247 V and Power is 3146.31 mW.
- At 80g excited acceleration maximum voltage observed is 376.5V and Power is 5590.3 mW.
- At 100gexcited acceleration maximum voltage observed is 426 V and Power is 8423.17 mW.

The maximum voltage is observed at the maximum force of 100g acceleration i.e., 426 V. The variation of response voltages with input excited accelerations are linear. These are satisfying the linear constitutive equation of the direct piezoelectric effect which is mentioned in international standards of American piezoelectricity. According to this equation the electrical displacement is directly proportional to the applied stress or pressure on the piezoelectric disc type actuator. The constant proportionality is called the piezoelectric coupled coefficient.

4.2.11 Acceleration dependence of EH at 80 Hz

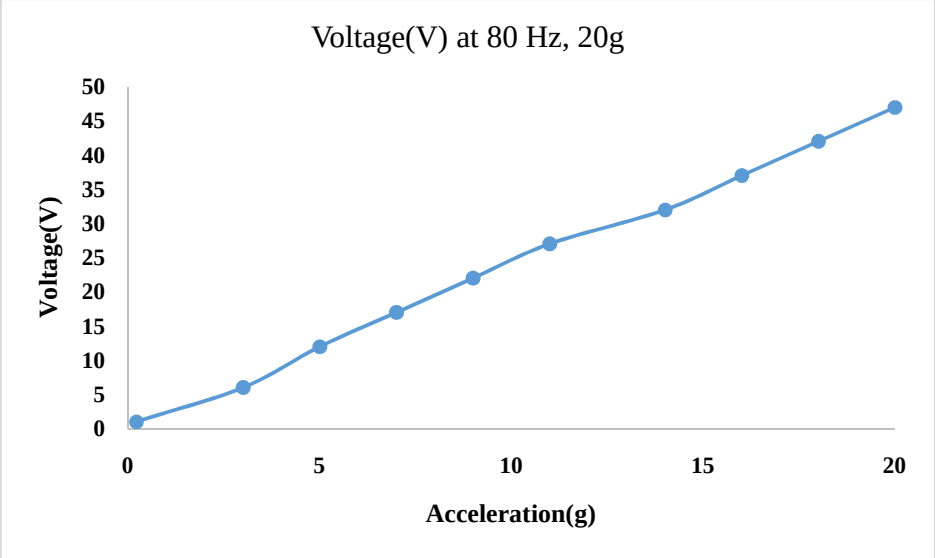

Fig. 4.59 Variation of voltage at 80 Hz under 0-20g acceleration

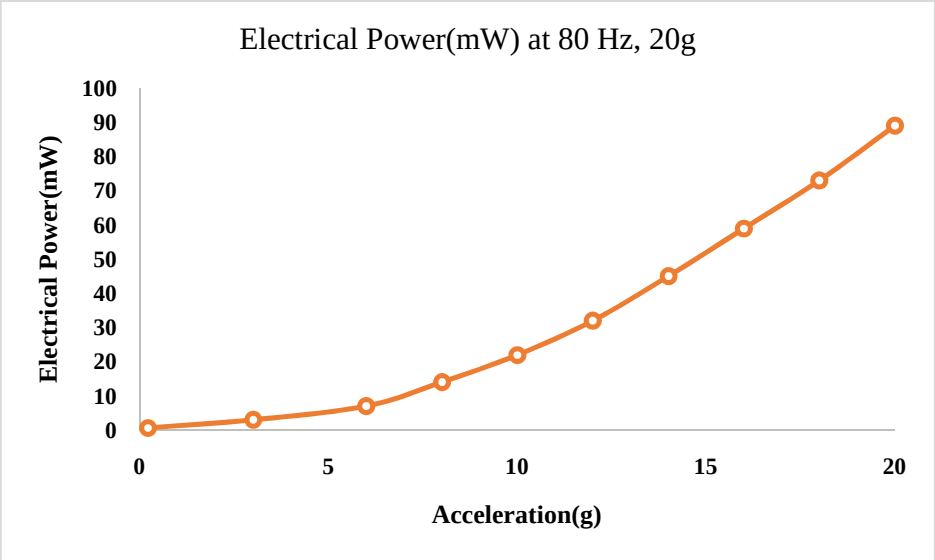

Fig. 4.60 Variation of power at 80 Hz under 0-20g acceleration

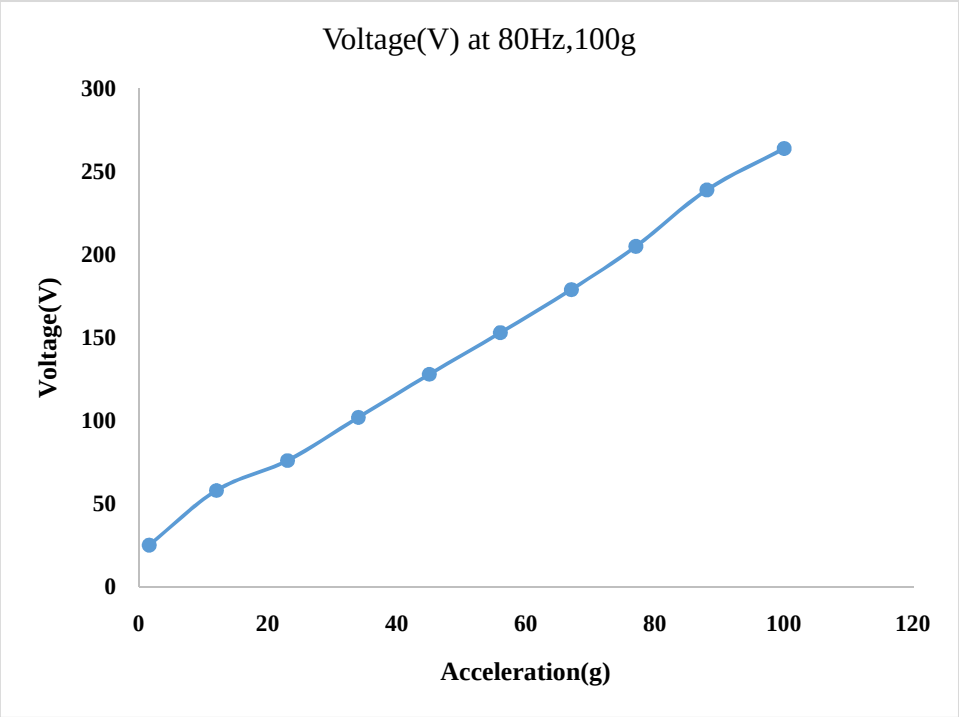

Fig. 4.61 Variation of voltage at 80 Hz under 0-100g acceleration

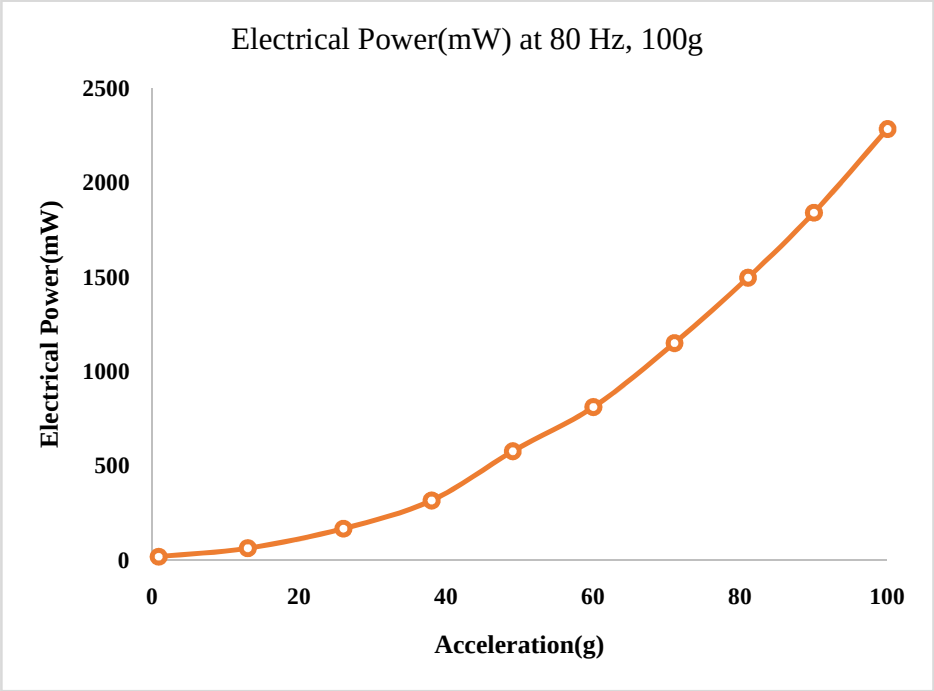

Fig. 4.62 Variation of power at 80 Hz under 0-100g acceleration

From Fig 4.59 to Fig.4.62 are shows the variation of voltage and power with respect to excited accelerations at 0-20g and 0-100g under the operated frequency of 80 Hz.

The following salient points are observed at the operated frequency of 80 Hz and at various excited accelerations.

- At 20g excited acceleration maximum voltage observed is 47 V and Power is 89 mW.
- At 40g excited acceleration maximum voltage observed is 118.13V and Power is 540 mW.
- At 60g excited acceleration maximum voltage observed is 160 V and Power is 1120 mW.
- At 80g excited acceleration maximum voltage observed is 220V and Power is 1494 mW.
- At 100gexcited acceleration maximum voltage observed is 264 V and Power is 2283 mW.

The maximum voltage is observed at the maximum force of 100g acceleration i.e., 264 V. The variation of response voltages with input excited accelerations are linear. These are satisfying the linear constitutive equation of the direct piezoelectric effect which is mentioned in international standards of American piezoelectricity. According to this equation the electrical displacement is directly proportional to the applied stress or pressure on the piezoelectric disc type actuator. The constant proportionality is called the piezoelectric coupled coefficient. This coefficient is in

times of 10^{-12} units, which plays a very important role in the generations of output voltage and power.

4.2.12 Acceleration dependence of EH at 85 Hz

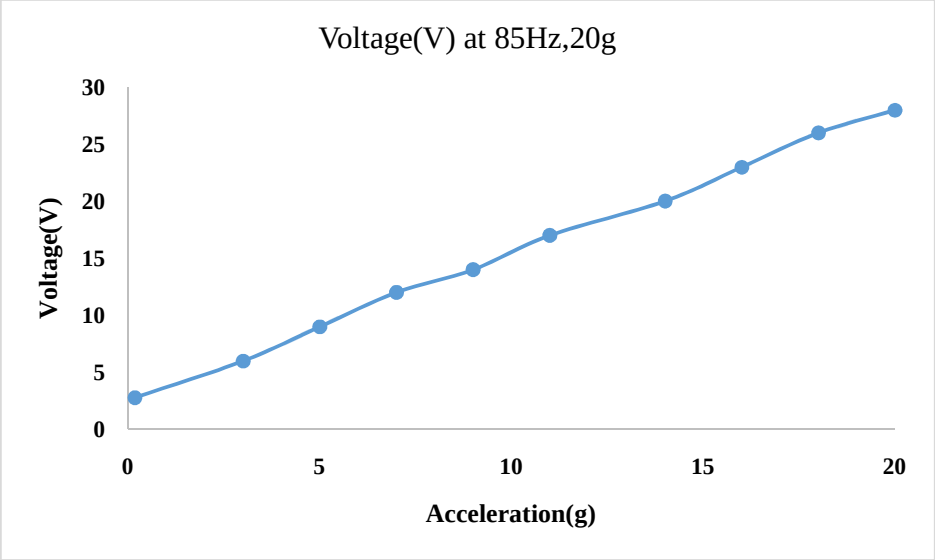

Fig. 4.63 Variation of voltage at 85 Hz under 0-20g acceleration

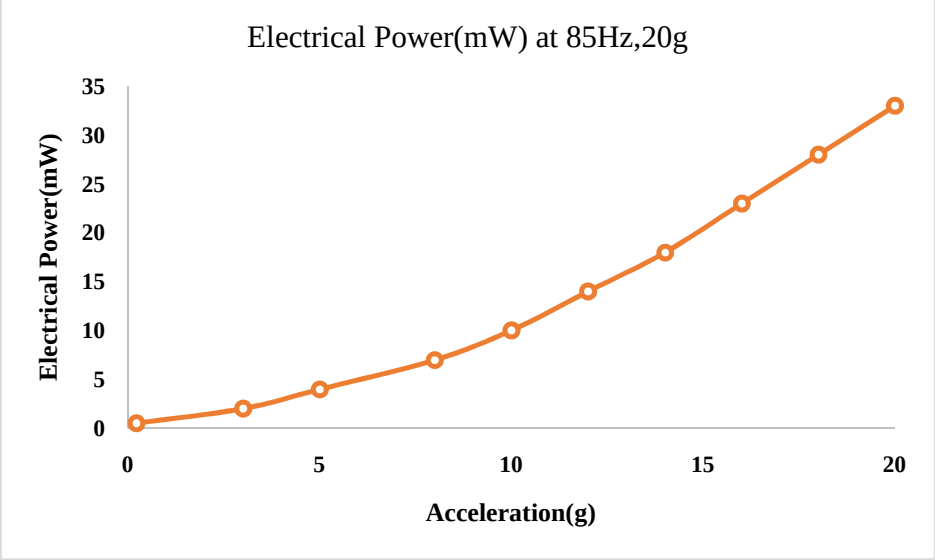

Fig. 4.64 Variation of power at 85 Hz under 0-20g acceleration

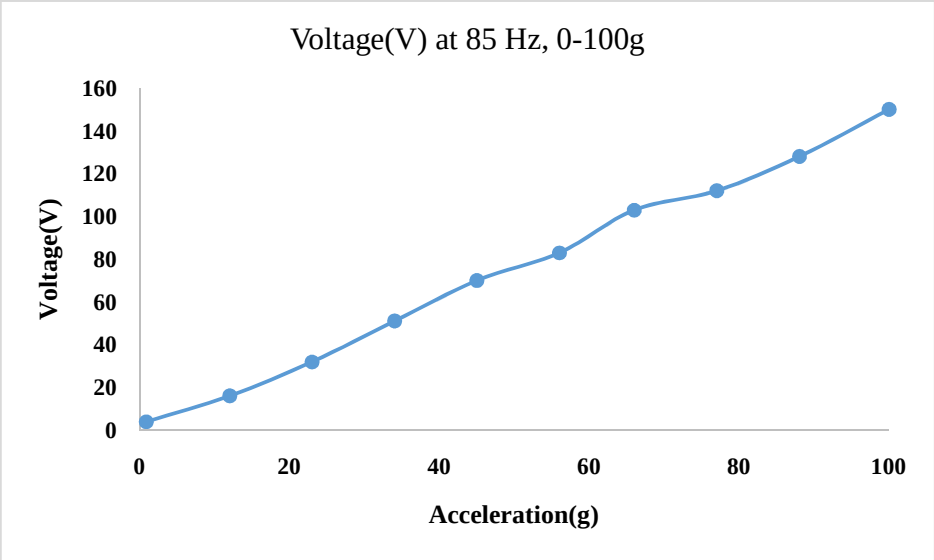

Fig. 4.65 Variation of voltage at 85 Hz under 0-100g acceleration

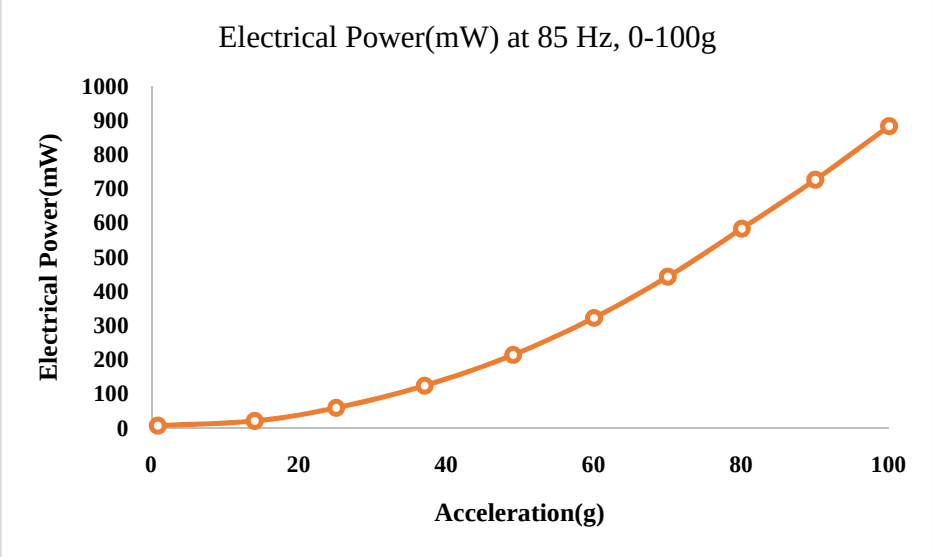

Fig. 4.66 Variation of power at 85 Hz under 0-100g acceleration

From Fig 4.63 to Fig.4.66 are shows the variation of voltage and power with respect to excited accelerations at 0-20g and 0-100g under the operated frequency of 85 Hz.

The following salient points are observed at the operated frequency of 85 Hz and at various excited accelerations.

- ❖ At 20g excited acceleration maximum voltage observed is 28V and Power is 33 mW.
- ❖ At 40g excited acceleration maximum voltage observed is 63V and Power is 180 mW.
- ❖ At 60g excited acceleration maximum voltage observed is 90 V and Power is 323 mW.
- ❖ At 80g excited acceleration maximum voltage observed is 120V and Power is 583 mW.
- ❖ At 100gexcited acceleration maximum voltage observed is 150 V and Power is 883 mW.

The minimum voltage is observed at the force of 20g acceleration i.e., 28V.The maximum voltage is observed at the maximum force of 100g acceleration i.e., 150V. The variation of response voltages with input excited accelerations are linear. These are satisfying the linear constitutive equation of the direct piezoelectric effect which is mentioned in international standards of American piezoelectricity. According to this equation the electrical displacement is directly proportional to the applied stress or pressure on the piezoelectric disc type actuator. The constant proportionality is called the piezoelectric coupled coefficient. Though, this coefficient is in times of 10^{-12} units, it may not affect to reduce the output voltage and power for charging the micro power operated electro mechanical devices.

4.2.13 Acceleration dependence of EH at 90 Hz

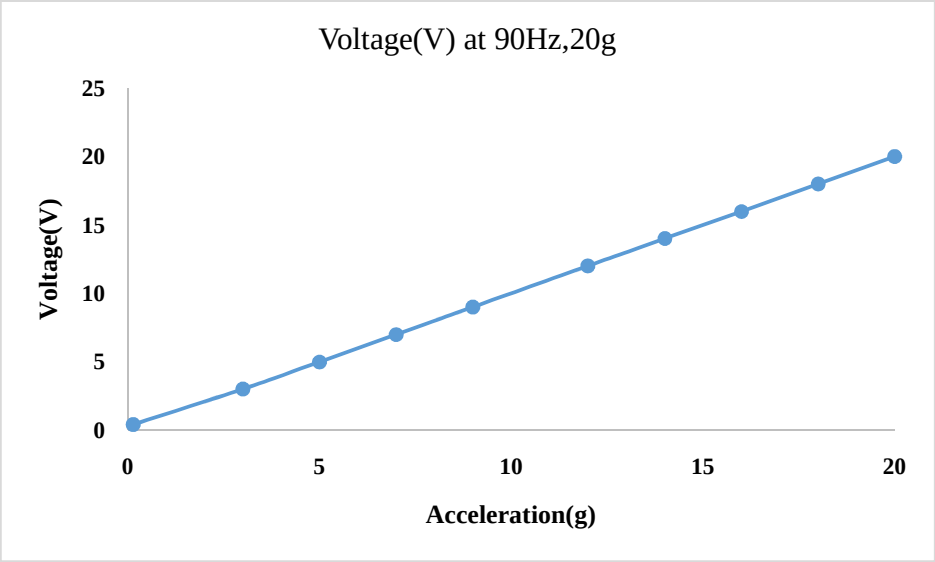

Fig. 4.67 Variation of voltage at 90 Hz under 0-20g acceleration

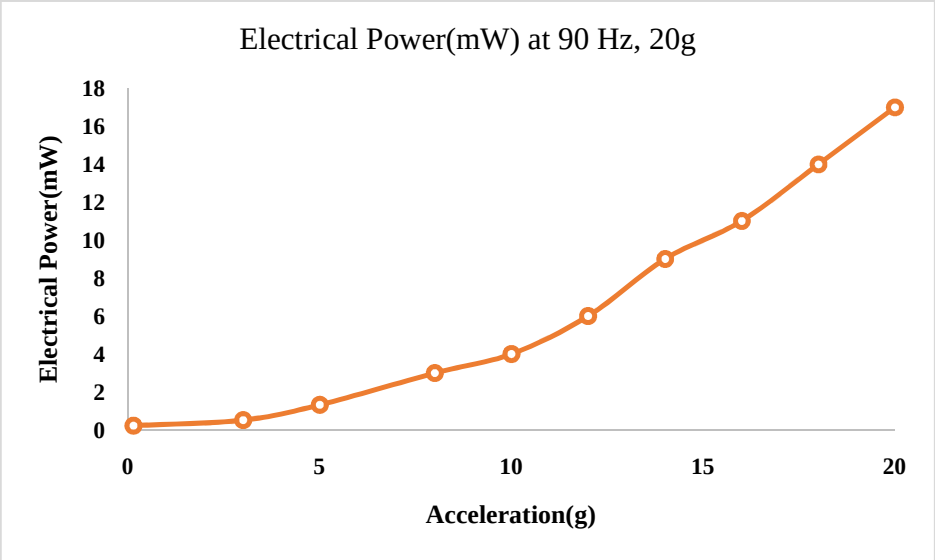

Fig. 4.68 Variation of power at 90 Hz under 0-20g acceleration

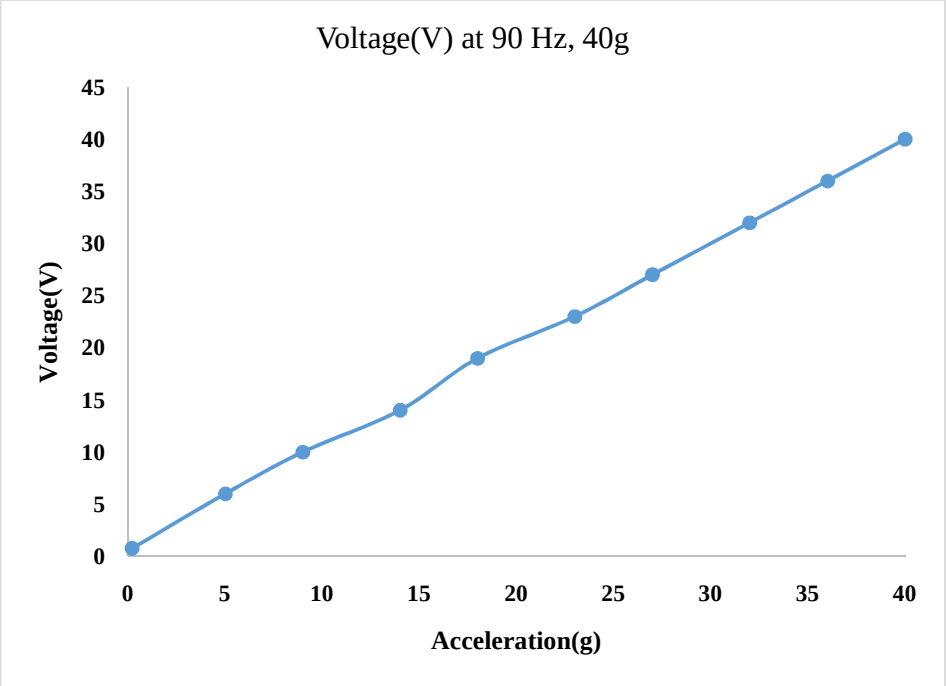

Fig. 4.69 Variation of voltage at 90 Hz under 0-40g acceleration

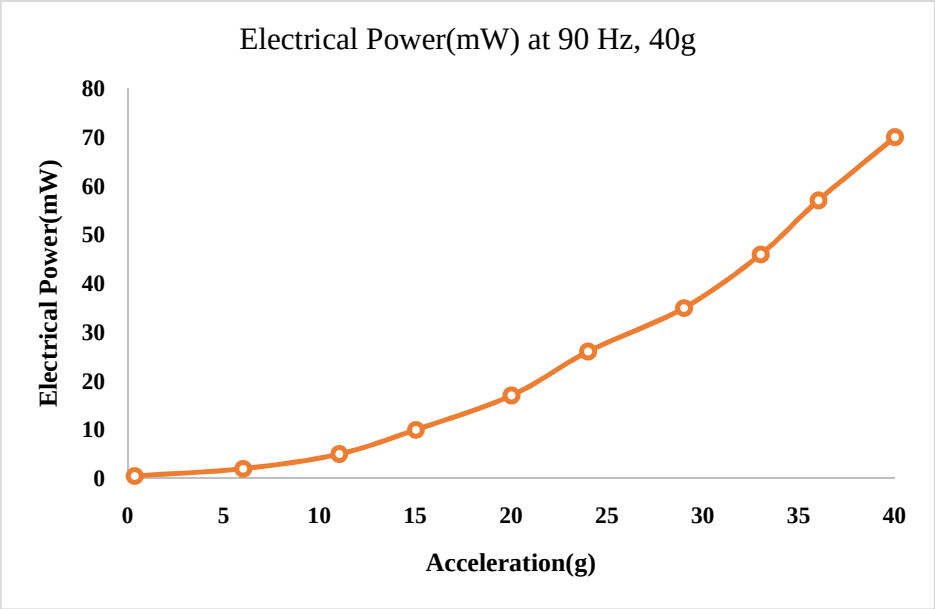

Fig. 4.70 Variation of power at 90 Hz under 0-40g acceleration

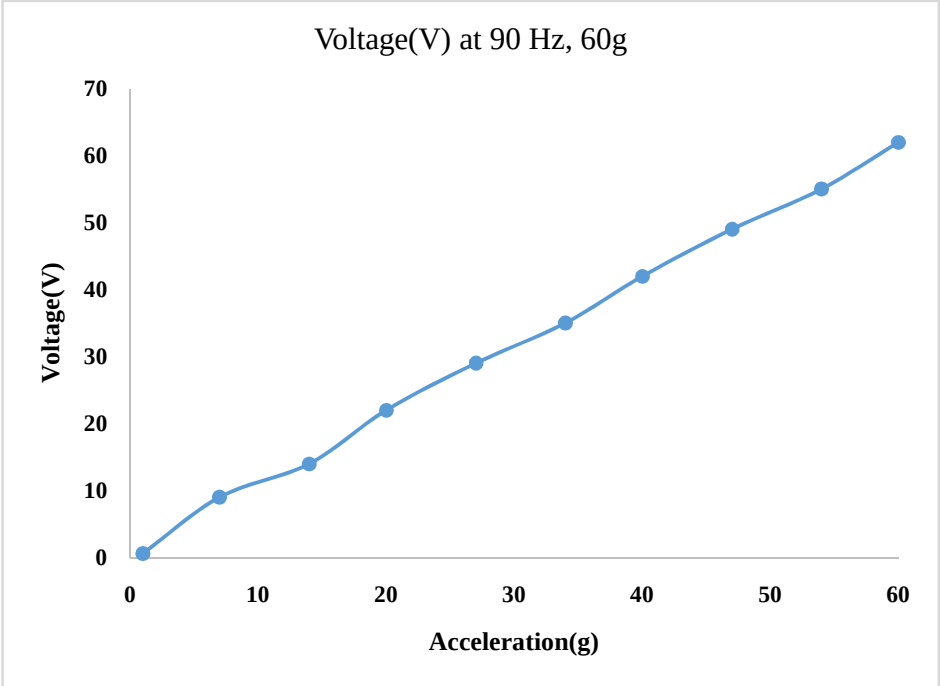

Fig. 4.71 Variation of voltage at 90 Hz under 0-60g acceleration

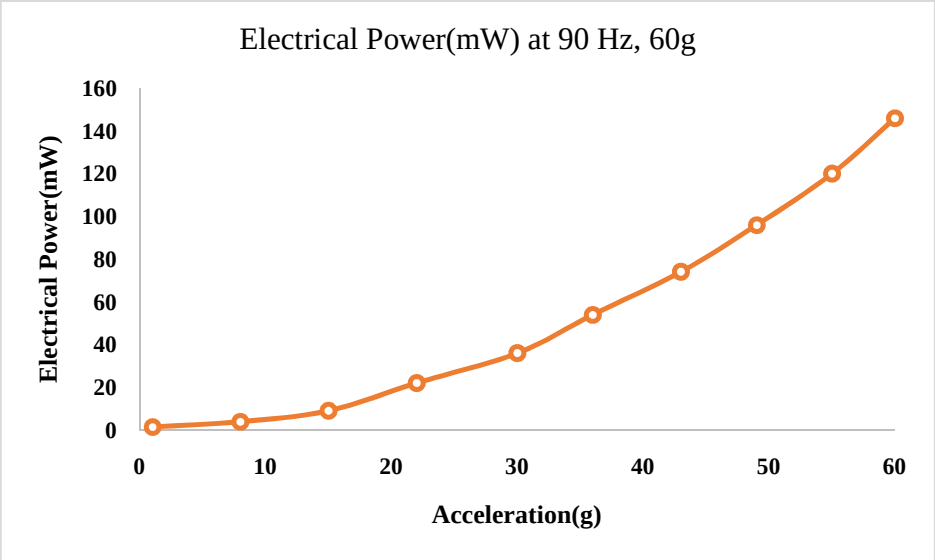

Fig. 4.72 Variation of power at 90 Hz under 0-60g acceleration

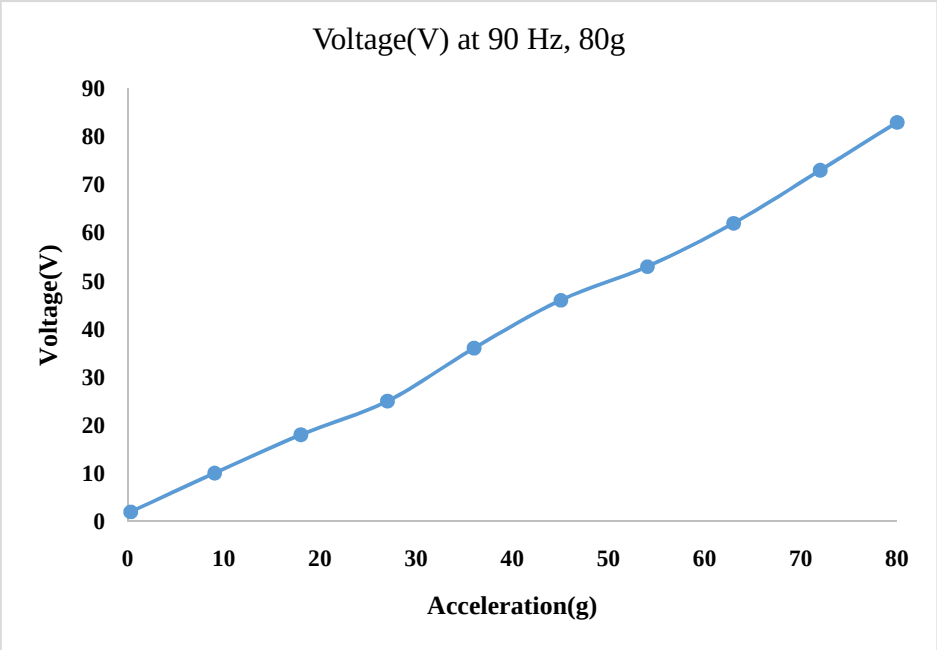

Fig. 4.73 Variation of voltage at 90 Hz under 0-80g acceleration

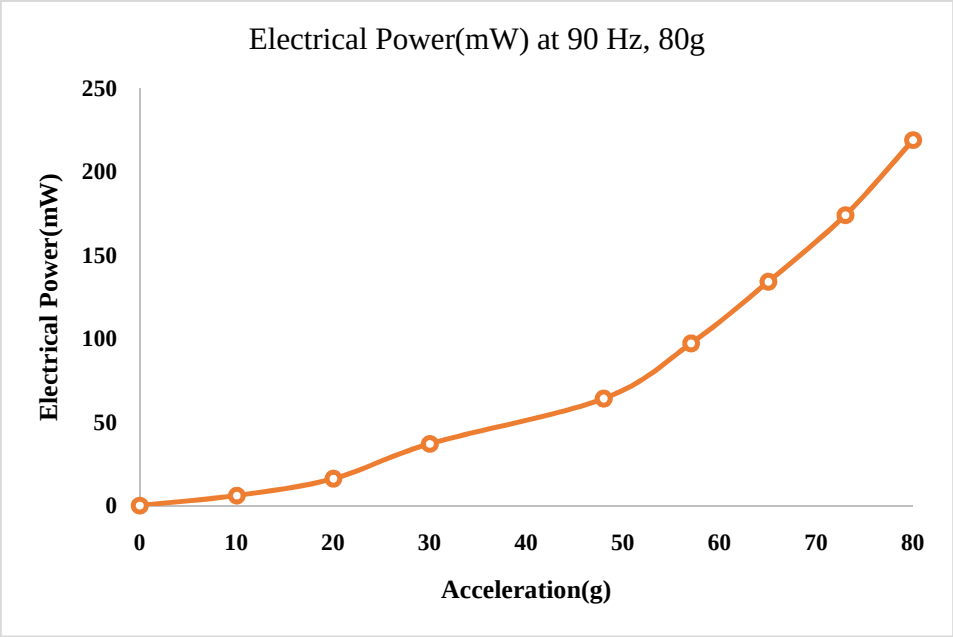

Fig. 4.74 Variation of power at 90 Hz under 0-80g acceleration

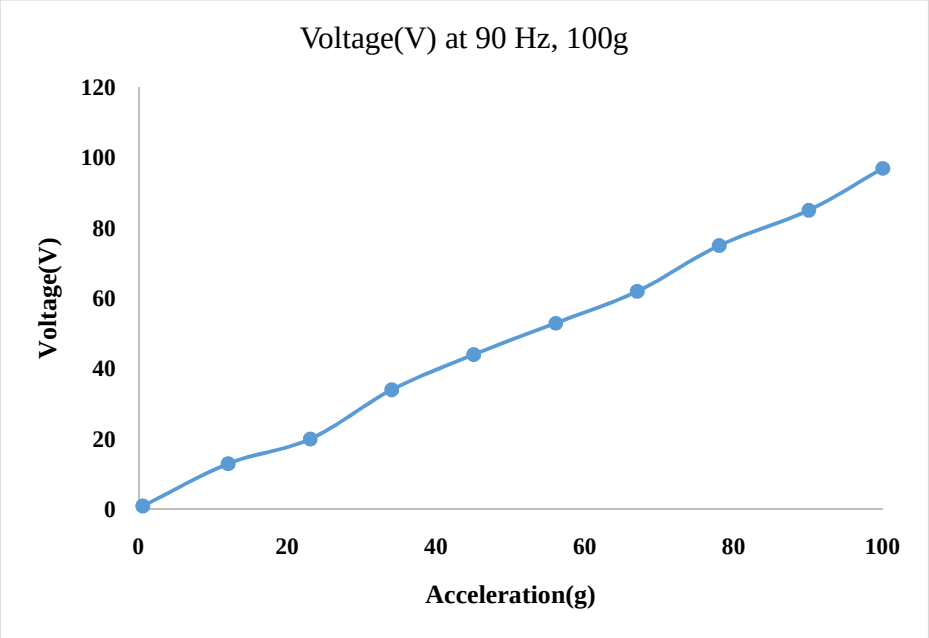

Fig. 4.75 Variation of voltage at 90 Hz under 0-100g acceleration

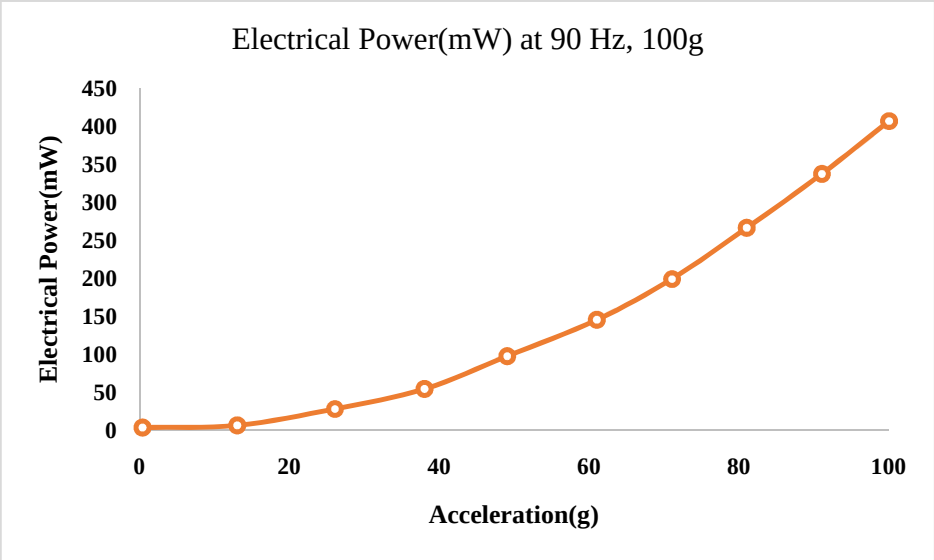

Fig. 4.76 Variation of power at 90 Hz under 0-100g acceleration

From Fig 4.67 to Fig.4.76 are shows the variation of voltage and power with respect to excited accelerations at 0-20g,0-40g,0-60g,0-80g and 0-100g under the operated frequency of 90 Hz.

The following observations are made at the operated frequency of 90 Hz and at various excited accelerations.

- At 20g excited acceleration maximum voltage observed is 20V and Power is 17 mW.
- At 40g excited acceleration maximum voltage observed is 40V and Power is 70 mW.
- At 60g excited acceleration maximum voltage observed is 62 V and Power is 146 mW.
- At 80g excited acceleration maximum voltage observed is 83V and Power is 219 mW.
- At 100gexcited acceleration maximum voltage observed is 97V and Power is 417 mW.

The minimum voltage is observed at the force of 20g acceleration i.e., 20V.The maximum voltage is observed at the maximum force of 100g acceleration i.e., 97V. The variation of response voltages with input excited accelerations are linear. These are satisfying the linear constitutive equation of the direct piezoelectric effect which is mentioned in international standards of American piezoelectricity. According to this equation the electrical displacement is directly proportional to the applied stress or pressure on the piezoelectric disc type actuator. The constant proportionality is called the piezoelectric coupled coefficient, which plays a crucial role in the analytical calculations of output voltage and power which was discussed in chapter 3.

4.2.14 Acceleration dependence of EH at 95 Hz

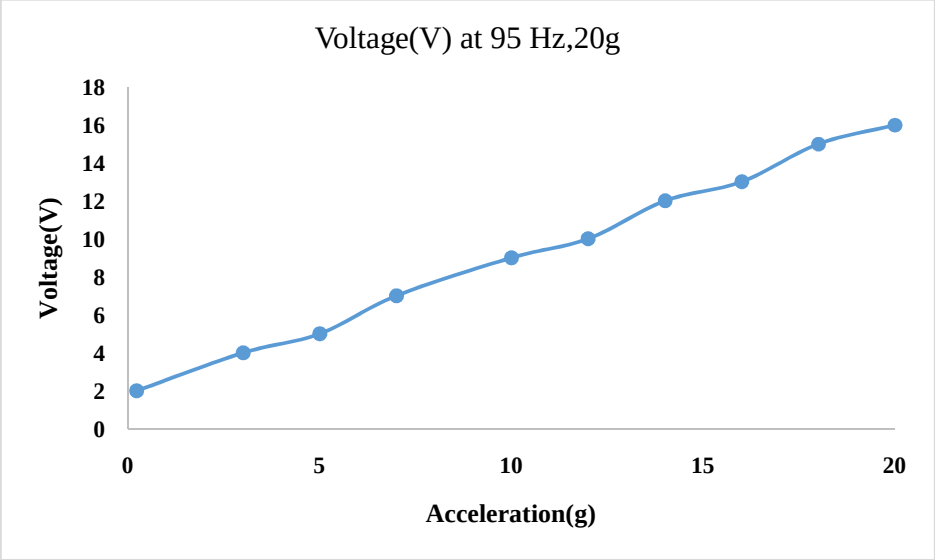

Fig. 4.77 Variation of voltage at 95 Hz under 0-20g acceleration

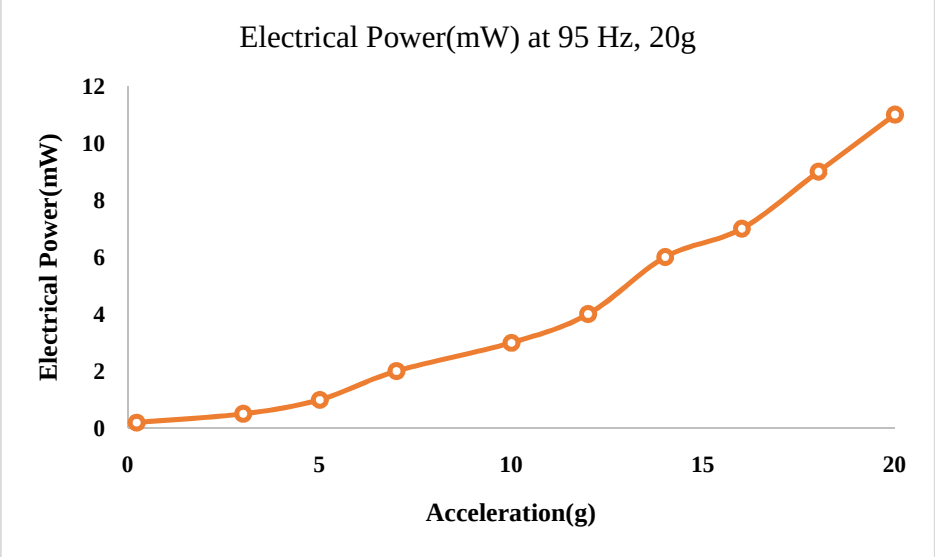

Fig. 4.78 Variation of power at 95 Hz under 0-20g acceleration

From Fig 4.77 to Fig.4.78 are shows the variation of voltage and power with respect to excited accelerations at 0-20g under the operated frequency of 95 Hz.

The following observations are made at the operated frequency of 95 Hz and at various excited accelerations.

❖ At 20g excited acceleration maximum voltage observed is 16V and Power is 11 mW, which is smaller than the 90Hz at 20g acceleration.

The maximum voltage is observed at the force of 20g acceleration i.e., 16V. The variation of response voltages with input excited accelerations are linear. These are satisfying the linear constitutive equation of the direct piezoelectric effect which is mentioned in international standards of American piezoelectricity. According to this equation the electrical displacement is directly proportional to the applied stress or pressure on the piezoelectric disc type actuator. The constant proportionality is called the piezoelectric coupled coefficient. This coefficient is 600 to 640 in times of 10^{-12} units, which plays essential role in the analytical calculations of output voltage.

4.2.15 Acceleration dependence of EH at 100 Hz

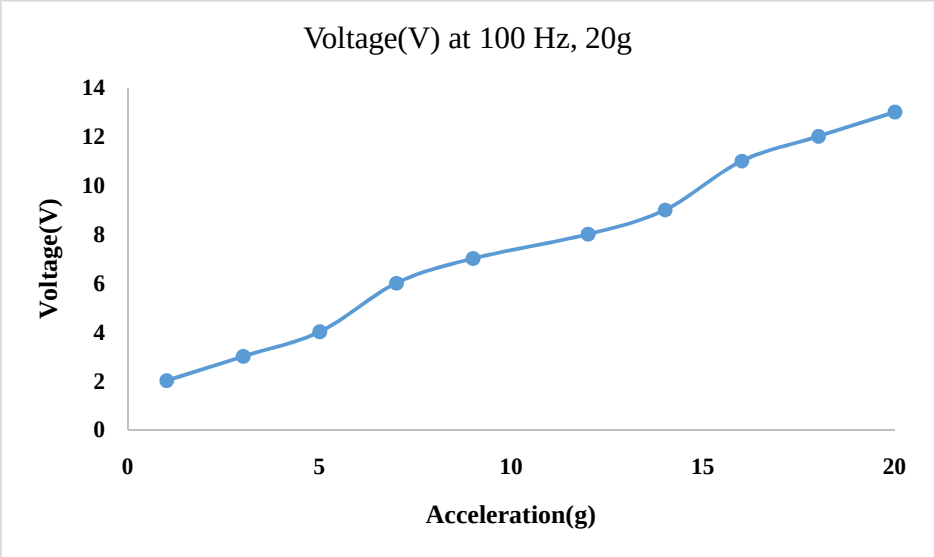

Fig. 4.79 Variation of voltage at 100 Hz under 0-20g acceleration

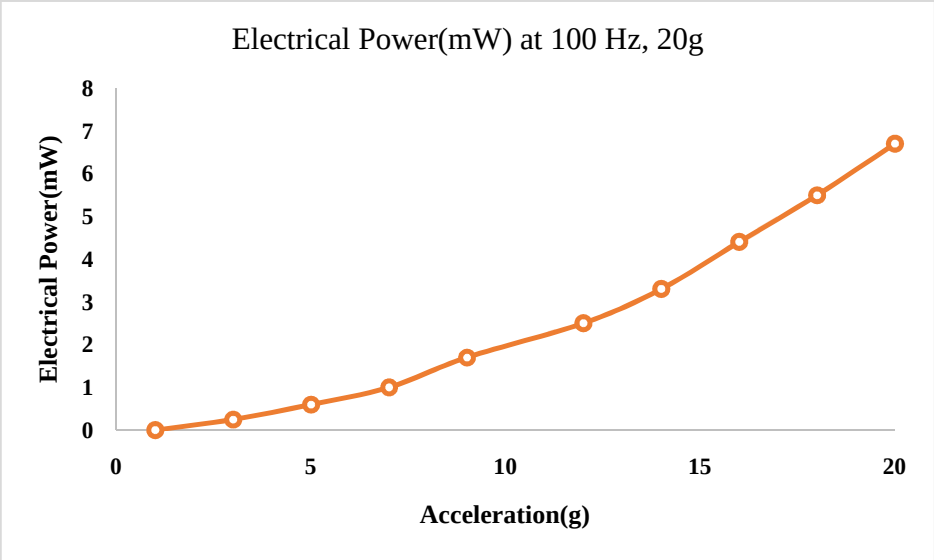

Fig. 4.80 Variation of power at 100 Hz under 0-20g acceleration

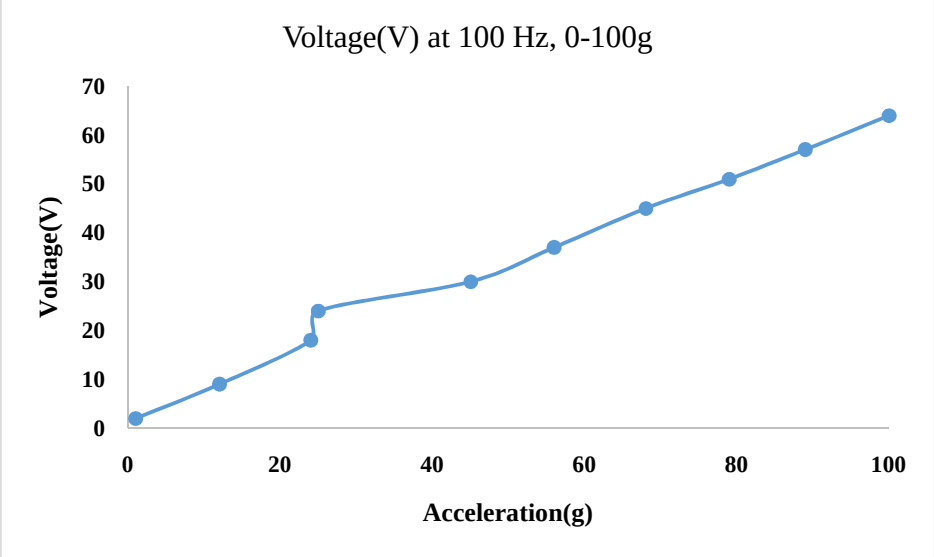

Fig. 4.81 Variation of voltage at 100 Hz under 0-100g acceleration

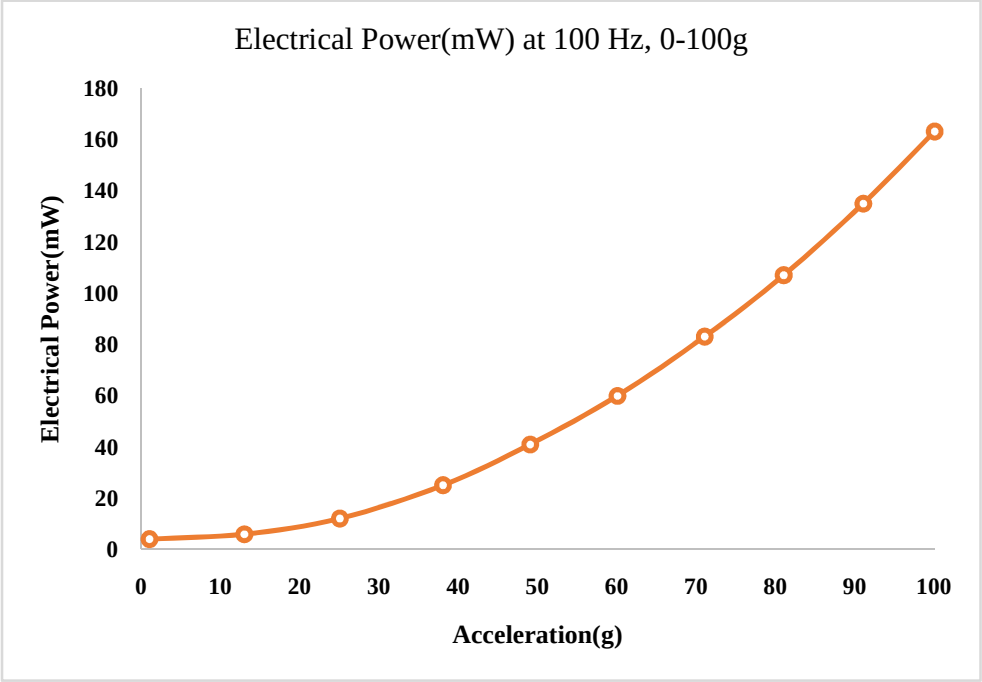

Fig. 4.82 Variation of power at 100 Hz under 0-100g acceleration

From Fig 4.79 to Fig.4.82 are shows the variation of voltage and power with respect to excited accelerations at 0-20g,0-40g,0-60g,0-80g and 0-100g under the operated frequency of 100 Hz.

The following observations are made at the operated frequency of 100 Hz and at various excited accelerations.

- At 20g excited acceleration maximum voltage observed is 13V and Power is 6.7 mW.
- At 40g excited acceleration maximum voltage observed is 28V and Power is 35 mW.
- At 60g excited acceleration maximum voltage observed is 40 V and Power is 60 mW.
- At 80g excited acceleration maximum voltage observed is 48V and Power is 106 mW.
- At 100gexcited acceleration maximum voltage observed is 64V and Power is 163 mW.

The minimum voltage is observed at the force of 20g acceleration i.e., 13V.The maximum voltage is observed at the maximum force of 100g acceleration i.e., 64V.

The variation of response voltages with input excited accelerations are linear. These are satisfying the linear constitutive equation of the direct piezoelectric effect which is mentioned in international standards of American piezoelectricity.

According to the constitutive equations of the piezoelectricity the electrical displacement is directly proportional to the applied stress or pressure on the piezoelectric disc type actuator. The constant of proportionality is called the piezoelectric coupled coefficient.

4.3 Summary of the chapter

In the chapter 3, as a prerequisite for designing the energy harvester and to know the limitations of the operating loads of the energy harvester, the mechanical and electrical properties of PZT disc type actuator have been studied.

In the chapter 4, the simulation studies of energy harvester have been done under the dependencies of frequency and acceleration as a prerequisite for designing the energy harvester. Simulation studies are also done at various frequencies and excitations of the energy harvester for optimizing the experimental work such as minimizing the time of experimentation and to evaluate the specific operated resonance frequencies for generating the maximum values of voltage and power

The direct piezoelectric transduction mechanism is applied on the piezoelectric disc type actuators. Distributed parameter model is considered and excited at various accelerations.

The output voltage and output power are measured and observed their behaviour with respect to input excited accelerations. It is observed that the output power is followed by the quadratic non linearity and is proven by the ohm's law ($P= V^2/R$) and the output voltage varied linearly with the input excitations; and these results are confirmed by the regression analysis.

Resonance and non resonance frequencies of the energy harvester are studied through simulation studies. The maximum values of voltage and power are observed at the resonance frequencies. The minimum values of voltage and power are observed at non resonance frequencies. Although the excitation of the acceleration is high, however, maximum voltage and power cannot be obtained if the energy harvester is not excited with resonance frequency.

At the resonance frequency, however, the piezoelectric constant does not vary with the various excitations but effects the development of dynamic strain in piezoelectric disc type actuator,

which can be considered as one of the reasons for obtaining the maximum generated values of voltage and power.

Simulation studies of energy harvester are quintessential to design and to know the operating frequencies of the energy harvesters; therefore simulation studies are done in this chapter 4.

In the next chapter, simulation results of energy harvester are validated by the experimental values of energy harvester. The validation of results is done at various frequencies but at 20g excitation based on the availability of experimental facility.

Chapter 5

Experimental Studies of Energy Harvester

5.1. Design procedure of energy harvester

Based on the prerequisite work of research, it is observed that the maximum researchers had contributed in the vibration energy harvesting is by using cantilever beam with tip mass for dynamic flexibility of the beam. PZT 5H rectangular unimorph and bimorph patches are used on the sub structure in the longitudinal direction in d_{31} mode. In this device there are three parts ie. lead material, PVC pipe and piezoelectric disc type actuators (PZT 5H). Pipe dimension is 15 mm X 28 mm, mass 5gm (10mm X 5mm) and piezo 35 mm X 0.2 mm. In a pipe there is one slot in which two piezo elements are placed and one lead mass is put in middle upper and bottom of the piezoelectric disc type actuators. The prototype model of energy harvester (EH) is shown in Fig 5.1(a) & (b).

5.1.1. Design of lead cylinder

Lead has good impact properties so it is selected as material for impacting. Lead is very soft, highly malleable, ductile, and a relatively poor conductor of electricity. It is very resistant to corrosion The shape of the hitting mass is cylindrical so that area of contact is larger and it can produce uniform impact force on piezoelectric disc type actuator. The dimensions are chosen as 5mm thickness and 10 mm diameter. Density of lead is 11.35 g/cm^3. Mass of piezoelectric elements as $m = V \times °$ Where, V= volume of hitting mass, ° =Density of lead

$$m = \frac{® d^2}{4} \times l \times ° \qquad (5.1)$$

Where, d= diameter of hitting mass= 10 mm, l= length of a mass= 5mm

m= 4.45 gm ≈ 5 gm

5.1.2 Design of PVC cylinder

The cylinder is to be designed to fit piezoelectric elements in it also to carry hitting masses in it. The inner and outer diameter of a cylinder is chosen as 28 mm and piezoelectric elements can fit properly in it. Cylinder is made with one compartment with 2 piezoelectric elements. This compartment carries a hitting mass.

The total length of cylinder is taken as 15 mm so that compartment length is 15 mm. This gives the enough space to hitting mass to oscillate. However the more accurate length of compartment can be found by experimental analysis.

The material for cylinder is plastic PVC (polyvinyl chloride) pipe as it is having good mechanical properties. PVC is general purpose plastic. It is amorphous in nature. It can be cut easily for manufacturing and it is cheap. The density of PVC is 1.4 g/cm^3.

Mass of cylinder, $M = V \times ° = 207$ gm

Where, V= volume of cylinder, density of PVC, ° = 1.4 g / cm^3

d_o = outer diameter of cylinder = 28 mm,

Table 5.1 Geometry properties of energy harvester

PVC pipe	15 mm X 28 mm
Piezoelectric disk	35 mm X 0.2 mm
Lead mass	5 gm

5.1.3 Material properties of piezoelectric disc type actuator

PZT disc is having a density of 7600 kg/m^3, Voltage Constant is 24.8x10^{-3} m^2/C, Relative Dielectric constant(K^T)= 1900, Young's modulus (E)= 6.3x10^{10} N/m^2,Piezoelectric Charge Constant (10^{-12}C/N or10^{-12} m/V) , d_{33}= 630 , PVC is having a density ° = 1.35 – 1.45 (g/cm^3), Modulus of elasticity (E)=51 GPa and lead Density ° = 11.3 g.cm^{-3}, Young's modulus (E)=16 GPa and Poisson's ratio(μ)=0.44[15]. The mass of the EH is 0.3 Kg.

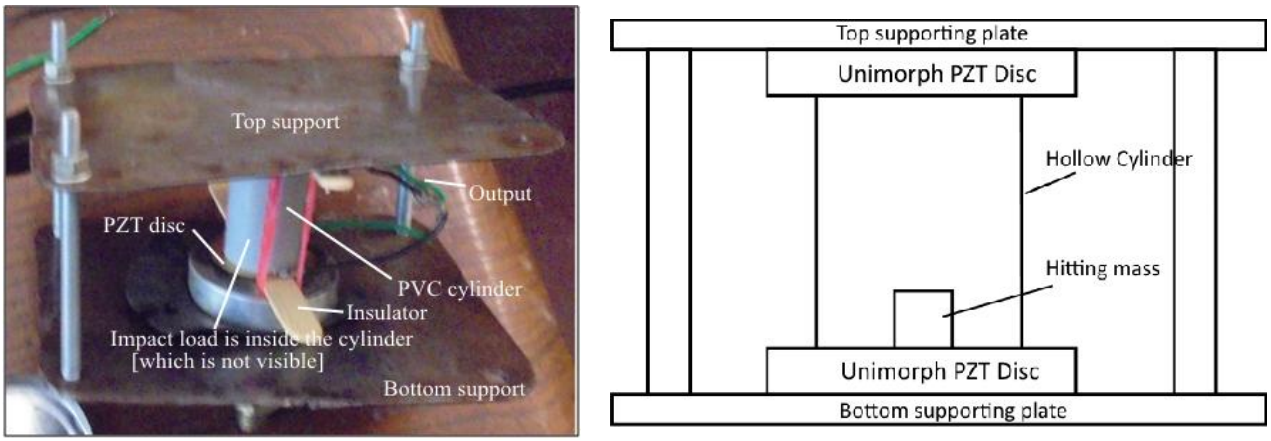

Fig. 5.1 (a) Prototype Model of Energy Harvester (b) Schematic diagram of EH

5.2 Experimental results

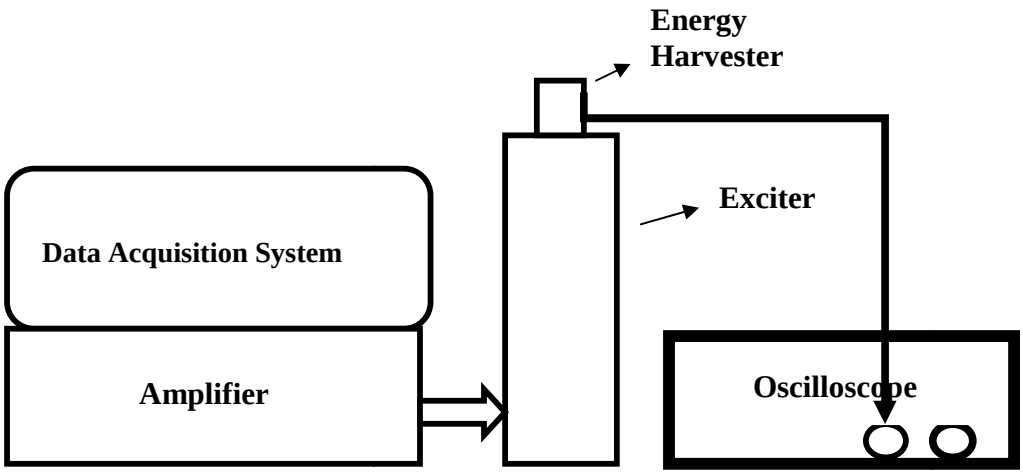

Fig.5.2 Schematic diagram of experimental set up with energy harvester

The schematic diagram of experimental setup with energy harvester is shown in Fig.5.2. It consists of four parts, i) Amplifier ii) Electro-dynamic exciter iii) Oscilloscope and iv) Data acquisition system. These parts are explained later briefly. Fig.5.4 represents the actual model of power oscillator.

5.2.1 Digital storage oscilloscope

Fig. 5.3(a) Digital signal oscilloscope

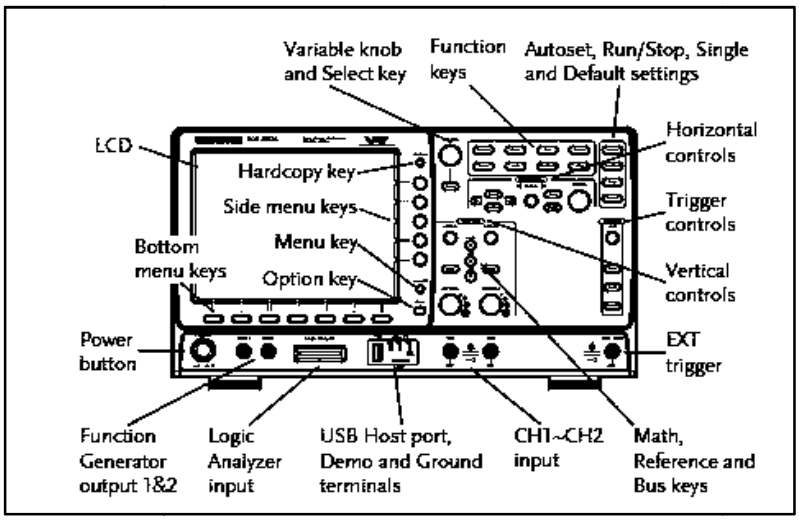

Fig. 5.3(b) Front panel of Digital signal oscilloscope

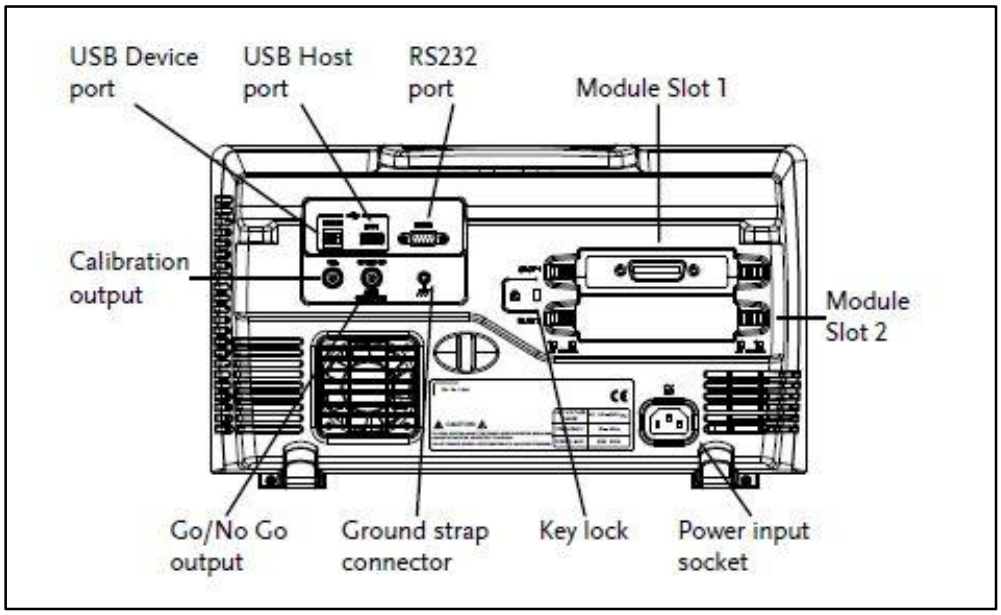

Fig. 5.3(c) Rear panel of Digital signal oscilloscope

Figure 5.3(a), (b) & (c) shows a digital oscilloscope model GWINSTEK GDS-2104A, is an instrument which used for converting the displaying the output of the energy harvester when it is under excitation during experimentation. And displays the analog signal and stores it in digital form for signal processing. Sinusoidal excitation is given to piezoelectric energy harvester through 20g Syscon vibration shaker. Fig.5.3(c) represents the rear panel of digital signal oscilloscope.

5.2.2 Power oscillator

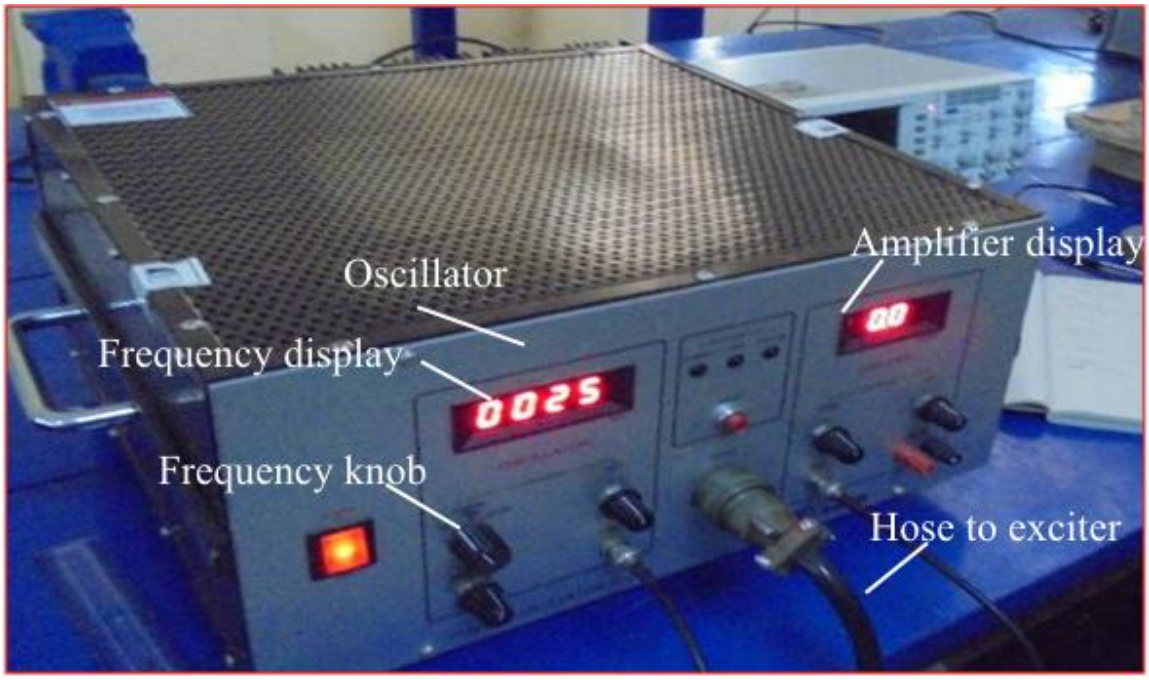

Fig.5.4 Oscillator with Amplifier

This power oscillator consists of two parts. One is Oscillator and another one is amplifier.

5.2.3 Electro-Dynamic Exciter

Fig.5.5 represents the complete experimental set up for testing the energy harvester. It consists of electro dynamic exciter for exciting the energy harvester, a four channeled digital signal oscilloscope, Oscillator, Amplifier and connecting cable. Prototype model of Energy harvester is shown in Fig.5.4. Oscillator can give frequency from 25 Hz to 20 KHz. In order to enhance maximum dynamic strain in the piezoelectric disc type actuator, the lead mass should impact more load with high amplitude, therefore operating the energy harvester at low frequencies such as 25 Hz to 100 Hz is preferred.

Fig.5.5 Electro dynamic exciter

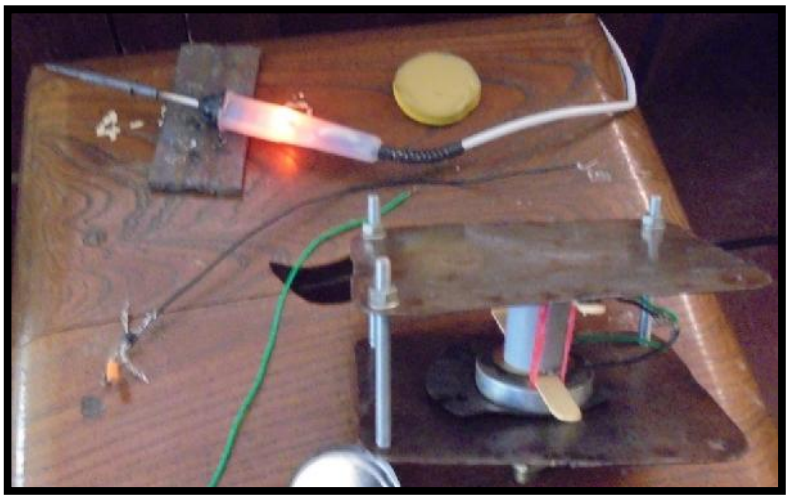

Fig.5.6 Prototype model of Energy Harvester

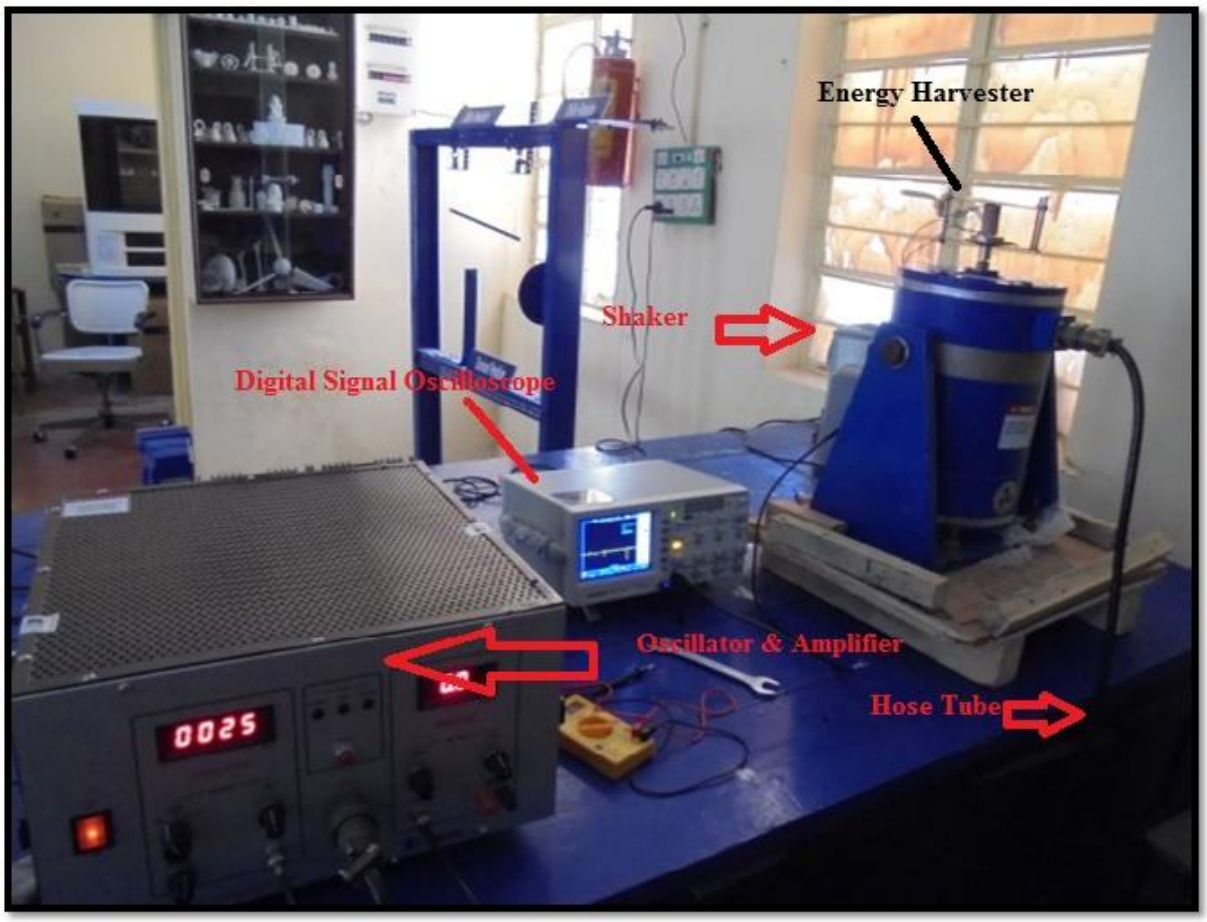

Fig.5.7 Energy harvester on Exciter

The total weight of the exciter is 40 kg. It can withstand payload up to 3 kg. The weight of the energy harvester is 0.3 kg.

5.3 Experimental results of Energy Harvester

5.3.1 Energy Harvester at 70 Hz at the input excitation of 20 g

The prototype model of energy harvester is mounted on exciter and excited through oscillator at various frequencies from 25 Hz to 100 Hz. The maximum voltage observed between 70 Hz to 80 Hz and at 90 Hz, therefore, energy harvester is tested experimentally at 70 Hz, 73.5 Hz, 75.5 Hz, 80 Hz and 90 Hz. The simulation results are validated with experimental results. The energy harvester is tested at the frequency of 70 Hz under the input excitation of 20g. The voltage verses time signal is recorded by digital signal oscilloscope. The variation of voltage with respect to

time under the excitation of 20g at the frequency of 70 Hz is shown in Fig.5.8. The observed peak voltage is 68 V.

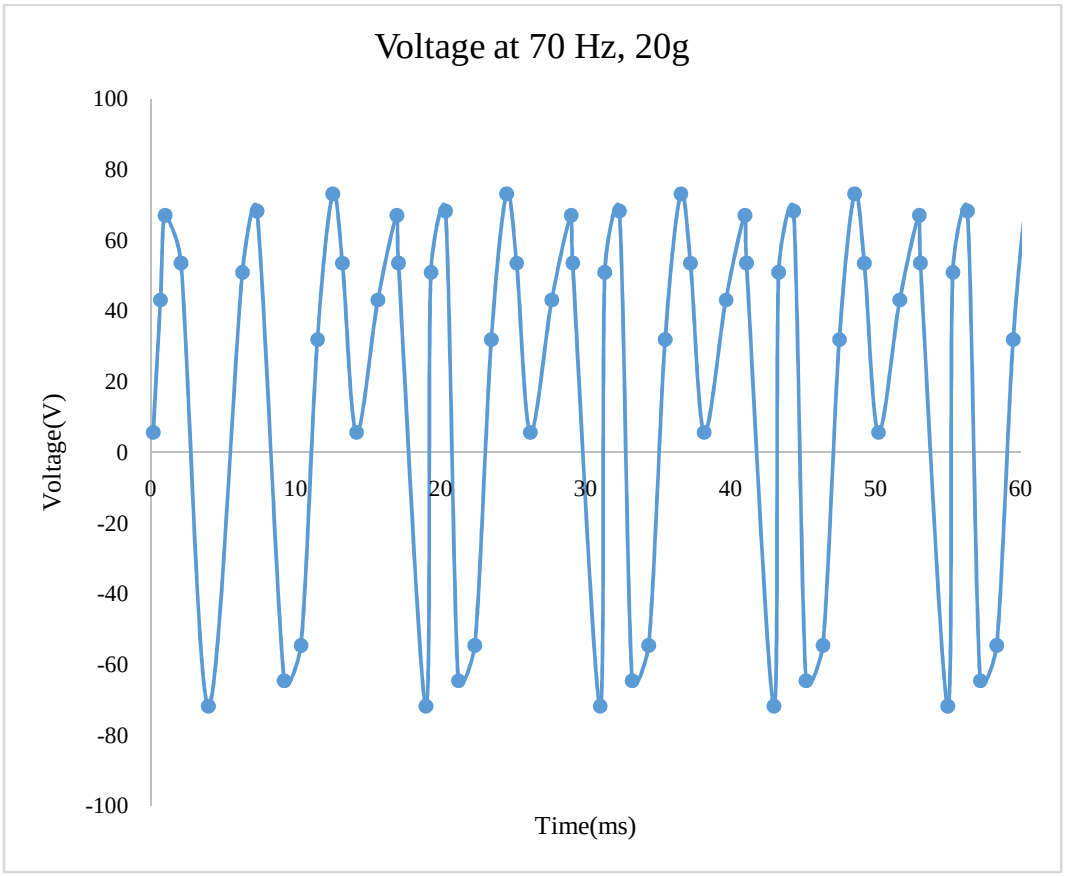

Fig.5.8 Output Voltage at 70 Hz

5.3.2 Energy Harvester at 73.5 Hz at 20g

The energy harvester is tested at the frequency of 73.5 Hz under the input excitation of 20g. The voltage verses time signal is recorded by digital signal oscilloscope. The variation of voltage with respect to time under the excitation of 20g at the frequency of 73.5 Hz is shown in Fig.5.9. The observed peak voltage is 115 V.

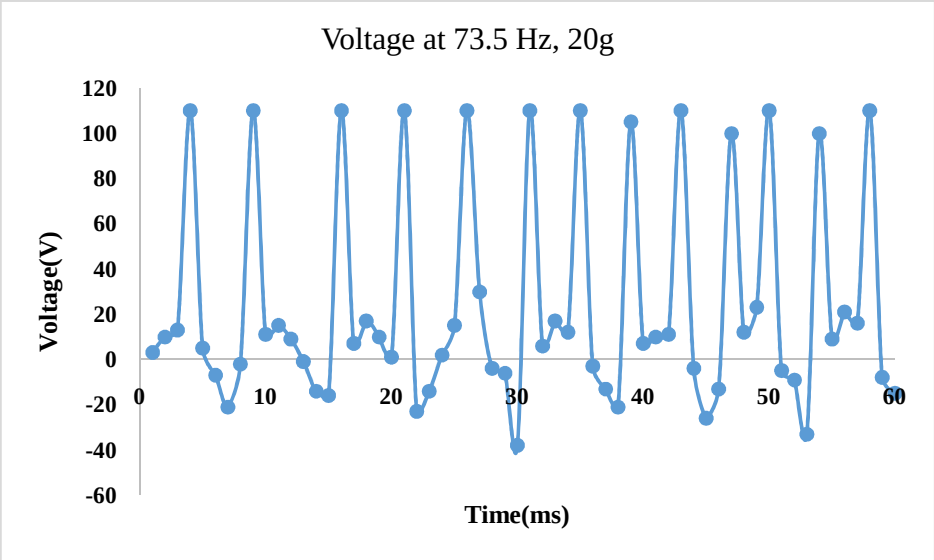

Fig.5.9 Output Voltage at 73.5 Hz

5.3.3 Energy Harvester at 75.5 Hz at 20g

The energy harvester is tested at the frequency of 75.5 Hz under the input excitation of 20g. The voltage verses time signal is recorded by digital signal oscilloscope. The variation of voltage with respect to time under the excitation of 20g at the frequency of 75.5 Hz is shown in Fig.5.10. The observed peak voltage is 85 V.

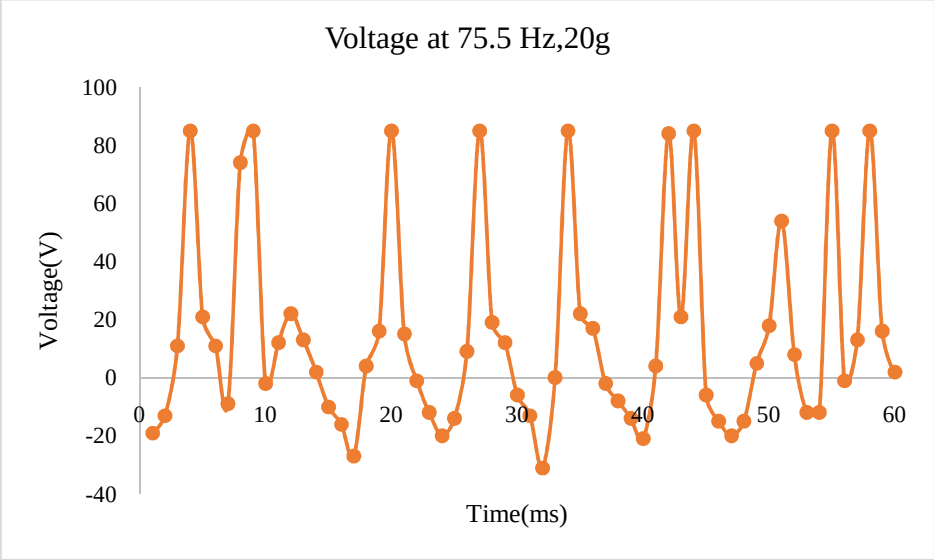

Fig.5.10 Output Voltage at 75.5 Hz

5.3.4 Energy Harvester at 80 Hz at 20g

The energy harvester is tested at the frequency of 80 Hz under the input excitation of 20g. The voltage verses time signal is recorded by digital signal oscilloscope. The variation of voltage with respect to time under the excitation of 20g at the frequency of 80 Hz is shown in Fig.5.11. The observed peak voltage is 50 V.

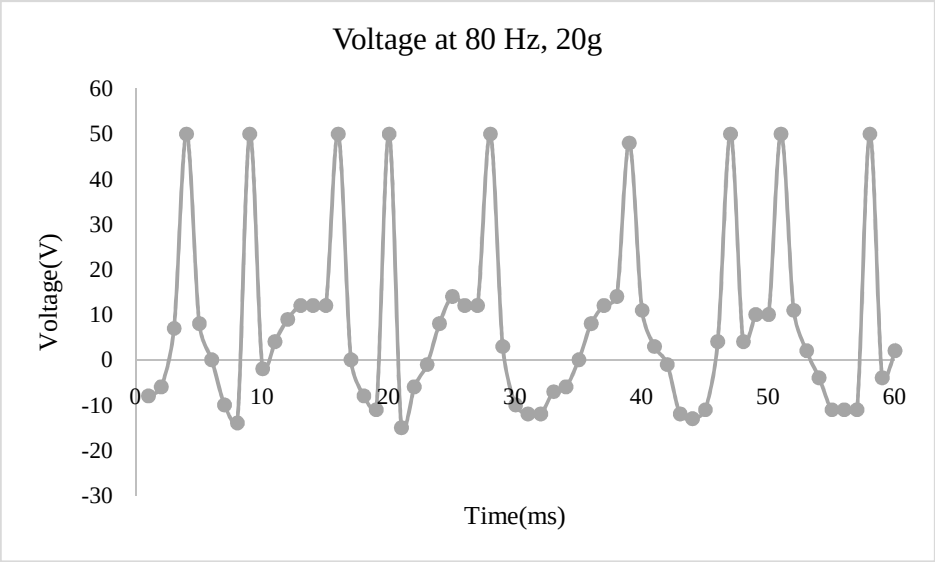

Fig.5.11 Output Voltage at 80 Hz

5.3.5 Energy Harvester at 90 Hz at 20g

The energy harvester is tested at the frequency of 90 Hz under the input excitation of 20g. The voltage verses time signal is recorded by digital signal oscilloscope. The variation of voltage with respect to time under the excitation of 20g at the frequency of 90 Hz is shown in Fig.5.12. The observed peak voltage is 19 V.

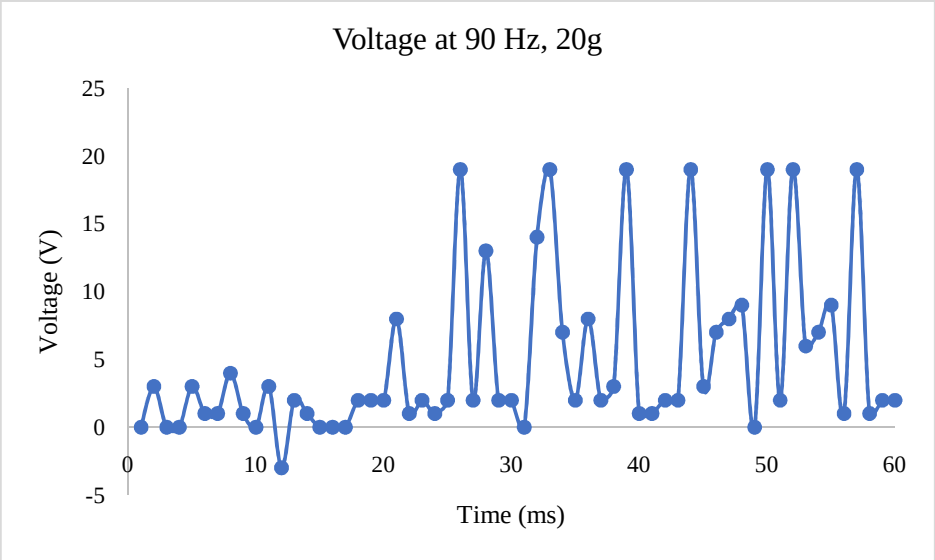

Fig.5.12 Output Voltage at 90 Hz

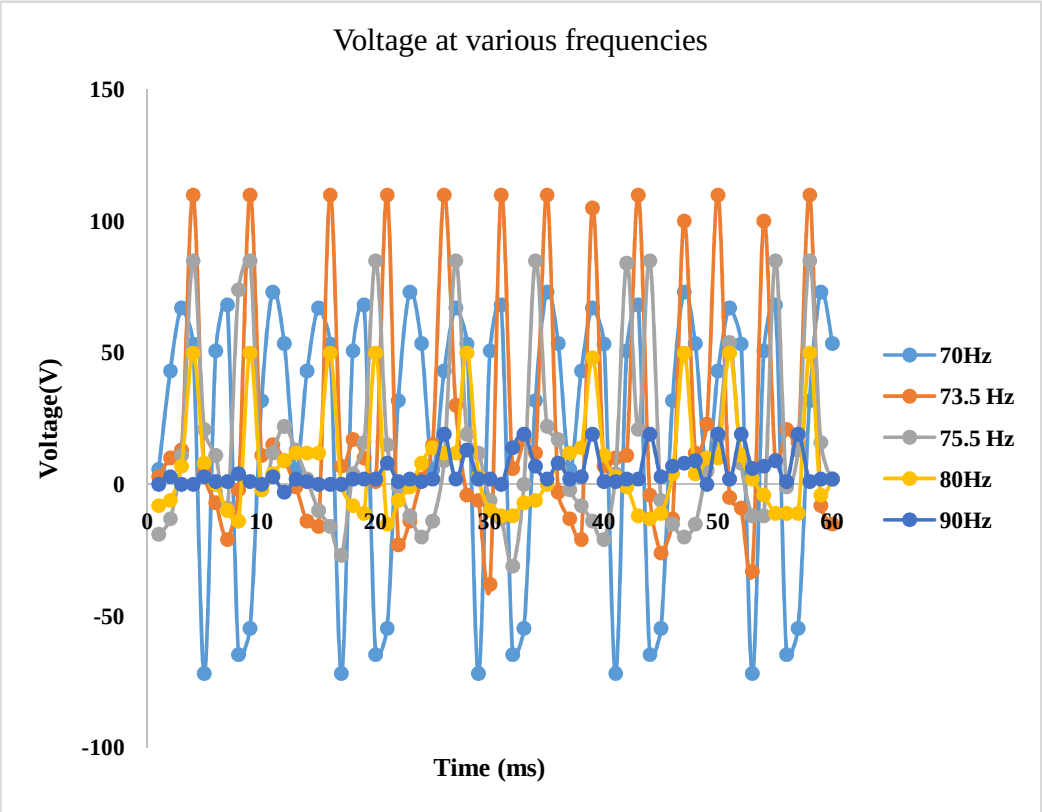

Fig.5.13 Output Voltage at various frequencies

The response of voltages at various frequencies such as 70 Hz, 73.5 Hz, 75.5 Hz, 80 Hz and 90 Hz is shown in Fig. 5.13. Through this figure the comparison of voltages in relation to other frequencies can be understood. The maximum voltage is observed at the frequency of 73.5 Hz under the input excitation of 20g.

5.3.6 Comparison of Analytical and Experimental results at various frequencies

Table 5.2 Comparison of analytical and experimental values at 20 g

Frequency (Hz)	Analytical Voltage in V	Experimental Voltage in V	% Error
70	73	68	7.4
73.5	110	115	4.3
75.5	92.17	85	8.4
80	47	50	6
90	20	19	5.3

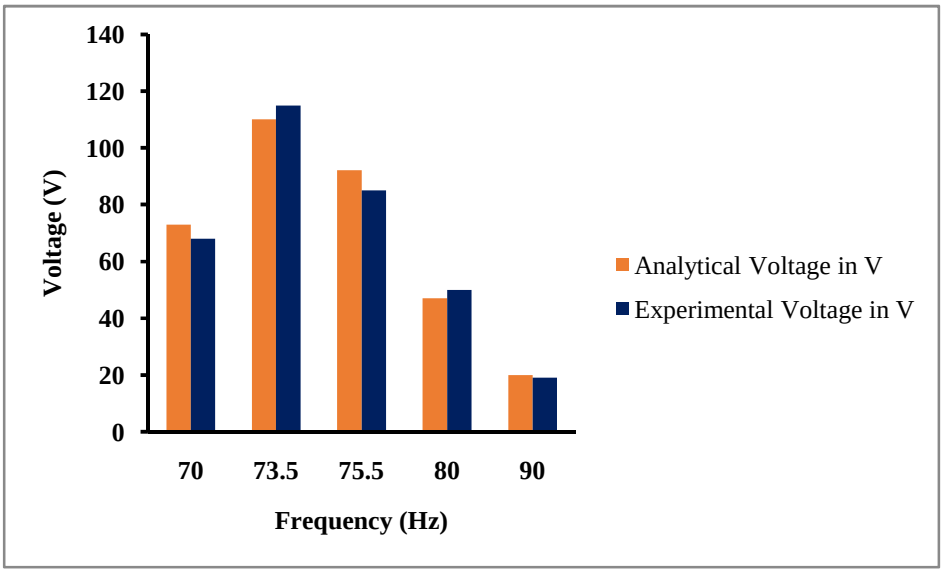

Fig.5.14. Comparison of analytical and experimental results at 20g

Analytical results which are described in the **chapter 4** are validated with the experimental results at the frequencies of 70 Hz, 73.5 Hz, 75.5 Hz, 80 Hz and 90 Hz. Table 5.2 shows the comparison of the results of analytical and experimental values at the frequencies of 70 Hz, 73.5 Hz, 75.5 Hz, 80 Hz and 90 Hz. More dynamic strain is observed at 73.5 Hz and the less dynamic

stain is observed at 90 Hz in the energy harvester. It may be understood based on the principles of piezoelectric energy harvesting [15] that the frequency at which the maximum voltage is obtained is considered as resonance frequency; therefore 73.5 Hz is the resonance frequency for this energy harvesting device.

5.4 Effect of temperature on energy harvester (EH)

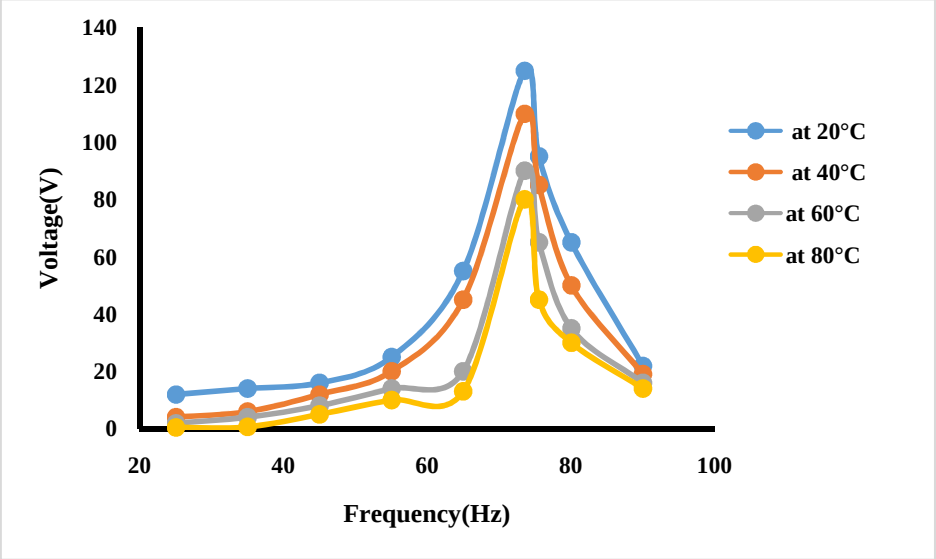

Fig.5.15 Output Voltage at various temperatures between 25 Hz to 90 Hz

Fig.5.15 shows the variation of voltage under various temperatures at the frequency range of 25 Hz to 90 Hz. In this figure the resonance frequency seems very closure to 80 Hz. It is required to draw the graph from the frequency range of 65 Hz to 90 Hz for observing the maximum voltage and optimum frequency value; therefore Fig.5.16 is drawn. The piezoelectric disc type actuators are heated in the electric oven at 20^0C, 40^0C, 60^0C and 80^0C for a period of one hour and tested on 20g exciter under sinusoidal excitation at the frequencies of 25 Hz, 35 Hz, 45 Hz, 55 Hz, 65 Hz, 70 Hz, 73.5 Hz, 75.5 Hz, 80 Hz and 90 Hz. The effect of temperature on the energy harvesting device is studied. At 20^0C: V peak is 122 V and at 80^0C: V peak is 80 V. The output power as a function of temperature can be calculated by the change of piezoelectric coupling constant that is proportional to piezoelectric constant and inverse of square root of dielectric constant [68].It may be the reason that the low temperature of the environment raises the brittle nature of the lead zirconate titanate; therefore, dynamic strain can be increased to

increase the output voltage generation. The value of coupling coefficient can be increased by decreasing of temperature. Fig.5.16 shows the variation of voltage at various temperatures under the excitation of 65 Hz to 90 Hz. The maximum voltage is observed at the frequency of 73.5 Hz and 20^0C.

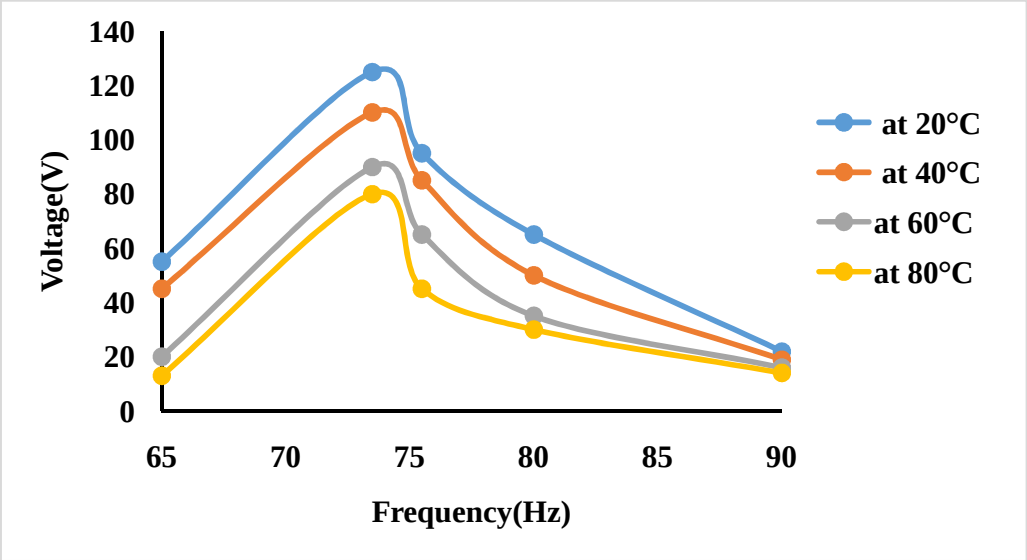

Fig.5.16 Output Voltage at various temperatures between 65 Hz to 90 Hz

5.5 Power Conversion from AC to DC

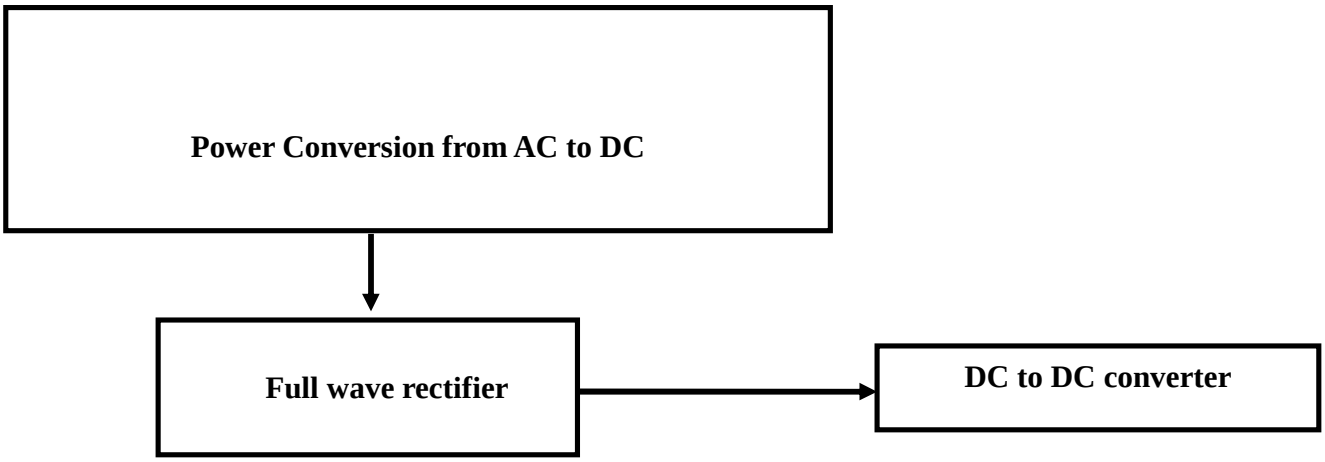

Fig.5.17 Pictorial presentation of power conversion

Effect of temperature on the performance of energy harvester is studied so far. Factually, the voltage is generated from energy harvester is alternating current (AC). Many power electronic devices functions on direct current but not on AC, therefore conversion of power is much needed. The pictorial presentation of power conversion is shown in Fig.5.17. Full wave rectifier is used to convert power from AC to DC. In order to study theoretically MATLAB Simulink tool is used, therefore Full wave rectifier circuit is shown in Fig.5.18.

5.6 Rectification of the output of energy harvester from AC to DC

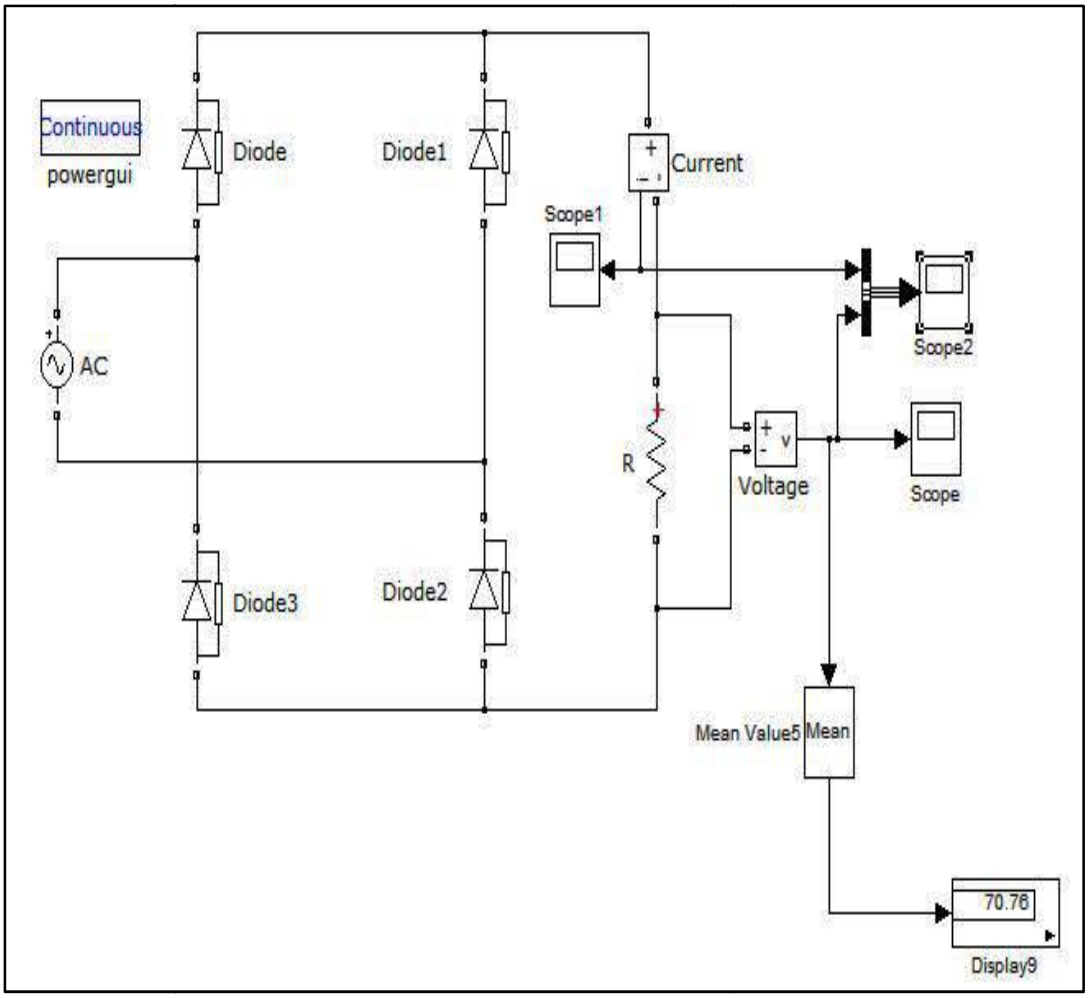

Fig.5.18 Simulink model of Full wave rectifier

A full wave rectifier is able to produce a positive half cycle for both the positive and negative half cycles (full wave) of the applied AC Voltage. The bridge rectifier accomplishes this by

using 4 diodes in a ‘bridge’ configuration.Fig.5.19 to Fig.5.21 shows the input parameters of Full wave rectifier. The input peak voltage is considered the maximum voltage and frequency obtained from analytical solutions i.e. 110 V and 73.5 Hz; therefore, AC to DC rectification is done for the voltage of 110 V at 73.5 Hz under 20g input excitation.

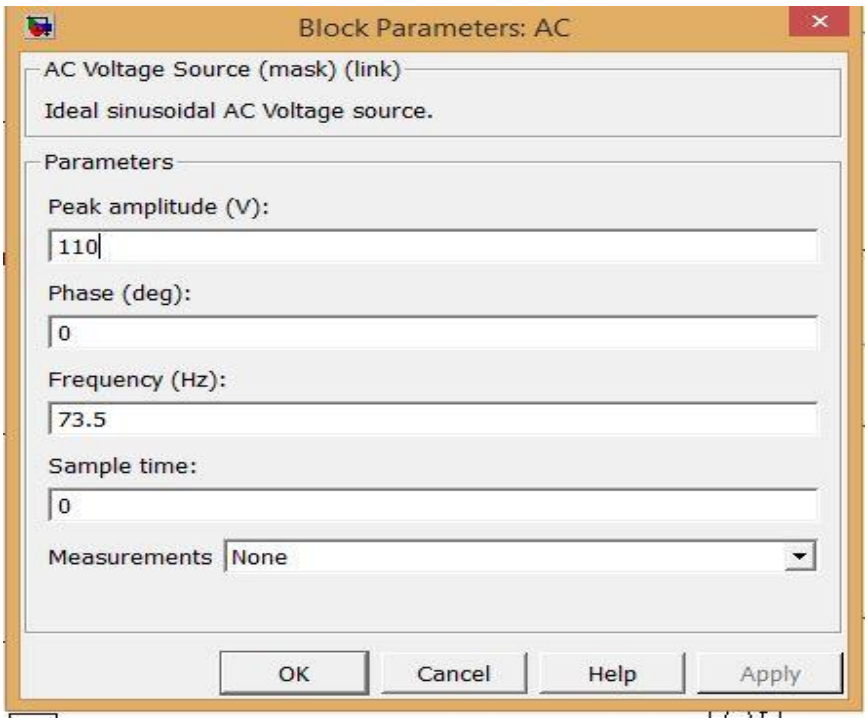

Fig.5.19 Simulink Block parameters of Full wave rectifier

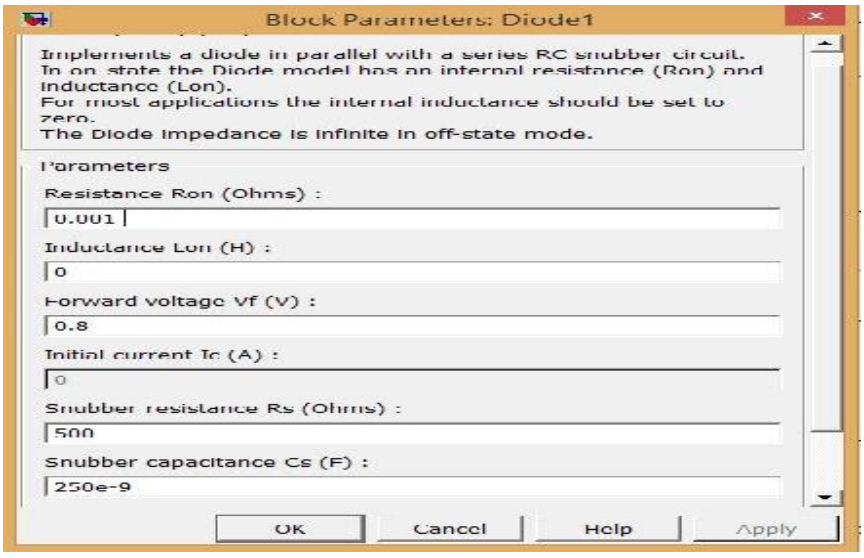

Fig.5.20 Simulink Diode Block parameters of Full wave rectifier

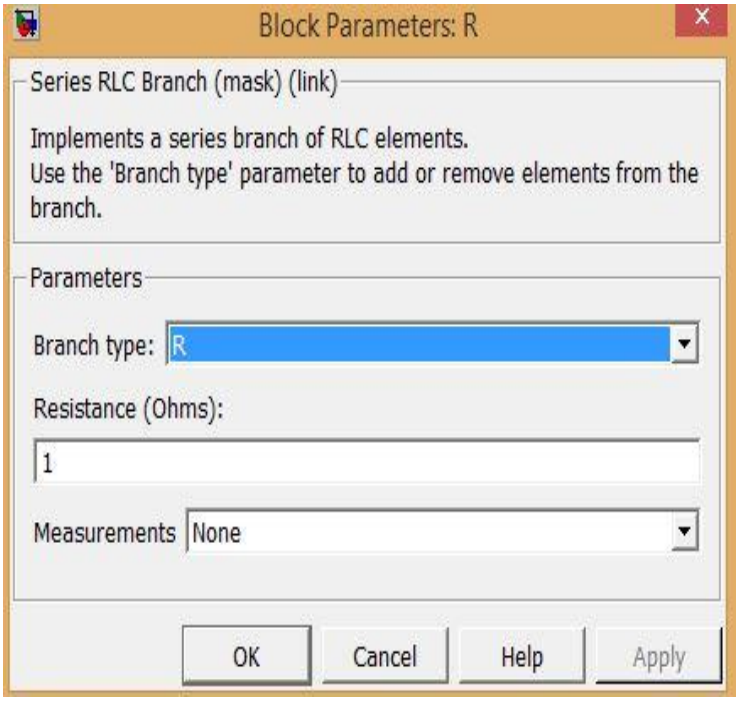

Fig.5.21 Simulink Resistance Block parameters of Full wave rectifier

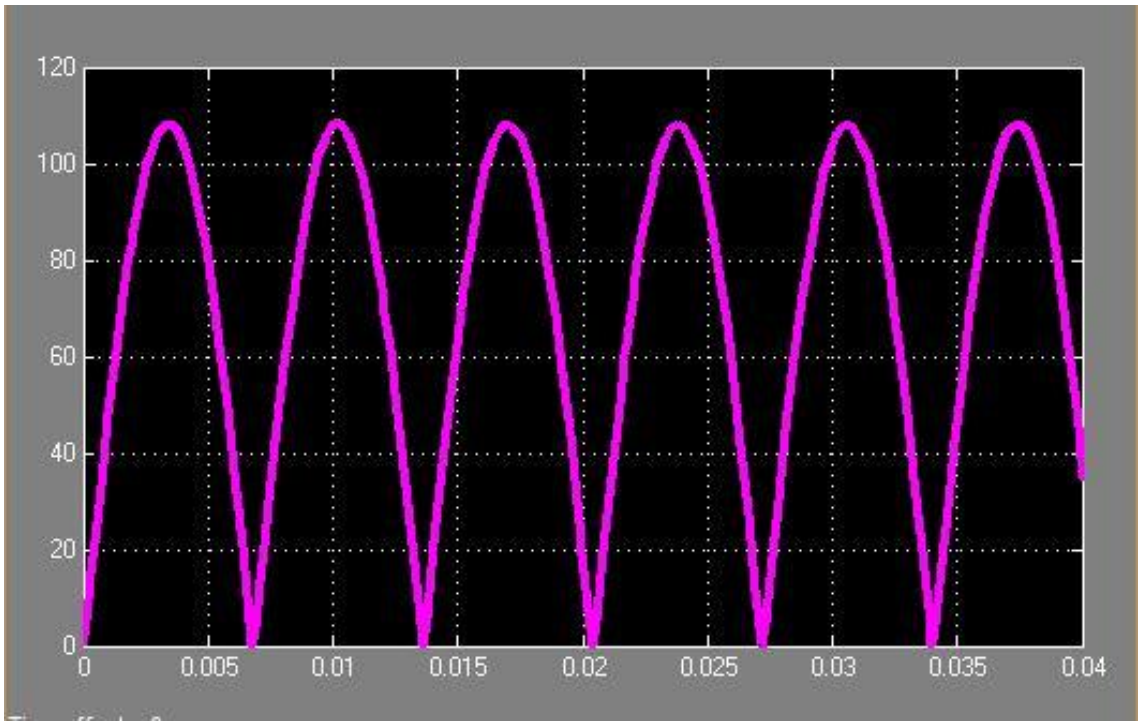

Fig. 5.22 DC Voltage from rectifier

Fig.5.22 shows the converted AC into DC voltage of 110 V.

5.7 Mathematical modelling of boost switching converter (BSC)

For converting DC to DC in maximum level BSC can be used and also it is a high efficient step up one. By assuming the continuous mode, the mathematical modelling is done for the BSC and the terminology is given to understand the design and operation principle of BSC, which is shown in Table 5.3.

Table 5.3 Terminology of BSC

Peak inductor current	i_{pk}
Min inductor current	i_0
Ripple Current	$\Delta i = (i_{pk} - i_0)$
Ripple Current Ratio to Average Current	$r = \Delta i / i_{av}$
Off Duty Cycle	$1 - D = T_{off} / T$
Switch Off Time	$T_{off} = (1 - D) / f$
Average and Load Current	$i_{av} = \Delta i / 2 = i_{load}$

The relationship of voltage and current for an inductor is: $i_{pk} = \frac{(V_{in} - V_{Trans})T_{on}}{L} + i_0$

For a constant rectangular pulse: $\Delta i = \frac{(V_{in} - V_{Trans})T_{on}}{L}$

When the transistor switches on the current is: $i_0 = i_{pk} - \frac{(V_{out} - V_{in} + V_D)T_{off}}{L}$

$$\Delta i = \frac{(V_{out} - V_{in} + V_D)T_{off}}{L}$$

Where V_D is the voltage drop across the diode, and V_{Trans} is the voltage drop across the transistor. Note that the continuous/discontinuous boundary occurs when i_o is zero.

By equating through delta i, we can solve for Vout: $\frac{(V_{in} - V_{Trans})T_{on}}{L} = \frac{(V_{out} - V_{in} + V_D)T_{off}}{L}$

$$V_{in}T_{on} + V_{in}T_{off} = V_{out}T_{off} + V_{Trans}T_{on} + V_DT_{off}$$

$$V_{in} - V_{Trans}D = (V_{out} + V_D)(1 - D)$$

$$V_{out} = \frac{V_{in} - V_{Trans}D}{(1-D)} - V_D$$

If the voltage drops across the transistor and diode is neglected then:

$$V_{out} = \frac{V_{in}}{1-D}$$

Fig.5.23 shows the simulink model of DC-DC Boost converter. Fig.5.24 shows the output parameters such as DC boosted voltage and Power. The observed maximized voltage is 220 V and power is 22 W. Off Duty cycle is considered as 0.5.

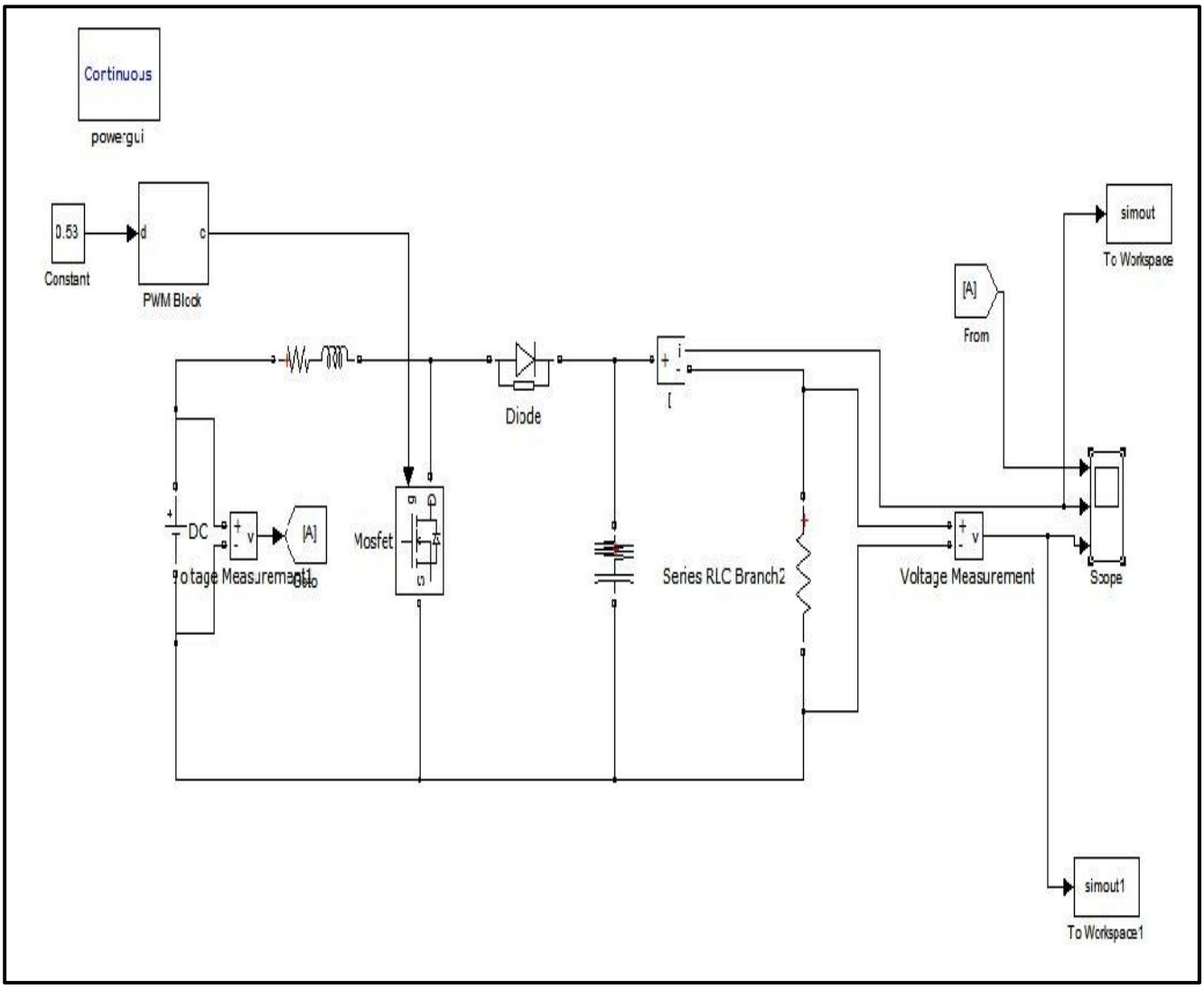

Fig. 5.23 Simulink model of DC-DC Boost converter

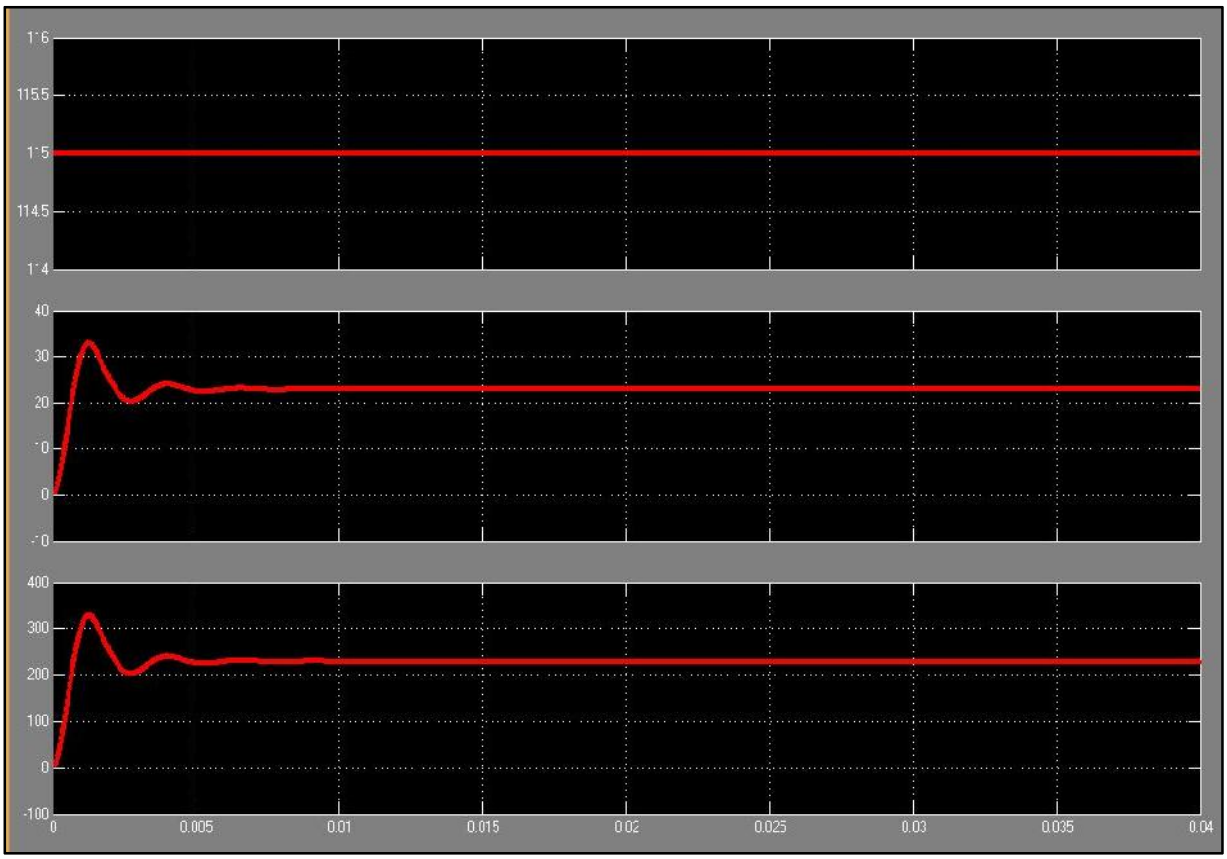

Fig. 5.24 Outputs of DC-DC Boost converter

5. 8 Summary of the chapter

In this chapter proto type model of a unimorph piezoelectric vibration energy harvester is developed. Analytical results are validated with experimentation at the frequencies of 70 Hz, 73.5 Hz, 75.5 Hz, 80 Hz and 90 Hz under the acceleration of 20g. The maximum voltage is observed at 73.5 Hz in both analytically and experimentally, which is considered as a resonance frequency for the presented energy harvesting device. As a case study, the effect of environmental factor on energy harvester is studied experimentally. The maximum voltage (122 V) is observed at the temperature of 20^0C, the reason may be temperature effects the brittleness variation of the lead zirconate titanate; therefore at low temperature raises the property of brittleness of the material and increases the piezoelectric constant which leads to increase the output voltage generation. As second part of this chapter, DC-DC Boost converter is designed to increase the DC output voltage and power by using MATLAB Simulink toolbox.

Chapter 6

Conclusions and Scope for Future Research

6.1 Results summary

i. In the chapter 3, the mechanical and electrical parameters of PZT discs are studied experimentally, generally, the limitations of applied loads are depended on the design of piezoelectric energy harvesters; therefore, the characterizations of piezoelectric disc type actuator are studied as a prerequisite to design the piezoelectric energy harvester and for doing experimentation. In this chapter, operating limiting values are observed. The maximum contact stress is observed as 11.4 MPa. If the operating stress is acted beyond the contact stress, the damage of PZT disc may be occurred which is shown in the chapter 3, Fig 3.12.

ii. The simulation studies of energy harvester are mentioned in chapter 4 and these studies are done under frequency and acceleration dependences by considering the damping factor of 0.001. The range of excited frequencies is from 25 Hz to 100 Hz. The maximum voltage is observed at 73.5 Hz.

iii. Harvesting the electrical energy through utilizing the vibrations at different excited frequencies including 25Hz to 100 Hz the reliability and sustainability of PZT wafers plays an important role under normal loading conditions. The output voltage curve is linear at excited lower frequencies and accelerations. Voltage curve becomes non-linear under lower frequencies and highly accelerated loads. It may be because of the Hertzian contact pressure causes to increase in the mobility of positive and negative charges in PZT.

iv. Analytical values are compared with experimentation, at the acceleration of 20g under the frequency of 73.5 Hz, the output voltage during experimentation is observed as 4.54% more than the obtained in analytical studies.

v. At 20^0C the generated voltage is 6.08% more than the normal temperature experimental value of 20g acceleration at 73.5 Hz.

vi. The generated optimum DC Voltage through simulation is 91.3% higher than AC Voltage which is generated during experimentation.

vii. Available DC Voltage can be used for operating the DC power devices such as fans for cooling engines, functioning of the LED lights , wireless sensors networks and electronic devices.

6.2 Conclusions

i. The theoretical analysis of piezoelectric constitutive equations revealed that the piezoelectric coupling coefficient plays the major role to maximize the output power; therefore, PZT-5H material is chosen in this dissertation. Electrical and mechanical properties are studied experimentally in the chapter 3 as a prerequisite to the design of the energy harvester. In the chapter 3, the limiting operating loads are observed. Among all properties, the value of contact stress is found significant for operating the energy harvester within the elastic limit.

ii. The selection of piezoceramic material is very important for developing maximum power generated energy harvester. The generation output voltage and power are depended the value of piezoelectric constant and dynamic strain.

iii. In the chapter 4, simulation studies of energy harvester have been done in support to the design of energy harvester under various frequencies and accelerations by considering the limiting conditions which are mentioned in the chapter 3. Resonance and non resonance frequencies are observed from the simulation studies of the energy harvester. These studies helped to generate maximum values of voltage and power by experimentation. The conceptual studies can be implemented in the simulation which are complex in experimentation for minimizing the wastage of material, operation time and finally capital.

iv. The optimum electrical load depends on electromechanical coupling but the maximum power outputs are affected and the order of the power outputs is same for all unimorphs. This observation supports the idea that the large power outputs are due to large dynamic flexibilities originating from the large elastic compliance values of the unimorphs.

v. The experimental studies of the properties of PZT-5H disc actuators divulged the limiting conditions of the operation of energy harvester, for increasing durable life. The analytical

model predicted the electrical voltages and power with good accuracy for all values of excitations.

vi. The output voltages of analytical method satisfied the linearity of theoretical method. The experimental results of energy harvester revealed that exciting the energy harvester at resonance frequencies leads to increase the output voltage. The analytical results are validated with experimental results and also good agreement is observed with the experimental values.

vii. The experimentation of energy harvester under different temperatures is done. It is found that the importance of temperature in optimizing the output voltage and power. By increasing the temperature of energy harvester leads to decrease the output voltage and decreasing the temperature of energy harvester leads to increase the output voltage. It may be due to increase of piezoelectric constant at low temperature, the output power raises. At high temperature, the piezoelectric constant may be decreased and leads to reduce the output power. At high temperature, the bond strength between the piezoceramic and the brass may be reduced.

viii. The output from piezoelectric transduction mechanism is alternating current. Direct current is required to operate low power DC devices and wireless sensor nodes in the satellites and to supply enough power and voltage; further, to optimize the output of energy harvester; the simulation study of power conversion is done. Simulated the AC voltage of energy harvester in DC-DC booster converter, it is found the maximum DC voltage, which can also be used for charging the electronic devices.

6.3 Scope for future work

- Novel devices of EH can be designed for maximum power output by using lumped mass EH on clamped free beams.
- Multistage EH devices with the help of rectangular PZT discs can also be constructed.
- Electric field plays a key role therefore one can look into this area of the manufacturing PZT discs in the future for gaining the maximum power output.
- Effect of environment on EH especially temperatures between -10^0C to 0 ^{0}C to be done. It can be more realistic in the lower temperature environment.

- There is a wide scope for vibration control and generating the electricity by using PZT discs for naval applications.
- There is a scope of increasing the output voltage by increasing the piezoelectric constant for aerospace and military applications.

References:

[1] Hua Bin Fang, Jing Quan Liu, Zheng Yi Xu, Lu Dong, Li Wang, Di Chen, Bing Chu Cai, Yue Liu, Fabrication and performance of MEMS-based piezoelectric power generator for vibration energy harvesting, Microelectronics Journal, Vol. 37 (2006), pp.1280–1284.

[2] Yuantai Hu, Ting Hu, Qing Jiang, Coupled analysis for the harvesting structure and the modulating circuit in a piezoelectric bimorph energy harvester, Acta Mechanica Solida Sinica, Vol. 20, (2007), pp. 134-145.

[3] Marco Ferraria, Vittorio Ferrari, Michele Guizzetti, Bruno Andò, Salvatore Baglio, Carlo Trigona Improved Energy Harvesting from Wideband Vibrations by Nonlinear Piezoelectric Converters, Procedia Chemistry, Vol. 1 (2009), pp.1203–1206.

[4] Huicong Liu, Chenggen Quan, Cho Jui Tay, Takeshi Kobayashi and Chengkuo Lee, A MEMS-based piezoelectric cantilever patterned with PZT thin film array for harvesting energy from low frequency vibrations, Physics Procedia,Vol.19 (2011), pp. 129–133.

[5] Meiling Zhu and Stephen Edkins, Analytical modelling results of piezoelectric energy harvesting devices for self-power sensors/sensor networks in structural health monitoring, Procedia Engineering, Vol. 25 (2011), pp. 195–198.

[6] Xianzhi Daia, Yumei Wen, Ping Li, Jin Yang, Ming Li, Energy harvesting from mechanical vibrations using multiple Magneto strictive and piezoelectric composite transducers, Sensors and Actuators, Vol. 66 (2011), pp. 94–101.

[7] N.H. Diyana, Asan G.A. Muthalif, M.N. Fakhzan, A.N.Nordin, Vibration Energy harvesting using single and comb-shaped piezoelectric beam structures: Modeling and Simulation, Procedia Engineering, Vol.41 (2012), pp. 1228–1234.

[8] L. Zhou, J. Sun, X.J. Zheng, S.F. Deng, J.H. Zhao, S.T. Peng, Y. Zhang, X.Y. Wang, H.B. Cheng, A model for the energy harvesting performance of shear mode piezoelectric cantilever, Sensors and Actuators, Vol. 179 (2012), pp. 185–192.

[9] Mahmoud Al Ahmad, H.N. Alshareef, Energy harvesting from radio frequency propagation using piezoelectric cantilevers, Materials Science & Engineering, Solid-State Electronics, Vol. 68 (2012), pp. 13–17.

[10] Huicong Liu, Chengkuo Lee, Takeshi Kobayashi, Cho Jui Tay, Chenggen Quan, Piezoelectric MEMS-based wideband energy harvesting systems using a frequency-up-conversion cantilever stopper, Sensors and Actuators, Vol. 186(2012), pp. 242– 248.

[11] Zhuming Liu, Lijie Li, Modeling of Energy harvesting device with segmented piezoelectric layer, Procedia Engineering, Vol. 47 (2012), pp.470–473.

[12] Hong jin Wangn, Qingfeng Meng, Analytical modelling and experimental verification of vibration-based piezoelectric bimorph beam with a tip-mass for power harvesting, Mechanical Systems and Signal Processing, Vol. 36(2013), pp.193–209.

[13] Zhongsheng Chen, Yongmin Yang, Zhimiao Lu, Yanting Luo, Broadband characteristics of vibration energy harvesting using one-dimensional photonic piezoelectric cantilever beams, Sensors and Actuators B :Physical, Vol.410(2013), pp. 5–12.

[14] Waleed Al-Ashtari, Matthias Hunstig, Tobias Hemsel, Walter Sextro, Enhanced energy harvesting using multiple piezoelectric elements: Theory and experiments, Sensors and Actuators A: Physical, Vol. 200(2013), pp. 138-146.

[15] M.N. Fakhzan, Asan G.A. Muthalif, Harvesting vibration energy using piezoelectric material: Modelling, simulation and experimental verifications, Mechatronics, Vol. 23 (2013), pp. 61–66.

[16] Jung Hoon Lim, Seong Su Jeong, Na Ri Kim, Seong Kyu Cheon, Myong Ho Kim, Tae Gone Park, Design and fabrication of a cross-shaped piezoelectric generator for energy harvesting, Ceramics International, Vol. 39(2013), pp. S641-S645.

[17] John Kymissis, Clyde Kendall, Joseph Paradiso and Neil Gershenfeld, Parasitic Power Harvesting in Shoes, IEEE International Conference on Wearable Computing, 1998, pp.1-8.

[18] Jose Luis Gonzalez, Antonio Rubio and Francesc Moll, Human powered piezoelectric batteries to supply power wearable electronic devices, International journal of Soc. Materials Engineering, Vol.10(2002), pp. 34-40

[19] S. N. S Jamaludin, Rosli A. Bakar and L. M. Gan, Design and development of actuation part of piezoelectric generator prototyping for alternative power generation, National Conference in Mechanical Engineering Research and Postgraduate Students (2010), pp.26-27.

[20] Pawan.S, Energy harvesting from passive human power using reverse electro wetting, IJESA Vol. 4(2014), pp. 1-7.

[21] G.J. Burger, T.S.J. Lammerink, J.H.J. Fluitman, **S.** Imai, M. Tokuyama & S. Hirose, Piezoelectric impact force sensor array for tribological research on rigid disk storage media,0-7803-2503-60 IEEE (1995).

[22] Kevin D. Champaigne & Jonathan Sumners Low-power electronics for distributed impact detection and piezoelectric sensor applications, IEEEAC paper 1149, Version 1, (2006).

[23] Marco Massarotto, Alfonso Carlosenal, Sergio Garriz and Jesu's M. Pintor, An impact technique for wide band characterization of piezoelectric accelerometers, Instrumentation and Measurement Technology Conference Warsav, Poland (2007), pp. 1-3.

[24] M. Renaud, P. Fiorini, R. van Schaijk and C. van Hoof, An impact based piezoelectric harvester adapted to low frequency environmental vibrations, Transducers, Denver, USA,(2009), pp. 21-25.

[25] E Jacquelin, S Adhikari and M I Friswell A piezoelectric device for impact energy Harvesting, Smart Matererial Structures, Vol. 20 (2011), pp. 1-13.

[26] P. Janphuang, D. Isarakorn, D. Briand, and N.F. de Rooij, Energy harvesting from a rotating gear using an impact type piezoelectric mems scavenger,Transducer, Vol.11(2011), pp. 5-9.

[27] M. Ferrari, M. Bau, F. Cerini & V. Ferrari Impact-Enhanced Multi-Beam Piezoelectric Converter for Energy Harvesting in Autonomous Sensors, Procedia Engineering, Vol.4(2012), pp. 418 – 421.

[28] Ki Hwan Baek, Seong Kwang Hong, Se Bin Kim, Jeong Hun Kim and Tae Hyun Sung Rectifier and structural design for efficient energy harvesting system from impact-based piezoelectric array, IEEE (2012).

[29] Chao Lu, Vijay Raghunathan and Kaushik Roy, Micro-scale energy harvesting, Circuits and Systems, Encyclopedia of Life Support Systems (2005).

[30] S. P. Beeby, M J Tudor and N M White, Energy harvesting vibration sources for micro systems applications, Measurement Science and Technology, Vol. 17 (2006), pp. R175–R195.

[31] Huan Tong, Bo-Lin Wang, Zhong-Can Ou-Yang, Electric potential generated in ZnO nanowire due to piezoelectric effect, Thin Solid Films, Vol. 516(2008), pp. 2708–2710.

[32] Ahmadreza Tabesh, and Luc G. Frechette, Ultra low power stand-alone circuitry for harvesting energy from a micro-power piezoelectric generator, Proceedings of Power MEMS 2008, Sendai, Japan, (2008),pp.9-12.

[33] R.M. Fain, M.A. Hopcroft and P.K. Wright, Development of a micro scale energy harvesting system for portable device recharging: a laptop case model, Power MEMS, Washington DC, USA, (2009).

[34] Manu Pallapa, Mohamed Aly Saad Aly, Albert I. H. Chen, Lawrence Wong, Ka Wai Wong, Eihab M. Abdel-Rahman and John Tze-Wei Yeow, Modeling and simulation of a piezoelectric micro-power generator, COMSOL Conference 2010 Boston.

[35] Brijesh Kumar, Sang-WooKim, Energy harvesting based on semiconducting piezoelectric ZnO nanostructures, School of Advanced Materials Science and Engineering, Nano Energy, Vol. 1 (2012), pp. 342–355.

[36] Jiyoung Chang, Michael Dommer, Chieh Chang & LiweiLin, Piezoelectric nanofibers for energy scavenging applications, Nano Energy, Vol. 1(2012),pp. 356–371.

[37] Xudong Wang, Piezoelectric nanogenerators Harvesting ambient mechanical energy at the nanometer scale, Nano Energy, Vol. 1(2012), pp. 13-24.

[38] Jin Yang, Yumei Wen, Ping Li, Xianzhi Dai, Ming Li, Design, analysis of broadband vibration energy harvester using magnetoelectric transducer, The Key Laboratory for Optoelectronic Technology & Systems, Ministry of Education, China (2009).

[39] Mao-Qugn Wei, Fu-Hsiang Ko, Tai-Ping Sun, Hsuen-Li Chen, Yung-Bin Lin, Efficiency enhancement and sensitive broadband 1Hz to 1kHz of power generator by recycling vibration energy on automobile, IEEE (2012).

[40] Lihua Tang, Yaowen Yang, and Chee Kiong Soh, Broadband vibration energy harvesting techniques, Springer Science, Business Media New York (2013).

[41] Louis Van Blarigan, Per Danzl, and Jeff Moehlis, A broadband vibrational energy harvester, Applied Physics Letters 100, 253904 (2012).

[42] V. R. Challa, M.G. Prasad and F. D. Fisher, Resonent frequency tunable vibration energy harvesting device, Stevens Institute of Technology, Castle Point on Hudson, Hoboken, NJ 07030 (2010).

[43] E. Minazara, D. Vasic and F. Costa, Piezoelectric generator harvesting bike vibrations energy to supply portable devices, Vol. 1(2008), pp. 508-513.

[44] Antonio Messineo, Andrea Alaimo, Piezoelectric Bender Transducers for Energy Harvesting Applications, Energy Procedia, Vol. 14, (2012) pp. 39-44.

[45] Hui Shen, Jinhao Qiu, Marco Balsi, Vibration damping as a result of piezoelectric energy harvesting, Sensors and Actuators A: Physical, Vol. 169 (2011), pp. 178-186.

[46] Joel Feenstra, Jon Granstrom, Henry Sodano, Energy harvesting through a backpack employing a mechanically amplified piezoelectric stack, Mechanical Systems & Signal Processing, Vol. 22 (2008), pp. 721-734.

[47] Mr. Suresh S. Balpande, Mr. Sudhir B. Lande, Mr. Sourabh Rungta, Mr. Maruti Tamrakar, Modeling and Comparative Evaluation of RF and PZT Micro-power Harvester for Wireless Sensors Network, 3rd International Conference on Intelligent Systems and Network (2009), pp. 14-16.

[48] No¨el E. duToit, Brian L. Wardle and Sang-Gook Kim, Design considerations for MEMS scale piezoelectric mechanical vibration energy harvesters, Integrated Ferroelectrics, Vol 71(2005), pp. 121–160, 2005.

[49] Shahab Mehraeen, S. Jagannathan, Keith A. Corzine, Energy harvesting from vibration with alternate scavenging circuitry and tapered cantilever beam, Industrial Electronics, IEEE Vol. 57, (2010), pp. 820-830

[50] Karthik Kalyanaraman, Jaykrishna Babu, Power harvesting System in Mobile Phones and laptops using piezoelectric charge generation, Proceedings of the World Congress on Engineering and Computer Science Vol. 1, (2010).

[51] Pisharody Harikrishnan, An optimal design for piezoelectric energy harvesting system, IEEE PES Innovative Smart Grid Technologies India(2011), pp. 244-247.

[52] Sujesha Sudevalayam, Purushottam Kulkarni, Energy Harvesting Sensor Nodes: Survey and Implications, IEEE communications surveys & tutorials, Vol. 13, third quarter (2011).

[53] M. C. B. Kumar, D. B. Prabhu, R. Akila, A. Gupta, M. Alagappan, N. M. Sundaram, Design and Simulation of MEMS Based Piezoelectric Vibration Energy Harvesting System, COMSOL Conference in Bangalore (2012).

[54] Shashank Priya, Robert D. Myer, Piezoelectric energy harvester, United state patent**,** patent no. US 7,649305, B2. JAN 19 (2012).

[55] H.S.Kim and J.S.Kim, A review of piezoelectric energy harvesting based on vibration, International Journal of precision engineering and manufacturing Vol. 12(2011), pp. 1129-1141.

[56] Roundy, S., On the effectiveness of vibration base energy harvesting, Journal of Intelligent Material Systems and Structures, Vol.16 (2005), pp. 45-52.

[57] S. Zhao & A. Erturk, Deterministic and band-limited stochastic energy harvesting from uniaxial excitation of a multilayer piezoelectric stack, Sensors and Actuators , Vol. 214 (2014), pp. 58–65.

[58] Anuruddh Kumar, Anshul Sharma, Rajeev Kumar, Rahul Vaish, Vishal S. Chauhan, Finite element analysis of vibration energy harvesting using lead-free piezoelectric materials: A comparative study, Journal of Asian Ceramic Societies, Vol. 2 (2014), pp. 138–143.

[59] Yuanlin Hu, Xin Liang, Wen Wang, A theoretical solution of resonant circular diaphragm-type piezo actuators with added mass loads, Sensors and Actuators A, Vol. 258 (2017), pp. 74–87.

[60] Nan Chen, Hyun Jun Jung, Hamid Jabbar, Tae Hyun Sung, Tingcun Wei, A piezoelectric impact-induced vibration cantilever energy harvester from speed bump with a low-power power management circuit, Sensors and Actuators A, Vol. 254 (2017), pp. 134–144.

[61] Isaku Kannoa and Hidetoshi Kotera, Crystallographic characterization of epitaxial Pb„Zr,Ti…O3 films with different ZrÕTi ratio grown by radio-frequency-magnetron sputtering, Journal of applied physics, Vol.93(2003), pp.1-5.

[62] Ching Chang Chun, Micro-structural Evolution in Lead Zirconate Titanate (PZT) Piezoelectric Ceramics, University of Connecticut - Storrs, ching-chang.chung@uconn.edu.

[63] RW Fox, AT McDonald, PJ Pritchard , Introduction to Fluid Mechanics, John Wiley and Sons, 8 Th Edition 2014.

[64] Quan and Shun-rong He, Two-dimensional analysis of piezoelectric/piezo magnetic and elastic media, Composite structures, Vol 69(2005), pp. 229-237.

[65] Seon-Bae Kim , Jung-HyunPark , HosangAhn, DanLiu, Dong-JooKim, Temperature effects on output power of piezoelectric vibration energy harvesters, Microelectronics Journal, Vol 42 (2011), pp. 988–991.

Appendix A

Effect of piezoelectric coupling coefficient in generating the power output

In this chapter studied the effect of piezoelectric coupling coefficient through the analysis of dimensions. Analysis of dimensions is the mathematical procedure which gives solution to engineering problems. And also helps to find out the role of importance of different parameters in analytical and experimental studies such a way designing of any product makes easy, builds confidence in the designer to fabricate the product and makes ease of understanding inferences within the research.

In general every mathematical modeling is the combination of dimensional and non-dimensional quantities in the form of dependent and independent variables. Analysis of dimensions leads to form the mathematical modelling provided dependent and independent quantities are known.

A.1 Merits of Analysis of dimensions [65]:

i) For forming mathematical modelling in terms of various parameters

ii) For knowing the relative importance of each parameters within the mathematical modelling.

iii) Planning for conceptual design of energy harvesters based on mathematical modelling.

iv) Planning for the fabrication of the vibration based energy harvesters.

v) Planning for experimentation of vibration based energy harvesters.

A.2 Dimensional homogeneity of equations:

The process of dimensional homogeneity plays a very important role in order to find out the algebraics missing in the process of developing a mathematical modelling; therefore dimensional homogeneity is a recommended method to adopt in all research works. The method of dimensional homogeneity is not confined to a particular engineering field rather it is applicable to all type of engineering fields of research. There are two types of mathematical modeling. One is rational and another one is irrational. In the rational type dimensional homogeneity exists and in irrational type dimensional homogeneity does not exist. Dimensional homogeneity is defined

by Fourier's law which states that any mathematical modelling of piezoelectricity should express the physical phenomenon and should be rational.

Generally, the mathematical modelling of any engineering and science problem is expressed with the combination of different variables. There are two types of engineering systems. One is a simple system and the second one is complex system. For the simple system mathematical modelling is easy based on the assumptions. In this system mathematical modelling yields good results. In the complex system, assumptions cannot be made, making mathematical modelling is very difficult because of involving so many variables and also no analytical solution is possible. At that time analysis of dimensions gives solution to make mathematical relations among variables especially forming a electromechanical coupled equations for the vibration based energy harvesters.

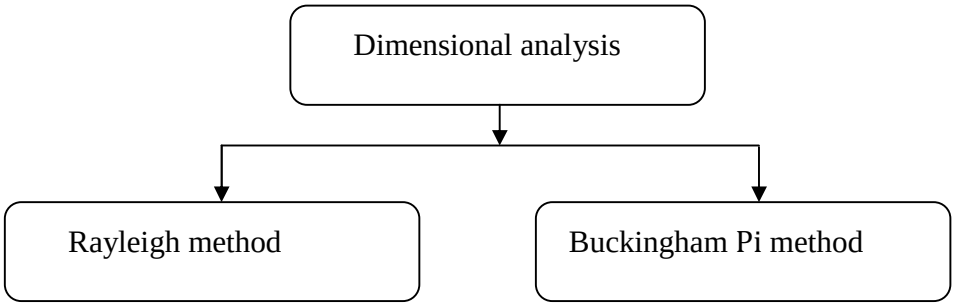

Fig A.1 Pictorial presentation of classification of Dimensional analysis

Dimensional analysis can be done by using two methods. One is Raleigh's method and another one is Buckingham's method. The pictorial presentation of classifications is shown in figure 4.1.

There are two theorems of Buckingham.

i) Theorem-I: It states that the relationship between independent dimensionless groups from all variables

ii) Theorem-II: It gives the formula of number of dimensionless groups (N_{dg})

$$N_{dg} = N_v - N_d$$

N_v is the number of variables and N_d is the number of dimensions

These dimensionless groups are called as Pi groups.

A.3 Rayleigh method [65]:

Rayleigh established this method in 1899, for determining the effect of temperature on the viscosity of a gas.

In this method a functional relationship of both dependent and independent variables is articulated in dimensionally homogeneous an exponential equation. Thus suppose '· ' is some function of variables · 1 ,· 2 ,· 3 ....: n . The equation can be established in the functional form:

· = f ·(· 2 · 3 .:.n ·

In the above functional form '· ' is the dependent variable, while · 1 ·,2 ·,3 ..:.n are the independent variables. Information is required about the dependent quantities and the independent quantities controls the variation of dependent quantities.

The exponential form of equation can be expressed as · = c (a 1 ·, b 2 ·, c 3 ..:.. n . In which c is the dimensionless constant which may be determined either from the physical characteristics of the problem or from experimental measurements. The exponents a, b, c …n are then evaluated on the basis that the equation is dimensionally homogeneous. The dimensionless parameters are then formed by grouping together the variables with like powers.

A.4 Buckingham Π method [66-67]:

The Buckingham Π method describes that if there are 'N_v' dimensional variables existed in a occurrence, which can be totally defined by 'N_d' fundamental dimensions and are related by a dimensionally homogeneous equation. The correlation among the 'N_v' variables can be expressed in the form of $(N_v - N_d)$ dimensionless and independent Π expressions. Mathematically, if any variable k_1 depends on the independent variables $k_2, k_3, k_4 ..... k_n$; the functional equation may be written as $k_1 = f(k_2, k_3, k_4 ..... k_n)$ which can be transformed to another functional relationship $f_1(k_2, k_3, k_4 ..... k_n) = P$ where P is a dimensionless constant. This is as if $x = f(y) = y^2 + P$

$$x - y^2 = f_1(x, y) = P$$

In accordance with the Buckingham theorem, a non-dimensional equation can thus be obtained in the following form. $f_2\left(\Pi_1, \Pi_2, \Pi_3 \ldots\ldots \Pi_{n-m}\right) = P_1$

Wherein every dimensionless Π - expression is expressed by coalescing 'N_d' quantities out of the total 'N_v' quantities with one of the residual $(N_v - N_d)$ quantities. The 'N_d' quantities can be appeared frequently in each of the Π terms and are subsequently entitled repeated variables. Thus the different Π terms may be established as

$$\Pi_1 = k_1^{a1} k_2^{b1} k_3^{c1} \ldots\ldots\ k_m^{m1} k_{m+1}$$

$$\Pi_2 = k_1^{a2} k_2^{b2} k_3^{c2} \ldots\ldots k_m^{m2} k_{m+2}$$

$$\Pi_3 = k_1^{a3} k_2^{b3} k_3^{c3} \ldots\ldots k_m^{m3} k_{m+3}$$

$$\Pi_4 = k_1^{a4} k_2^{b4} k_3^{c4} \ldots\ldots k_m^{m4} k_{m+4}$$

$$\ldots\ldots\ldots\ldots\ldots\ldots\ldots\ldots\ldots\ldots$$

$$\Pi_{n-m} = k_1^{an-m} k_2^{bn-m} k_3^{cn-m} \ldots\ldots k_m^{mn-m} k_{m+1}$$

In the above equation each individual equation is dimensionless and the exponents a,b,c,d…m etc., are determined by considering dimensional homogeneity for each equation so that each Π term is dimensionless. The final general equation for the phenomenon may then be obtained by expressing any one of the Π terms as a function of the others as

$$\Pi_1 = f_1\left(\Pi_2, \Pi_3, \Pi_4 \ldots\ldots \Pi_{n-m}\right)$$

$$\Pi_2 = f_2\left(\Pi_2, \Pi_3, \Pi_4 \ldots\ldots \Pi_{n-m}\right)$$

$$\Pi_3 = f_3\left(\Pi_2, \Pi_3, \Pi_4 \ldots\ldots \Pi_{n-m}\right)$$

$$\Pi_4 = f_4\left(\Pi_2, \Pi_3, \Pi_4 \ldots\ldots \Pi_{n-m}\right)$$

A.4.1 Outline procedure for Buckingham method:

The following is the outline of the procedure to be followed when the dimensional analysis is carried out by the Buckingham Π-method.

i) List all the quantities both dependent and independent existed with in the occurrence.

ii) Write down the dimensions of existed variables.

iii) The variables of 'N_d' is served as repeating variables. These variables should not be dimensionless. No two 'N_d' variables have the same dimensions.

iv) A dependent variable should not be considered as a repeating variable for obtaining a good functions of mathematical modelling.

v) Write down the general equations of various Π expressions and expressed with the products of repeating variables. Then find out the unknown powers by using algebraic equations.

vi) By repeating the above step, the number of dimensional equations of the Π terms can be obtained.

vii) Final equation for the physical phenomenon can be obtained with Π terms.

Piezoelectric linear constitutive equations:

The constitutive equations[48] for PZT are

$$S = s \pm + d\ E$$

$$D = d \pm + £\ E$$

Where S is the strain

$$s\ \ is\, the\, compliance = \frac{1}{Youngs\, modulus} = \frac{1}{E}$$

$$\pm\, is\, the\, mechanical\, stress\,,\ D\, is\, the\, electric\, displacement\,,\ E\ \ is\, the\, electricfield$$

$$d\ \ is\, the\ piezoelectric\, charge\, constant$$

$$£\ \ is\, the\, dielectric\ \ permittivity\, constant$$

Dimensions of properties are $\pm = ML^{-1}T^{-2}$

$$E = M^{1/2}L^{-1/2}T^{-1}, \quad s = M^{-1}L^{1}T^{2}$$

$$d = M^{-1/2}L^{-1/2}T^{1}, \; D = M^{1/2}L^{3/2}T^{-1}$$

$$S = M^{0}L^{0}T^{0}, \quad £ = M^{-1}L^{-3}T^{4}I^{2}$$

Number of relevant variables (n) = 7, Number of repeated variables (m) = 4

Number of dimensional groups = n - m = 3

Repeated variables are ±, E and d and the remaining variables are S, D, s and £

$$®_1 = ± \; S^a D^b s^c £^d$$

$$M^0L^0T^0I^0 = ML^{-1}T^{-2}\left(M^0L^0T^0\right)^a\left(M^{1/2}L^{3/2}T^{-1}\right)^b\left(M^{-1}L^1T^2\right)^c\left(M^{-1}L^{-3}T^4I^2\right)^d$$

By comparing the powers on both sides $®_1 = ± \; s$

$$®_2 = E \; S^a D^b s^c £^d$$

$$M^0L^0T^0I^0 = M^{1/2}L^{-1/2}T^{-1}\left(M^0L^0T^0\right)^a\left(M^{1/2}L^{3/2}T^{-1}\right)^b\left(M^{-1}L^1T^2\right)^c\left(M^{-1}L^{-3}T^4I^2\right)^d$$

$$M^0L^0T^0I^0 = M^{1}{}_2L^{-1}{}_2T^{-1} \; M^0L^0T^0{}^{\,a} \; M^{1}{}_2L^{3}{}_2T^{-1}{}^{\,b} \; M^{-1}L^1T^2{}^{\,c} \; M^{-1}L^{-3}T^4I^2{}^{\,d}$$

Therefore $®_2 = E \; s^{1/2}$

$$®_3 = d \; S^a D^b s^c £^d$$

$$M^0L^0T^0I^0 = M^{-1/2}L^{-1/2}T^{1}\left(M^0L^0T^0\right)^a\left(M^{1/2}L^{3/2}T^{-1}\right)^b\left(M^{-1}L^1T^2\right)^c\left(M^{-1}L^{-3}T^4I^2\right)^d$$

$®_3 = d \; D^{1/2}s^{-1/4}$

According to Buckingham pi theorem $f\left(®_1, ®_2, ®_3\right) = 0$

$$f\left(± s, E\, s^{1/2}, d\, D^{1/2}s^{-1/4}\right) = 0$$

$$d\, D^{1/2}s^{-1/4} = f\left(Ts, Es^{1/2}\right)$$

$$D = f\left(\frac{\pm\ {}^{2}s^{5/2}}{d^{2}}\ \frac{E\ {}^{2}s^{3/2}}{,\ d^{2}}\right)$$

$$D = f\left(\pm\ {}^{2}s^{5/2}d^{-2}, E\ {}^{2}s^{3/2}d^{-2}\right)$$

$$D = f\left(\pm\ {}^{2}s^{5/2}d^{-2}\right)$$

$$D = f\left(E\ {}^{2}s^{3/2}d^{-2}\right)$$

$$D = f\left(\pm\ {}^{2}s^{5/2}d^{-2}, E\ {}^{2}s^{3/2}d^{-2}\right)$$

Therefore Electric charge is the function of applied stress, Elastic compliance, Electric field, piezoelectric coupling coefficient. By observing the above relations the effect of piezoelectric coupling coefficient causes to enhance the output voltage generation from piezoelectric disc type actuators.